CHR
KHR

Internationale Kommission für die Hydrologie des Rheingebietes

International Commission for the Hydrology of the Rhine Basin (CHR)

Generation of Hydrometeorological Reference Conditions for the Assessment of Flood Hazard in large River Basins

Papers presented at the International Workshop held on March 6 and 7, 2001 in Koblenz

Edited by:
P. Krahe
D. Herpertz

Lelystad, December 2001
CHR-Report no. I-20

International Commission for the Hydrology of the Rhine Basin (CHR)

Generation of Hydrometeorological Reference Conditions for the Assessment of Flood Hazard in large River Basins

Papers presented at the International Workshop held on March 6 and 7, 2001 in Koblenz

Edited by:
P.Krahe
D.Herpertz
Bundesanstalt für Gewässerkunde, Koblenz - FRG

Lelystad, December 2001

CHR-Report no. I-20

ISBN 90-36954-18-5

Foreword

The International Commission for the Hydrology of the Rhine basin (CHR) is an organisation in which the scientific institutes of the Rhine riparian states formulate joint hydrological measures for sustainable development of the Rhine basin. The CHR's mission and tasks essentially are the expansion of knowledge of the hydrology in the Rhine basin and contributing to solutions of cross-border problems.

In response to recent flooding events in the Rhine basin, revised integrated management strategies were initiated which aim at improving the protection against high water by taking into account hydraulic, ecological and socio-economic functions of the entire river system on a transnational level. From the perspective of a long-term sustainable and resilient river basin development, hydrological studies on the effect of decentral flood reduction measures have become an important issue in the spatial planning process. Though high water management in itself is not a CHR task, the organisation is responsible for the study of hydrological principles that provide the basis for alternative and advanced river management practices in the Rhine basin.

A current CHR project, "Development of Methodologies for the Analysis of the Efficiency of Flood Reduction Measures in the Rhine Basin on the basis of Reference Floods (DEFLOOD)", was established within the scope of the IRMA-SPONGE programme. This project develops concepts and methods which facilitate hydrological assessments of the effect of decentralised flood reduction measures at the supraregional level. The CHR set up a project working group which comprises representatives of the Bundesanstalt für Gewässerkunde in Koblenz, the Bundesamt für Wasser und Geologie in Bern, the ETH Zürich, the Institute of Inland Water Management and Waste Water Treatment (RIZA) in Arnhem and the University of Trier.

The DEFLOOD project is part of the IRMA-SPONGE umbrella project which is financially supported by the EU's joint operational programme IRMA (Interregional Rhine-Meuse Activities). The IRMA-SPONGE project comprises 13 innovative, transnational, mutually consistent and complementary projects concerned with the study of flood prevention and potential damage. The overall aim is to develop instruments to support the spatial planning process in the Rhine and Meuse basins. NCR (Nederlands Centrum voor Rivierkunde) is responsible for the overall management. To further ensure scientific quality an International Scientific Advisory Committee (ISAC) is set up.

A special focus within the DEFLOOD project lies on the generation and application of standardised hydrometeorological scenarios which serve as a basis for integrated river basin modelling approaches in large river basins. In this context the international workshop "Generation of Hydrometeorological Reference Conditions for the Assessment of Flood Hazard in Large River Basins" was initiated in order to provide a platform for exchange of knowledge between experts on the fields of hydrological and hydrometeorological research.

The collection of technical papers of this workshop presented here documents the need for the generation of well-defined hydrometeorological boundary conditions in the context of hydrological modelling of extreme floods. Furthermore, the status quo of applicable methods available in the riparian countries of the River Rhine basin was determined. Some essential methodological questions regarding the generation of hydrometeorological input data required for the assessment of future flood hazard arose and could be discussed.

All speakers and other participants are thanked for their contributions, which enabled us to realise the workshop and this publication. We thank the EU and the IRMA-SPONGE project coordinator NCR for their financial support.

Contents

Introduction

The aim of this workshop was to accentuate the importance of hydrometeorological conditions for the origin of flooding in large river basins and to advance the scientific exchange of experience in relevant fields of research. Furthermore, an overview of the latest level of knowledge in German- and Dutch-speaking regions was given.

In order to allow for fruitful discussions the number of participants was limited. Fourteen speakers lectured on five pre-set subjects and gave an outline of the latest level of knowledge on the determination and regionalisation of measured precipitation. In addition, spokespersons of current projects in the Rhine basin working on hydrological modelling of the catchment area were invited. To these working groups a forum was provided in which the demands of the hydrological modellers on hydrometeorological research could be formulated. Altogether about 30 scientists from the fields of hydrometeorology and hydrology participated in the workshop.

The main theme of the workshop was the definition of hydrometeorological reference conditions for the estimation of flood hazard. This comprises for one the classification of precipitation patterns, and for two, various methods for estimating extreme precipitation as well as the largest possible constellation of precipitation distribution with regard to discharge formation. For example, how can "unfavourable" precipitation scenarios be created for large areas? Discussions were held on which approaches and methods, such as e.g. stochastic precipitation generators or meso-scale meteorological models, were suitable for which temporal and spatial scale. Furthermore, consideration was given to meteorologically-based estimations of the greatest possible precipitation on the catchment area and the problems of deriving probabilities and trends on the basis of historical data.

The intention was to identify deficiencies in research by exchanging experience in the field of hydrometeorology with regard to the demands made by hydrological modellers. At the same time, the exchange of ideas by scientists from various fields of work could be stimulated.

During the two-day workshop the following five subjects were treated:

- Topic 1: Approaches to the development of methods for the determination of maximised regional values (2 lectures)
- Topic 2: Estimation and classification of spatial/temporal patterns of extreme precipitation events (3 lectures)
- Topic 3: Modelling of extreme precipitation events of long duration (meso-scale meteorological modelling and stochastic precipitation generators) (4 lectures)
- Topic 4: Temporal trends of precipitation series, especially with regard to extreme behaviour and spatial development (2 lectures)
- Topic 5: Application of procedures for the determination of extreme precipitation events for questions concerning hydrology and water resources management (3 lectures)

In the concluding debate the most important arguments of the workshop were summarised and discussed.

Conclusions from the workshop

The lectures on topics 1 and 2 showed that based on measured precipitation data and meteorological evidence statements on the statistics of the extreme values in a region can be made. This includes scenarios of extreme and maximum probable regional precipitation depth. Although the majority of the procedures presented allow to give information on the precipitation of a region, the spatial reference of statistics on the next larger regional level is lost.

Results for areas of approx. 20 km² to 30 000 km² were presented. For the application of the procedures the temporal and spatial disaggregation of the regional values is still necessary. This is essential in order to convert the precipitation statistics into time series of precipitation required for hydrological modelling. In one lecture the corresponding methods for the spatial and temporal disaggregating of precipitation were described.

It was found that many of the procedures mainly refer to convective precipitation events or to the occurrence of a single precipitation event. A fact which is reflected in the rainfall duration steps chosen in most procedures, which are typically 3 to 72 hours. Thus the question arises whether these statistics can be used for frontally-bound precipitation events of long duration, which represent the flood-causing precipitation for example in the Rhine basin.

However, it was also shown how scenarios of extreme, spatially distributed precipitation for large regional units can be set up with plausible assumptions from historically-measured precipitation distributions in conjunction with a classification of precipitation patterns.

The lectures and discussions under topic 3 showed that there exist both stochastic and meso-scale meteorological models for the creation of small(meso)-scale precipitation areas for large regional units. Some of these procedures, however, require the atmospheric general circulation expressed as classified indices as a driving element. The great significance of the atmospheric circulation on the precipitation process was emphasized in all the lectures. Consequently, the problem of the creation of precipitation scenarios for large river basins is shifted to the modelling of the atmospheric general circulation.

In both the lectures and the following discussions emphasis was placed on the significance of this knowledge and the modelling of circulation parameters, for example the duration and the succession of certain current situations of heavy precipitation. However, during the workshop it was not possible to discuss the related existing methods in more detail. Nonetheless, this subject matter should definitely be pursued further.

In addition, it was understood from the lectures that the validation of the procedures was not yet complete. In the discussion it was stressed that a comprehensive validation is indispensable. Furthermore, emphasis was put on the necessity to point out the uncertainty of the methods for the generation of precipitation. Moreover, comparisons of the various techniques should be used to assure the accuracy of the results.

The lectures and discussions on topic 4 explained the non-stationarity of the precipitation series and once more pointed out the significance of the wide-ranging atmospheric circulation. The resulting consequences for the evaluation of statistics of extreme values of precipitation time series were discussed. Suggestions were made for extending the trend analyses of hydrometeorological quantities to analyses of statistical quantities, which describe the spatial/temporal patterns of precipitation as well as the atmospheric circulation.

For the fifth topic examples of hydrological applications in conjunction with synthetically-produced hydrometeorological time series were presented. These lectures again explained the need, formulated from the aspect of hydrological modelling, for synthetically-produced precipitation data for design purposes. Approaches to producing hydrometeorological time series were also mentioned. But here, as in the discussions of the first three topics, open questions remained regarding the spatial scale and possibilities for sound validations.

At the workshop the state of the art for the creation of hydrometeorogical boundary conditions could be highlighted. The advantages, disadvantages and restrictions of various procedures were discussed. With regard to future projects, the numerous methods and their complexities indicate a strong need for generally valid instructions on the creation of synthetic precipitation series and their application in hydrological models. Hydrologists and meteorologists should tackle this subject matter together. With this intention the workshop has made a step into the right direction.

Peter Krahe and Dorothe Herpertz
Bundesanstalt für Gewässerkunde
Koblenz

Dipl.-Met. Peter Krahe
Dr. Dorothe Herpertz
Bundesanstalt für Gewässerkunde
Kaiserin-Augusta-Anlagen 15-17
56068 Koblenz

krahe@bafg.de
herpertz@bafg.de

Agenda
of the Workshop
Generation of Hydrometeorological Reference Conditions for the Assessment of Flood Hazard in large River Basins
held on March 6 and 7, 2001 in Koblenz

Topic 1: Approaches to the development of methods for the determination of maximised regional values

Gabriele Malitz (Deutscher Wetterdienst, Hydrometeorology, Berlin, Germany)
Evaluation of notable, extreme and probable maximum areal values of precipitation depth and precipitation supply in large river basins

Dietmar Grebner (Institute for Atmospheric and Climate Sciences, ETH Zurich, Switzerland)
Spatial and temporal patterns of precipitation fields of extreme events in Switzerland and concepts for precipitation scenarios

Topic 2: Estimation and classification of spatial/temporal patterns of extreme precipitation events

Alfred Helbig (Dept. Climatology, Fac. Geography/Geosciences, Univ. of Trier, Germany)
Spatio-Temporal Structure of Precipitation during Flood Events in the Moselle Basin

Angela Hinterding (Institut für Geoinformatik, Westfälische Wilhelms-Universität Münster, Germany)
InterNied - A geostatistical interpolation procedure for hourly measured precipitation data

Andras Bardossy (Institut für Wasserbau, Universität Stuttgart (IWS), Germany)
Spatio-temporal disaggregation of precipitation for hydrological modelling

Topic 3: Modelling of extreme precipitation events of long duration (meso-scale meteorological modelling and stochastic precipitation generators)

Daniela Jacob (Max-Planck-Institut für Meteorologie, Hamburg (MPI), Germany)
Simulated precipitation characteristics in the River Rhine basin

Georg Skoda (Institute of Meteorology and Geophysics, University of Vienna, Austria)
How to use meso-meteorological models to predict cases of extreme precipitation

Gerd Bürger (Potsdam Institute for Climate Impact Research (PIK), Potsdam, Germany)
Precipitation scenarios from expanded downscaling

Jules Beersma, T. Adri Buishand and Rafał Wójcik (Royal Netherlands Meteorological Institute (KMNI), De Bilt, The Netherlands)
Rainfall generator for the Rhine basin: multi-site simulation of daily weather variables by nearest-neighbour resampling

Topic 4: Temporal trends of precipitation series, especially with regard to extreme behaviour and spatial development

Christian Schönwiese (J.W. Goethe University, Institute for Meteorology and Geophysics, Frankfurt a.M., Germany)
Observed long-term precipitation trends in Central Europe and some preliminary remarks on change in extremes

Laurent Pfister and Lucien Hoffmann (Centre de Recherche Public - Gabriel Lippmann, Cellule de Recherche en Environnement et Biotechnologies (CREBS), Luxembourg)
Evidence of a climate-induced change in maximum streamflow of the Alzette river (Grand-Duchy of Luxembourg)

Topic 5: Application of procedures for the determination of extreme precipitation events for questions concerning hydrology and water resources management

Jürgen Ihringer (Institut für Wasserwirtschaft und Kulturtechnik (IWK) der Universität Karlsruhe, Germany)
Employing extreme precipitation events for estimating extreme runoff

Karl-Gerd Richter, Martin Ebel and Karl Ludwig **(**c/o Dr.-Ing. Karl Ludwig, Beratender Ingenieur Wasserwirtschaft Wasserbau, Karlsruhe, Germany)
Application of a Water Balance Model for Calculating the Impact of Extreme Rainfall Events

Harvey J. E. Rodda (Peter Brett Associates, UK**)**
The Development of A Stochastic Rainfall Model for UK Flood Modelling

Topic 1: Approaches to the development of methods for the determination of maximised regional values

Generation of hydrometeorological reference conditions for the assessment of flood hazard in large river basins (Proceedings of International Workshop, Koblenz, 6. and 7. March 2001). CHR-Report No. I-20

Evaluation of notable, extreme and probable maximum areal values of precipitation depth and precipitation supply in large river basins

Gabriele Malitz
Deutscher Wetterdienst, Hydrometeorology
Berlin, Germany

Abstract Taking large parts of the Rhine catchment basin as an example the projects KOSTRA; REWANUS; MGN/NIEFLUD, PEN, and "MAGWANUS" are presented, with regard both to methodical aspects and the results. Within the framework of the coordinated regionalisation of heavy precipitation (KOSTRA), especially the selective heavy precipitation depths, determined with extreme value statistics, for duration levels from D = 24 h and return periods of T = 100 a in the time spans summer, winter (October to April) and the whole year are of interest for large river catchment basins. The KOSTRA heavy precipitation depths for the winter period are based on precipitation measurements, whereby the precipitation in the form of snow was liquefied before determination of the precipitation depth. If, when the snow melts, the precipitation stored therein coincides with heavy rainfall, extreme values, which are higher than the winter KOSTRA values, can occur. Consequently, the REWANUS values in the winter half-yearly period, those concerning the occurrence probability of extreme values of total precipitation (the sum of rainfall and snowmelt), are of considerable importance, above all in areas in which snow is hydrologically relevant. Based on time series of approximately 30 years, extreme value statistics of precipitation and total precipitation allow at the most statements up to return periods of 100 years. Flood protection structures that are designed for greater safety cannot be measured in this way. For risk appraisals the theoretically largest precipitation depth (probable maximum precipitation, PMP), that is physically possible in an observed area for a given duration at a certain time of year, is of importance. With the scope of the MGN and NIEFLUD projects an empirical path was taken with the maximisation in order to determine the presumably greatest regional precipitation depths, also in Germany's river basins. The very high precipitation values that result from the definition of PMP are, however, not used directly for the dimensioning of water management structures. The designed safety-serving elements of reservoirs are nearer to these values. Work is being done on the derivation of precipitation extreme values (PEN) in Germany that are relevant for water management practice. Thereby the region between the KOSTRA heavy precipitation depth of the return period of a hundred years and the presumably greatest precipitation is to be sounded out subject to the duration level. Work on the quantification of values between the extreme REWANUS value and the presumably maximum total precipitation is planned ("MAGWANUS").

INTRODUCTION

In recent years severe floodings have occurred in several parts of the world, both as localised flash floods and as basin-wide floods. The meteorological causes of floods are storm rainfalls in small river basins, persistent rainfall in large river basins or sudden melting of snow, which is often linked with heavy rainfall. Floods pose the greatest overall and most widely distributed natural risk to life within Europe. That is why there is a pressing need of hydrometeorological information on notable, extreme and probable maximum values of precipitation and of precipitation supply from meltwater release and rain at the same time. A series of problem solving oriented projects – for example KOSTRA, REWANUS, MGN, NIEFLUD - had been set up by the DWD's hydrometeorologists:

notable	← additional indirect measurement through remote sensing (radar),
areal	← computation of areal precipitation from point measurements directly,
values	← computation of areal precipitation supply by means of a model
extreme	results of extreme value statistics:
areal	← KOSTRA, PEN (with regard to precipitation)
values	← REWANUS (with regard to precipitation supply)
probable	results of estimation procedures:
maximum	← MGN (with regard to precipitation, duration: hours, area ≤ 1,000 km²)
areal	← NIEFLUD (with regard to precipitation, duration: days, area > 1,000 km²)
values	← MAGWANUS (with regard to precipitation supply, duration: days)

Fig. 1 Ways to get notable, extreme and probable maximum areal values of precipitation depth and precipitation supply

The importance of precipitation supply is demonstrated with an example of a hydrological winter half year in Fig. 2. Precipitation depths result from measurements both of liquid as well as solid precipitation (Fig. 2b). Stored in the snow cover (Fig. 2a), the precipitation does not immediately have to turn into runoff. The values of the precipitation supply in fact give the hydrologically effective contribution decisive for the formation of the runoff (Fig. 2c). In spite of precipitation there is practically no precipitation supply in January and February. In March and April there are notable values of precipitation supply generated from meltwater release plus rain. In November the notable values of precipitation supply result mainly from the notable values of rain.

EXTREME VALUE STATISTICS

A statistical evaluation of the extreme values of heavy rainfall is made following the selection of annual or partial series and is adjusted through mathematical distribution functions (WMO 1981). Such evaluation permits the computation of the statistical mean of the heavy precipitation depths to be expected as a function of the duration (minutes to days) and the return period (annuality). No certain pronouncement can be made for return periods (in years) more than three times the number of measured years. For this a 30-year series of precipitation depths must be available to determine a return period of almost one hundred years. The heavy rainfall point statistics gleaned from a station are valid in the case of long-duration precipitation for areas of approximately 20 km² around the station.

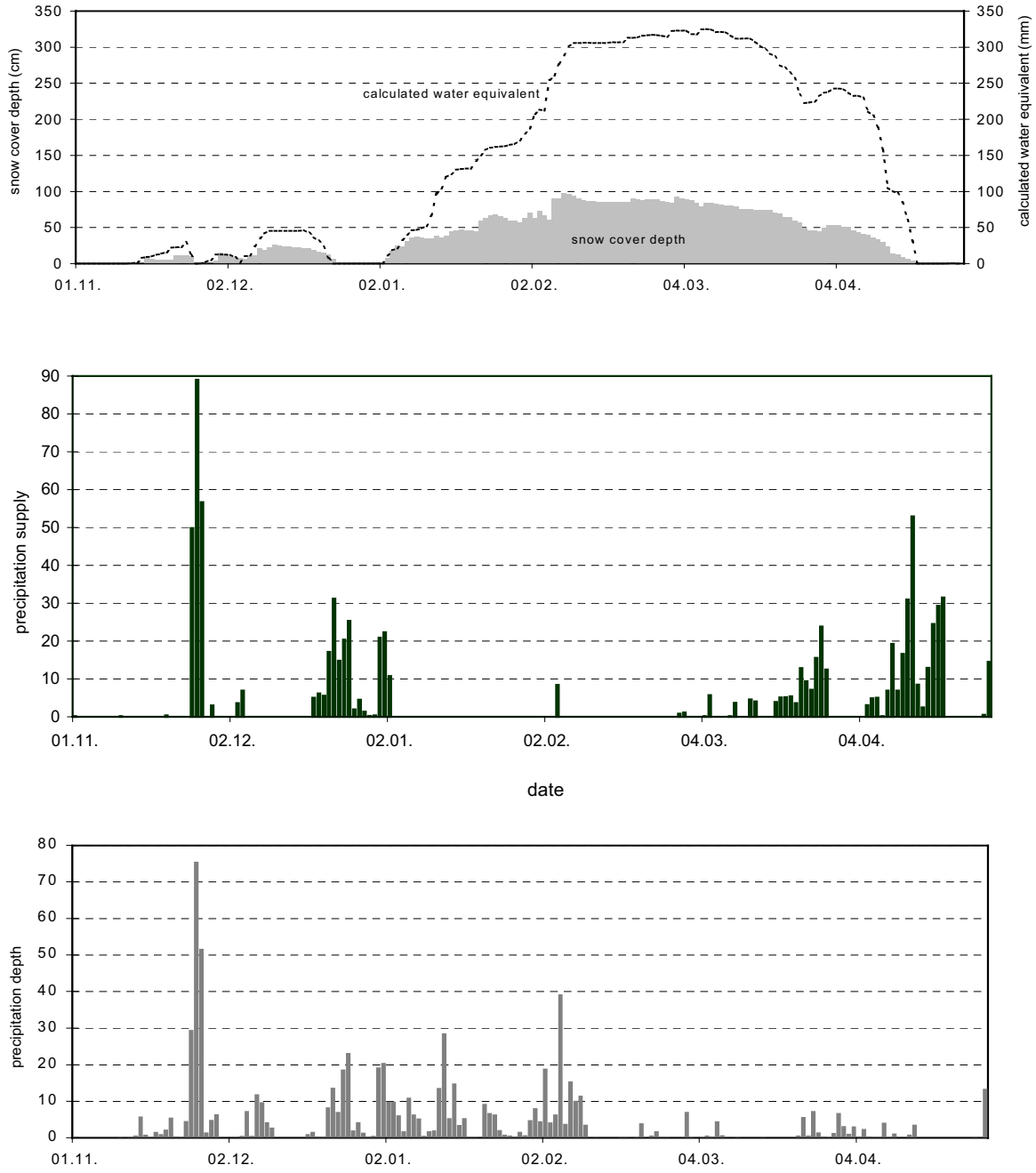

Fig. 2 a, b, c Example for the importance of precipitation supply (in mm)

The extreme values statistics statement starts for every duration D (precipitation duration including interruptions) of a partial or annual series which is determined from a series of registered or measured precipitation depths (Fig. 3). Each series of heavy precipitation depths hN(D;T) is adjusted to the theoretical distribution function by a regression calculation, where T is the return period (annuality) (DVWK 1985). The distribution function is represented as straight line on squared paper with hN(D;T) on the y-axis and ln T on the x-axis. The parameter u(D) is the ordinate section for ln T = 0 and the parameter w(D) gives the gradient of the straight line. In order to obtain clear precipitation depths over all durations, a double logarithmic compensation of the parameters u(D) and w(D) in duration range I (5 minutes to 60 minutes) and duration range II (60 minutes to 12 hours) was carried out. The aim of co-ordinated heavy rainfall regionalisation in Germany (project KOSTRA) was not only to process heavy rainfall point statistics, but also to represent the spatial distribution of heavy

rainfall depths for selected durations (between 5 minutes and 72 hours) and relevant return periods (between once a year and once in 100 years) on maps with adequate spatial resolution for the durations and return periods (DWD 1990, 1997).

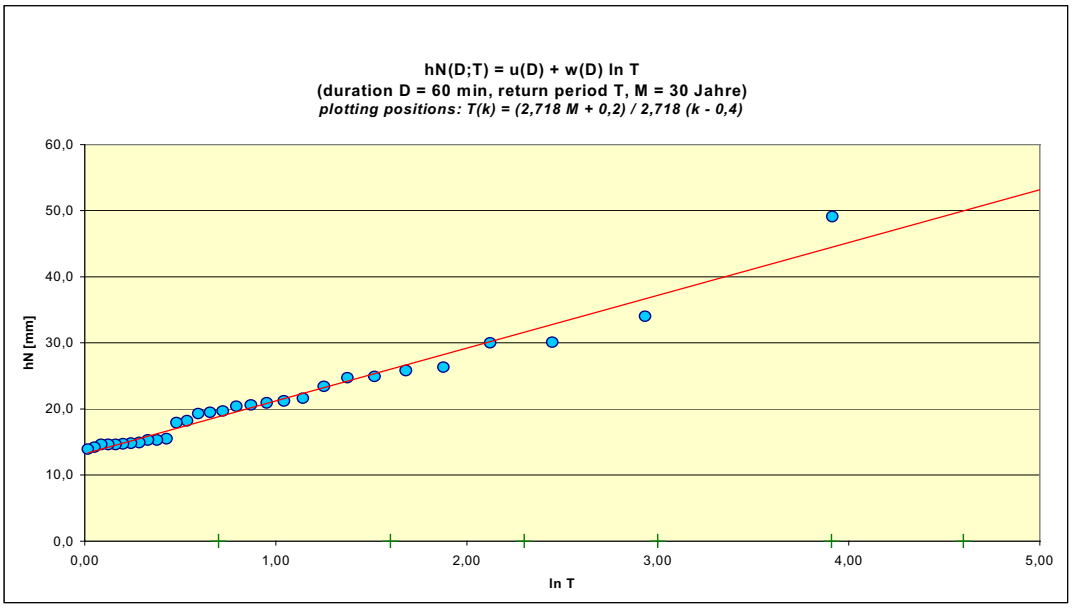

Fig. 3 Example of partial series from the plotting positions of heavy point precipitation depths registered at a station

Building on these point evaluations, a regionalisation of heavy rainfalls covering the area was made with the aid of a complex regionalisation method which especially contains the orographically modified variogram analysis.

For all regionalisation methods, the various error influences (uncertainties) must first be weighed against each other in order to arrive at a given maximum possible spatial resolution with a certain confidence interval on the basis of the density and distribution of the stations as well as the evaluation period and the computational method. Purely computational methods to transfer the point results to the areas can normally only deliver a very rough spatial distribution because in this case significant influences through the weather situation with differently operating precipitation mechanisms and orography with windward and lee-side effects remain ignored. Without such additional information, the station results are valid only in a relatively small area around the station. The results of regionalisation are recorded in grid representations with a resolution of 8.45 km by 8.45 km per grid field (Fig. 4). In this way, the KOSTRA values of the heavy precipitation depths are obtained even for locations without precipitation measurement series.

In hydrological practice, however, a relationship must be established between the precipitation depths from the point determinations of heavy rainfall statistics and the runoff from the river basin. Consequently, in this case too, the areal precipitation must be known. In order to take that areal effect into account, many depth-area-duration relationships of the precipitation were developed in the form of areal reduction curves. In this context, the factor by which the amount of the statistically determined point precipitation of a given duration and return period is to be multiplied in order to obtain the areal precipitation depth for a given area for the same duration and return period is designated as reduction factor. As some investigations show, for certain regions characteristic reduction factors exist which vary mainly only in relation to the size of the area and the duration of the precipitation. Short precipitation durations are related to small areas and precipitation of long duration to large river basins. Accordingly, the reduction factor mostly has a value of around 0.9 to 1.0.

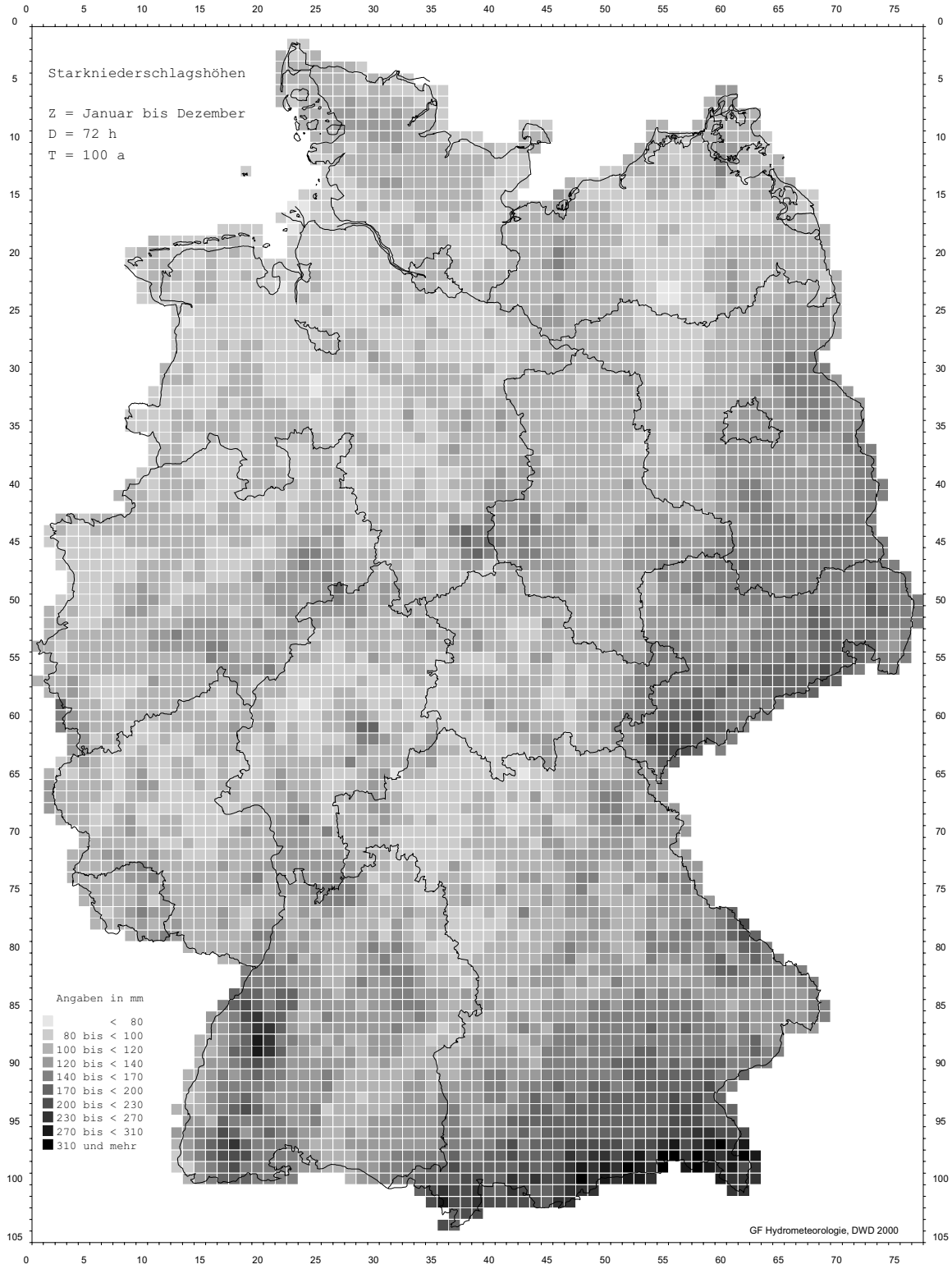

Fig. 4 Heavy precipitation depths in Germany (KOSTRA values)
Duration: 72 hours
Return period: 100 years
January – December

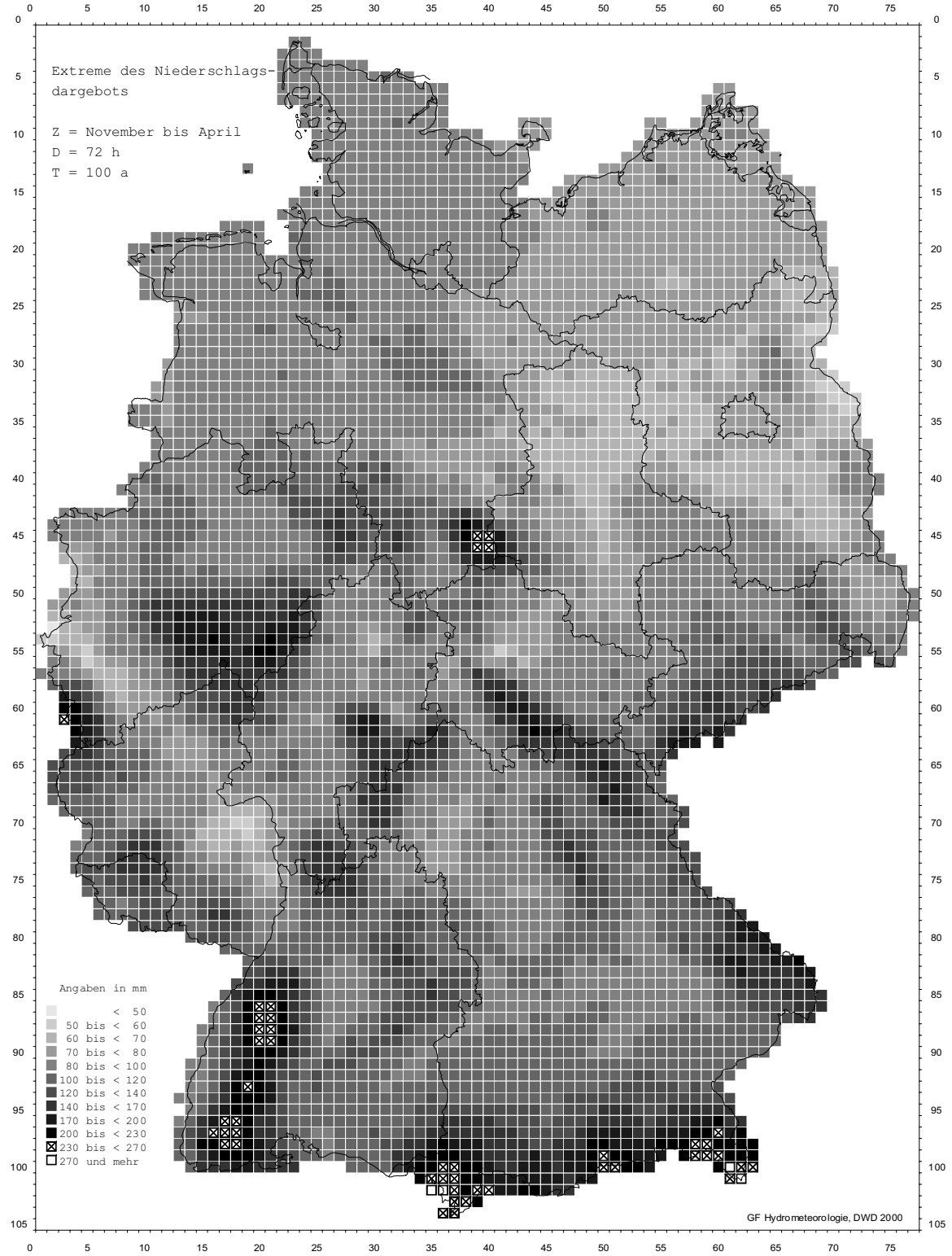

Fig. 5 Extreme values of precipitation supply (REWANUS values)
Duration: 72 hours
Return period: 100 years
November – April

Precipitation depths are obtained from measurements; values of precipitation supply are found with the aid of models. The snow cover model SNOW-K enables the daily calculation of meltwater release out of the snow cover, taking into account the liquid precipitation, by continuous simulation of the development of the snow cover (RACHNER et al. 1997). The optimisation of the model parameters and the verification of the derived results are obtained, relative to the location, by means of all available measured values of the water equivalent of the snow cover. The daily values of the precipitation supply arrived at in this way are subjected to an extreme value statistical analysis (project REWANUS) with the support of the KOSTRA investigations.

Regionalisation is obtained dependent on station-related point results. Mean winter precipitation plays an important role in this regionalisation procedure. Regional climatological influencing factors in the river basins of Germany were taken into account with very well confirmed regression relationships. On the basis of these regressions, the regionalisation of station-related extreme values, calculated for all climate and precipitation stations, was obtained by distance-dependent interpolation on the middle point of the grid areas (resolution of 8.45 km by 8.45 km per grid field). As a result of the REWANUS investigations, grid-oriented extreme values of the precipitation supply in the hydrological winter half year for durations of D = 0.5 d to D = 10 d are available with a blanked coverage in the form of regionalised cartological representations (Fig. 5).

The KOSTRA heavy precipitation depths for the winter time period are based on measurements both of liquid as well as solid precipitation, whereby the precipitation fallen as snow is liquefied before the precipitation depth (in mm) is determined. Stored in the snow cover, the precipitation does not immediately have to turn into runoff, or not completely. On the contrary, the values of the precipitation supply in fact give the hydrologically effective contribution decisive for the formation of the runoff. Therefore the REWANUS values, the information about the occurrence probability of extreme values of the precipitation supply, are of great significance, above all in the snow-hydrologically relevant regions. This is especially true of areas in medium and high sites in the mountains (> 400 m).

ESTIMATING PROCEDURES

Heavy rainfall statistics allow, given the normally available time period of about 30 years, conclusions for return periods of up to 100 years. Flood structures which are meant to be built with greater safety, cannot be based on these statistics. The Probable Maximum Precipitation (PMP) was therefore defined conceptually as the theoretically greatest precipitation depth of a given duration for a specified catchment area at a specified season which is physically possible (without regard to climate changes). This definition represents the upper limit of a possible heavy precipitation event (WMO 1986).

In effect there are several possibilities for quantifying the PMP. With the maximisation, an empirical path was taken by the Deutscher Wetterdienst to investigate the probable maximum precipitation depths in Germany. In order to be able to estimate PMP, knowledge of the meteorological values and processes which impose a limit on precipitation depth is necessary. Of course the water vapour content of the air plays an important part. Multiplying the precipitation depth measured in an extreme heavy precipitation event by the maximising factor gives the maximised precipitation depth. The maximising factor is the relation – depending on the region and the season – of the theoretically greatest water vapour content of the atmosphere to the water vapour content which is available over a specific area during an observed extreme heavy precipitation event of a certain duration. By adopting an optimal degree of effect of the precipitation process, this maximising factor already implicitly contains the appropriate wind influence.

Within the project MGN, the large number of computationally evaluated probable maximum regional precipitation depths for selected regions was regionalised, i.e. transferred to the other regions of Germany, and represented in maps of the maximised areal precipitation depths for durations from D = 1 h to D = 72 h (DVWK 1997). The main focus was on relatively short precipitation durations of less than a day and relatively small regional areas. In the follow-up project NIEFLUD above all the probable maximum areal precipitation depths were processed for heavy rainfalls of several days´ duration and covering a wide area (> 1,000 km²) in Germany's river basins.

The precipitation database did not have to be restricted to the approximately 200 stations recording precipitation during the day and having high time resolution of around 30 year precipitation time series. Data could be obtained from the around 4,500 stations measuring precipitation once a day and having a longer observation period. The high spatial density of these stations permitted the areal precipitation depths for Germany's river basins to be calculated directly from the measured point precipitation depths. Therefore the use of precipitation-duration-area relationships as well as the execution of regionalisation were dispensable for the quantification of the probable maximum areal values of precipitation.

The maximisation procedure in the project NIEFLUD consists of three steps demonstrated in Table 1 and Fig. 6:

- In the first step, the maximum multiple of extreme areal precipitation depths (MxPrec) for given river basin, duration and season is marked off in the special form (Table 1).
- In the second step, unrealistic differences between the marked maximum MxPrec values of all durations (columns in Fig. 6) are evened out by logarithmic smoothing – for each river basin of interest. It is worth mentioning that the marked maximum MxPrec values are derived from extreme precipitation depths in summer, autumn or spring.
- In the third step, in order to be on the safe side, a supplementary amount depending on the length of the time series has to be taken into account – the longer the time series the smaller the supplement. In the project NIEFLUD, the length of the time series is more than 50 years. Therefore a supplement of 30 mm is sufficient. In this way the last step results in probable maximum areal precipitation depths in terms of duration in a specific river basin (dots in Fig. 6).

Table 1 Special form for marking off the maximum multiple of extreme areal precipitation depths for given river basin, duration and season

River basin: Upper Elbe (4,259 km²)
Dew point station: Wahnsdorf 51°12'N 13°68'E (246 m above sea-level)
Period of time: January 1931 to December 1998
68 years (24837 days)

Season: summer

Duration: 5 days

maximum persisting 12-h 1000-hPa dew point: Td_12h = 20.9°C
maximum atmospheric water vapour content: MaxWc = 52.6 mm

representative 1000-hPa dew point for the precipitation event: Td_Rpr
water vapour content estimated for the precipitation event: Wc

extreme areal precipitation depth: Prec
multiple of extreme precipitation depth: MxPrec

Factor = MaxWc/Wc MxPrec = Factor · Prec

Rank	Date	Prec[mm]	Td_Rpr[°C]	Wc[mm]	Factor	MxPrec[mm]
1	1954/07/11	159.6	12.9	28.2	1.9	298.1
2	1983/08/05	154.8	12.5	27.2	1.9	299.5
3	1937/07/14	152.9	11.6	24.8	2.1	**324.9**
4	1937/07/13	149.8	11.5	24.6	2.1	320.8
5	1937/07/12	148.5	11.5	24.5	2.1	318.7
6	1937/07/15	147.3	11.6	24.8	2.1	312.0
7	1954/07/12	141.4	13.2	29.1	1.8	255.5
8	1954/07/10	138.9	12.6	27.5	1.9	265.8
9	1983/08/06	137.4	12.4	27.0	1.9	267.8
10	1978/08/11	131.6	14.6	33.0	1.6	209.5

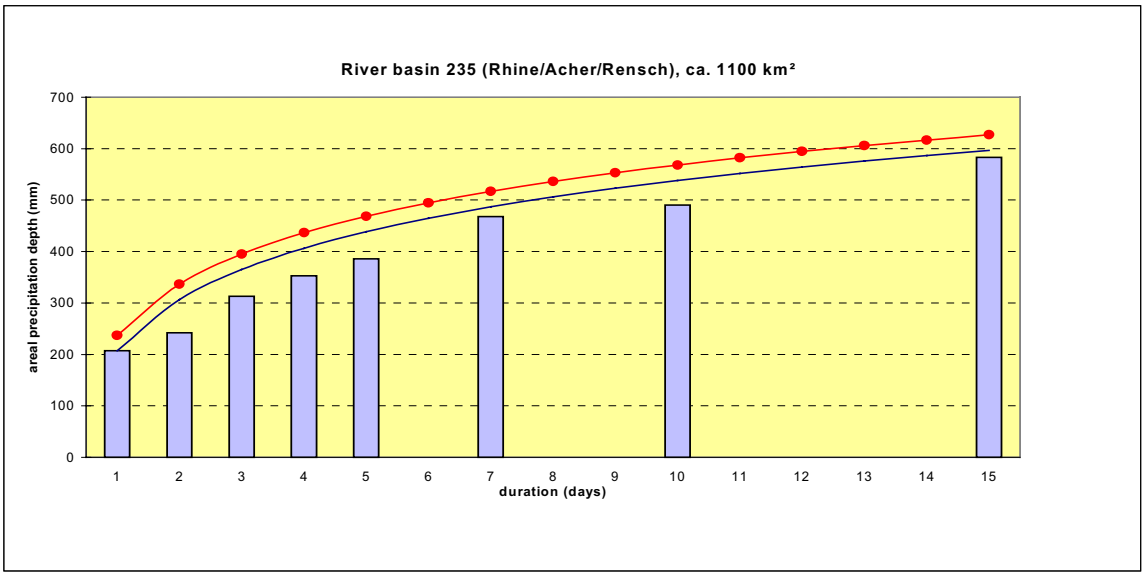

Fig. 6 Probable maximum areal precipitation (dots) after smoothing out the multiples of extreme areal precipitation depths (columns) by a logarithmic graph

Together with the notable areal precipitation depths and the date of a few precipitation events, probable maximum areal precipitation depths in terms of duration in several river basins of different area size are listed in Table 2.

Table 2 Notable and probable maximum areal precipitation depths for several river basins in Germany

river basin			notable areal precipitation [mm] with date of end			probable maximum areal precipitation [mm]		
number	rivers	km²	3 days	5 days	10 days	3 days	5 days	10 days
23	**Upper Rhine/ Neckar**	27.624	**102** 1978-05-24	**107** 1978-05-23	**135** 1998-11-01	**240**	**287**	**352**
247	**Main, Kinzig**	4.277	**107** 1982-10-08	**115** 1982-10-10	**155** 1982-10-14	**259**	**304**	**364**
235	**Rhine/Acher/ Rensch**	1.114	**170** 1978-05-24	**173** 1978-05-23	**195** 1978-05-24	**395**	**469**	**568**

Individual investigations using maximisation calculations for a few stations have also been carried out by other authors. Although these investigations were also carried out very meticulously, they always hold the danger that – because of the small number of stations and the comparably short length of the precipitation supply series as well as the sometimes unrepresentative investigation period – the values calculated are by a long way not the probable maximum precipitation depths in those specific regions (HAUCK 1983). As opposed to this, all individual results were evaluated in a temporal and spatial context at every step in both maximisation projects of Deutscher Wetterdienst in the search for the probable maximum areal precipitation depths in Germany.

The procedures for the evaluation of PMP cannot be standardised. There is also no objective procedure to permit sure statements about the accuracy of the PMP estimates. Nevertheless, comments about accuracy can be made. In relation to this, the following factors are especially to be taken into account (WMO 1986):

- exceedance of the estimated PMP over the maximum observed precipitation depths for the surrounding climatologically homogeneous region,

- number and severity of the available recorded precipitation events in the region in question for the longest possible time series,
- number, character and interrelationship of the maximising steps,
- reliability of the model used in relation to the precipitation description and other meteorological variables,
- probability of the individual meteorological variables used in the model being excessive in relation to the occurrence of very rare events.

The resulting very high precipitation depths, according to the definition of the PMP, are therefore not directly used in dimensioning hydrological structures. The safety elements designed into barrages approach these values in their calculations. In this way the use and the potential danger of the installation in the case of failure are weighed up against each other. Also taken into consideration is an estimation of the construction methods as well as the necessary building and running costs for a specified construction in a specified region. An optimisation of these various needs, however, can only be arrived at through close co-operation among meteorologists, hydrologists and engineers. Parallel to this, relevant extreme values of precipitation in Germany are processed for subsequent use in hydrological practice. In addition - depending on the duration - the area between the KOSTRA heavy precipitation depths of the 100 year return period and the PMP is to be sounded out by the project PEN.

OUTLOOK

In an hydrological regime, the flood characteristics can change quite dramatically even without changes in the variability of precipitation but with changes in the variability of precipitation supply.
Given the normally available time period of about 30 years, statistical REWANUS investigations of extreme precipitation supply allow conclusions for return periods of up to 100 years. At present there is no imagination of probable maximum values of precipitation supply. Following the definition of PMP, the probable maximum precipitation supply is the theoretically greatest precipitation supply of a given duration for a specified river basin which is physically possible. In the planned project MAGWANUS probable maximum values of precipitation supply of 0.5 up to 10 days´ duration are to be quantified for areas which are in potential danger of combined rain/melt floodings.
Finished, current and planned projects focused on extreme and probable maximum areal values of precipitation depth and precipitation supply in large river basins are symbolised in Fig. 7. The sign * stands for the fact that some of these projects yield point values of precipitation depth and precipitation supply.

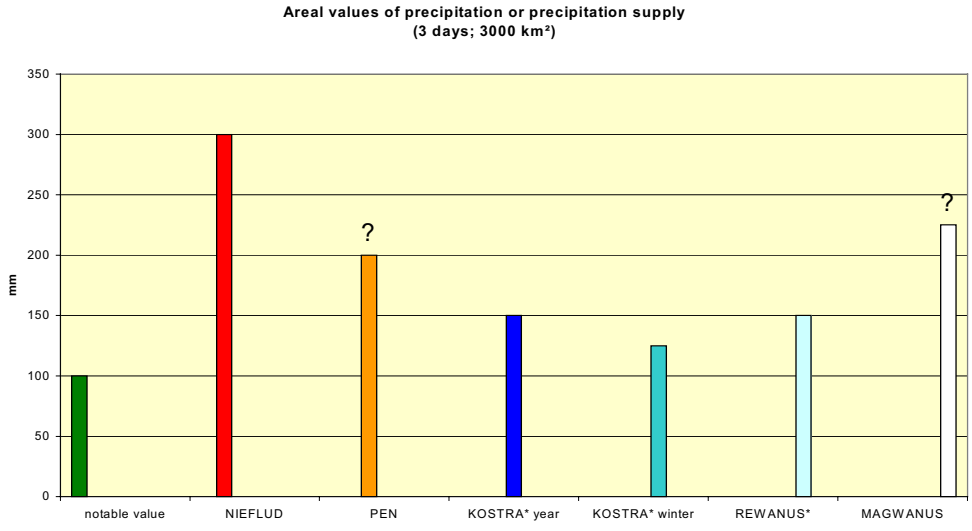

Fig. 7 Finished, current and planned projects focused on extreme and probable maximum areal values of precipitation depth and precipitation supply.

Anyway the columns of projects in Fig. 7 serve as examples for quantifying the values of precipitation depth and precipitation supply.

REFERENCES

DWD (1990) Starkniederschlagshöhen für die Bundesrepublik Deutschland, Offenbach a. M.

DWD (1997) Starkniederschlagshöhen für Deutschland (KOSTRA-Atlas), Offenbach a. M.

DVWK (1985) Niederschlag – Starkregenauswertung nach Wiederkehrzeit und Dauer, DVWK-Regeln zur Wasserwirtschaft 124, Hamburg und Berlin.

DVWK (1997) Maximierte Gebietsniederschlagshöhen für Deutschland, DVWK-Mitteilungen 29, Bonn.

Hauck, E. (1983) Beiträge zur Wahl des Bemessungshochwassers und zum vermutlich größten Niederschlag, DVWK-Schriften 62, Berlin und Hamburg.

Rachner, M., H. Matthäus, G. Schneider (1997) "Echtzeitvorhersage der Schneedeckenentwicklung und der Wasserabgabe aus der Schneedecke, Erste Ergebnisse aus dem Projekt SNOW-D", DWD-GF HM in "Deutsche Gewässerkundliche Mitteilungen" (DGM), Heft 3, 1997, S. 98-106.

WMO (1981) Selection of Distribution Types for Extremes of Precipitation. WMO-No. 560, Geneva.

WMO (1986) Manual for Estimation of Probable Maximum Precipitation, Operational Hydrology 332, Report No. 1, Second Edition, Geneva.

Dr. G. Malitz
Deutscher Wetterdienst (DWD)
Geschäftsfeld Hydrometeorologie
Referat HM 2
Lindenberger Weg 24
D- 13125 Berlin

gabriele.malitz@dwd.de

Generation of hydrometeorological reference conditions for the assessment of flood hazard in large river basins (Proceedings of International Workshop, Koblenz, 6. and 7. March 2001).
CHR-Report No. I-20

Spatial and temporal patterns of precipitation fields of extreme events in Switzerland and concepts for precipitation scenarios

Dietmar Grebner
Institute for Atmospheric and Climate Sciences ETH
Zürich, Switzerland

Abstract Generalized and individuel analyses of precipitation fields were carried out for the area of Switzerland. Generalized means depth-area relationships for non calendaric durations of precipitation ranging from 3 to 72 hours. An important property of the relationships is that they were derived through storm centred areal integration of the precipitation. The analyses have been done separately for the parts of Switzerland on the north, inside and south of the Alps, according to influences of the mountains. The storm centred generated relationships involve the disadvantage that they are only conditionally applicable to individual hydrologic watersheds. However the advantages are, that the relationships give information about the precipitation power of the atmosphere over a particular size of area within the analysed duration intervals during the observed most intensive events of the record period. Further, they are basic to PMP estimations and, together with the findings from the analyses of the individual events of heavy precipitation, they can be used for precipitation scenarios.

For cyclonic caused heavy precipitation events on the south and inside the Alps, only some few circulation types of the atmosphere are suitable. They produce typical precipitation distributions in space and time. North of the Alps, the spectrum of potential circulation conditions for heavy cyclonic precipitation is larger. Accordingly, the patterns of spatial precipitation distribution and also the boundary conditions for the scenarios are more numerous. Concerning convective events, the 3 zones distinguish only through the precipitation intensities, but not through different circulation patterns and distribution chracteristics.

INTRODUCTION

Precipitation is the result of the combination of several hydro-thermodynamic process components. The contribution of each of them is limited through the energetic conditions of the climate in a region. The precipitation power of an event depends on how much of these components are how close to their optimum contribution. The higher the combined degree the more intensive and infrequent is an event.

For rainfall runoff purposes, the process components can be grouped into (i) the hydro-thermodynamic conditions within the atmosphere, (ii) the migration of this system related to the earth surface, and (iii) the influence of the orography on the precipitation generation of the system. The hydro-thermodynamic conditions define the precipitation type (through convective lifting or cyclonic ascent of the air), the horizontal extent of precipitation generation, the course of the precipitation intensity, and the spatial distribution of precipitation within a time interval. The thermal properties of a system limit the water vapour content in the air and control the altitude of the snowfall line in space and time as well as the contribution of snowmelt water to the runoff in case of a snow cover. Due to the migration of a precipitation system, the precipitation generated in the atmosphere per unit area will be spread over a larger ground area. For a stationary system, therefore, the observed precipitation amounts represent approximately the precipitation power of the system. Regarding the runoff

concentration in a catchment, however, a specific migration of the precipitation system may be more efficient than the local maximum amounts in the case of stationarity of the system. In any case, the runoff concentration in a catchment is sensitive to both, the position of the centre of the precipitation field and the temporal course of intensity. The orography can have an intensifying or reducing effect on the generation and deposition of precipitation, depending on the scale considered and on the location of the precipitation system relative to the orography.

DEPTH-AREA-DURATION RELATIONSHIPS

The precipitation amount within a specific duration, averaged over a defined area decreases with increasing size of the area. The reliability of the detectable decrease depends on the density of the gauging network. The densest precipitation gauging network in the analysed region consists of daily observing stations. To find the important areal precipitation events for specific durations in the data records, a temporal resolution of the records is required which is clearly higher than the duration in question. An additional available network of automatic stations yield high resolved registrations. However, the density of this network is substantially smaller and more irregular than of the daily observing stations. For the analyses of the precipitation fields, therefore, the daily observations were subdivided in calendaric hourly time steps by means of the automatic stations. That way, the daily gauging network could be used for the analysis of the areal precipitation for quasi-noncalendaric durations down to 3 hours (Fig. 1)

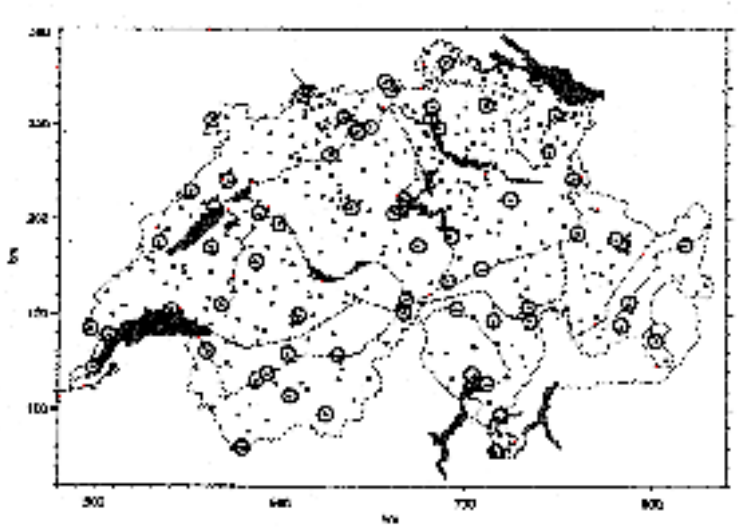

Fig. 1 Used precipitation gauging network. Dots: daily observing stations; encircled dots: automatic stations.

The data series of the automatic stations were available for the years 1981 to 1993 and limited the analysis to these 13 years. The areal precipitation properties of 8 duration intervals between 3 and 72 hours were investigated. Because of the orographic segmentation of Switzerland and the corresponding different climatic boundary conditions for precipitation systems, the area was subdivided into 8 zones (Fig. 2). For each of them, the depth-area-duration characteristics were derived.

The selected precipitation fields were interpolated on a 2x2 km2 grid and storm centred integrated. The considered areal precipitation and the resulting DAD relationships are, therefore, basically not restricted to individual hydrologic catchments, except if the watersheds are formed by the main alpine crests. The latter applies for the two inner Alpine zones, the Rhone above the Lake of Geneva (Wallis, Zone 4/5) and the Swiss section of the Inn basin (Engadin, Zone 8), respectively (Fig. 2). Both are approximately identical with the hydrological catchments. Through the storm centred integration, the areal precipitation represents the precipitation power of the atmosphere for each area size and duration interval.

In each zone and for each duration interval, the depth-area-duration relationships were derived for the 26 most important events. An envelope curve was fitted to each of these families of curves, and frequency analyses were performed (Ihringer, 1992). The envelope curves represent for each area the largest observed precipitation in the record period and the statistical depletion curves (Figs. 3-5) indicate the areal precipitation of specific return periods. The shapes of these curves, however, are not the depletion course of events.

For the curve branches over areas larger than 400 km2 in each zone, the DAD curves of cyclonically caused precipitation systems show for different durations of course different amounts of areal precipitation, but the depletion of the curves are very similar (Figs. 3 a, b) Between the zones, however, the depletions are differing more, in particular comparing the three main areas, on the north, inside and on the south of the Alps (Figs. 3 b, 4 and 5). The steep depletion up to large areas of the southern Zones 6 and 7 is mainly caused through the limitation of the precipitation fields by the national border. Italian data series were not obtainable. Nevertheless, the derived DAD relationships are representative for the area concerned because the locations of the fields of heavy events are hardly different (Figs. 6 and 7 b, c).

Further, on the north, an increasing frequency of strong cyclonic precipitation is to find from west to east (Zone 1 to Zone 3). This increase coincides with the zonal gradient of point precipitation (e.g. Zeller et al., 1976-1992). The higher number of heavy events in Zone 3 is partly caused through precipitation fields which are centred on the south of the Alps but extend across the mountain range and affect considerably also the northern Zone 3, as is still explained later on (Fig. 6 a).

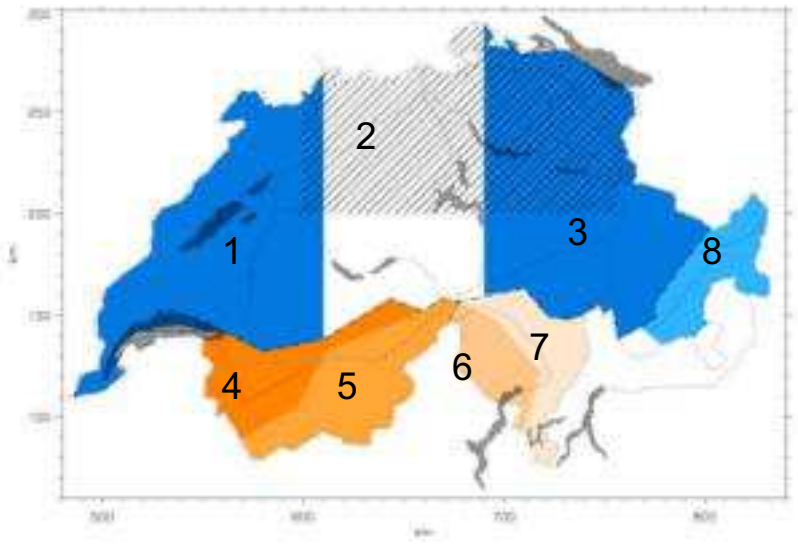

Fig. 2 Subdivision of the investigated area in 8 zones for taking into account the varying climatologic boundary conditions for the precipitation systems.

Through the air mass properties on the south of the Alps differing decisively from the north, high precipitation amounts and systematically large spatial differences of precipitation amounts occur. For the short distance from Zone 6 to the adjacent Zone 7, the areal precipitation amounts of the DAD differ by a factor close to 2 (Figs. 5 a, b and Figs. 7 a-c).

The inner-Alpine areas are partly shielded through the orography against the northern as well as against the southern precipitation systems. The intensity of the precipitation systems get reduced. The orography defines also the sectors of the wind directions from which the individual basins are exposed to intensive precipitation systems. Therefore, the location and the pattern of the precipitation fields in inner Alpine basins are controlled through the orography.

a

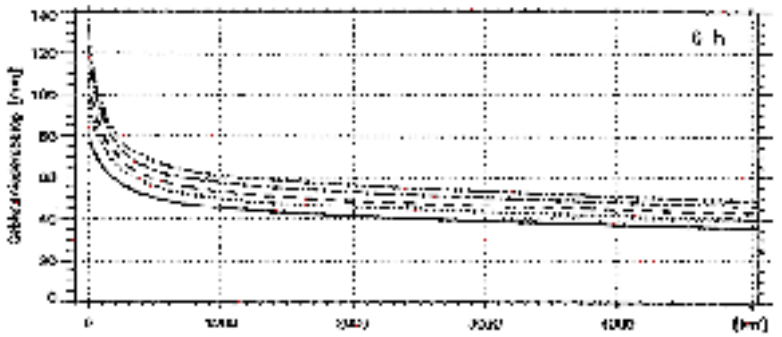

b

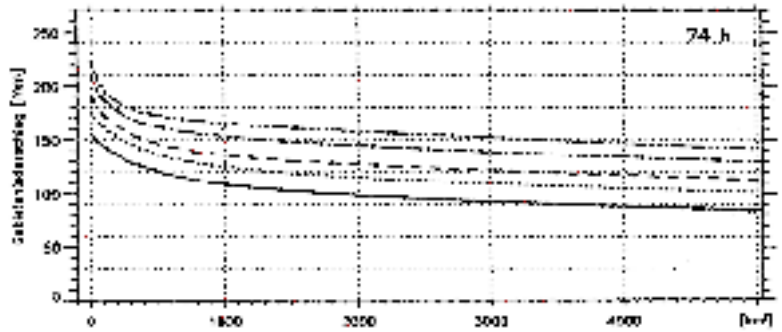

Fig. 3 Absolute depth-area relationships of the north-Alpine Zone 3 for the two durations 6 and 24 hours. The families of curves represent different return periods ranging from 2 years (bottom) up to 50 years (top).

The Rhone catchment above the Lake of Geneva is affected by precipitation systems of climatically different origin. The lower half of the basin is exposed to Atlantic conditioned properties of the atmosphere. The upper half and a strip along the southern mountain crest of the basin are covered by Mediterranean precipitation systems at the southern slope of the Alps (Fig. 6 b and 7 b-d). In the upper part (Fig. 4 b), therefore, the precipitation amounts over areas up to 1500 km2 are significant larger than in the lower part of the basin (Fig. 4 a). The respective precipitation patterns in each of the two areas are strongly controlled through the air stream direction and are approximately congruent in similar cases (Fig. 7). Therefore, each of the two types can be generalised through averaging the individual precipitation fields and transforming into percentage isopleths.

Like the Rhone basin, also the Swiss part of the Inn catchment (Engadin, Zone 8) is mainly affected from the south (Figs. 7 b and c). However, the precipitation power of heavy events, their frequency and durations are less than in the Rhone basin.

a

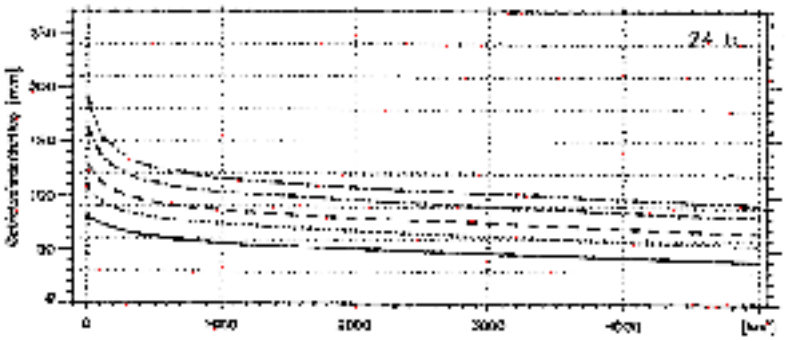

(continued p. 25)

b

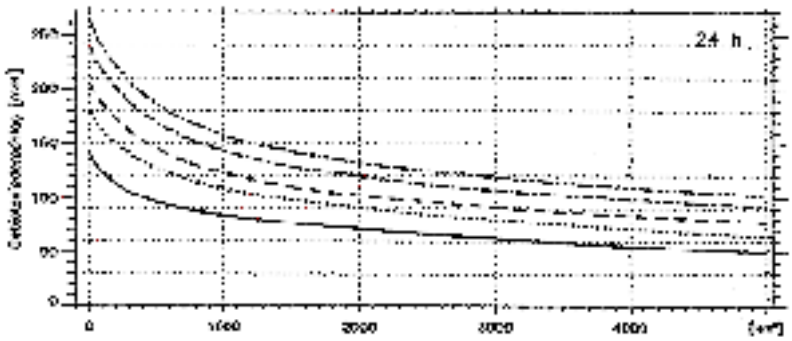

Fig. 4 As Figure 3, but showing the relationships of the inner Alpine area Wallis for 24 hours. a) Lower portion of the basin (Zone 4); b) upper portion (Zone 5).

a

b

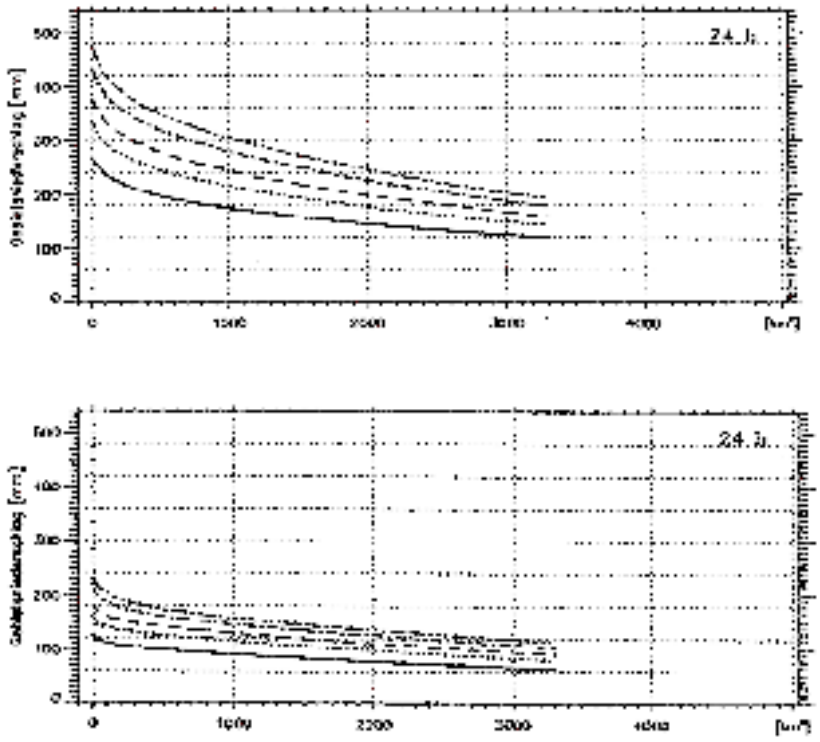

Fig. 5 As Figure 3, but showing the relationships of the area on the south of the Alps for 24 hours. a) Western part of the area (Zone 6); b) eastern part (Zone 7).

ANALYSES OF EVENTS

The DAD relationships represent precipitation amounts averaged over a specific area and a specific time interval. However, the runoff reacts also on the course of precipitation in time and space. Such informations as well as how far the precipitation patterns are controlled by the atmospheric dynamic or by the orography can be found through analyses of individual events.

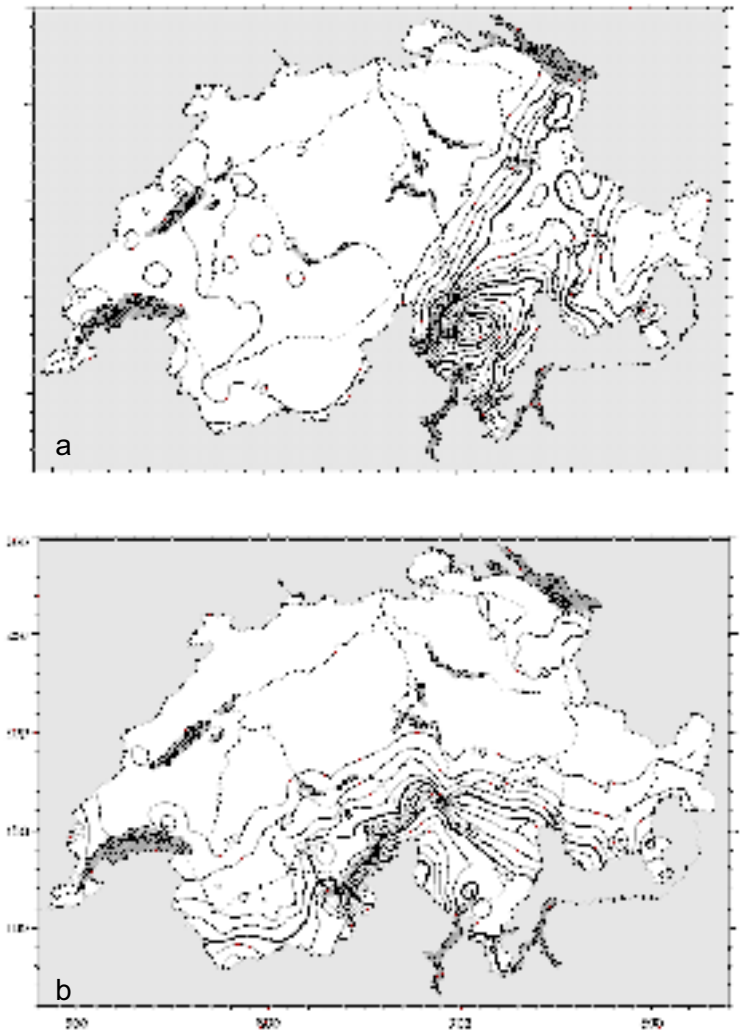

Fig. 6 Two examples of precipitation fields generated and centred on the south of the Alps. The equidistances of the isohyets are 10 mm up to 100 mm/d and 20 mm for larger amounts. a) Precipitation generation across the mountain range; one day amounts of 17. July 1987. b) Covering the south and inner Alpine areas, maximum amounts for 24 hours (24. September 1993) during the "Brig-event".

The meteorological contribution to the generation of floods consists of the two phases, the course of the weather conditions during the antecedent period and the conditions during the main phase of an event. The relevant length of the antecedent period may cover several months. After a marked development of the antecedent period, even a moderate rain event is able to cause an important flood, as showed a specific example in northern Alpine Switzerland in May 1999 (Grebner und Roesch, 1999; BWG, 2000). At that time, the antecedent period to be considered goes back to an extraordinary snowfall period in February, followed by repeated rain periods, in particular in April. In the beginning of May, a strong snowmelt loaded the discharge along the mountain edge. At the same time, the whole area was affected by two succeeding rain phases, centred in the wet pre-Alpine area, causing extended floods though the return periods of the areal precipitation did not exceed 50 years in any duration interval. Due to the two adjacent effects, snowmelt and rainfall, most of the northern Alpine area of Switzerland was affected by floods.

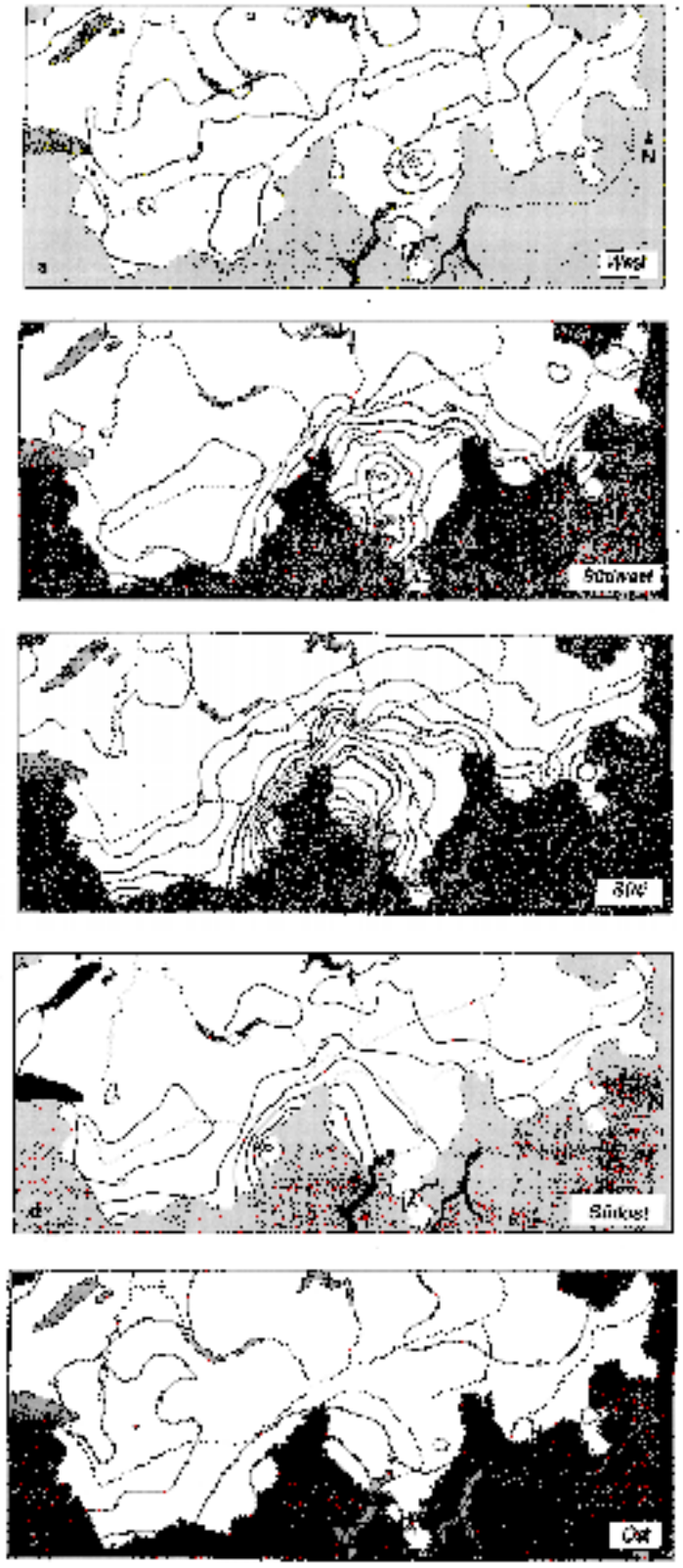

Fig. 7 Averaged spatial precipitation distributions of one day amounts occurring with specific wind directions: a) west (12 events), b) south-west (53 events), c) south (20 events), d) south-east (18 events), e) east (24 events).

The development of a flood requires a sufficient altitude of the snowfall line. In the area of Switzerland, all observed cyclonically caused heavy precipitation are possible or are even favoured under such a warm condition. An intensification of the runoff concentration usually arises, if the rainfall intensity increases during an event. This increase can be caused through the thermodynamic

property of a precipitation system or through its migration. On the north of the Alps, the former causes an increase of the intensity usually in the first half of an event. Due to the migration, the precipitation intensity may get stronger nearly up to the end of an event. But in both cases, the intensities remain in the range of cyclonic activities up to some 15 mm/h. Whereas on the south of the Alps and in the inner-Alpine Zones along the mountain crest, being affected from the south, convective like precipitation intensities of more than 50 mm/h are possible even still at the end of a long lasting cyclonic precipitation event.

The precipitation duration of individual intensive cyclonic systems over an area is usually less than 3 days. On the northern edge of the Alps, however, the duration can get few days longer in cases when fronts become stationary along the mountain range. Long periods of precipitation up to more than 30 days are possible in the case of specific conditions of the pressure pattern of the planetary scale, which controls cyclonic precipitation systems. Series of precipitation systems may be steered over an area or catchment in a succession of usually 1 to 2 days. Weather situations like that constitute a high risk for floods particularly in large river catchments. Corresponding examples are the floods of: Mississippi, July 1993; Lago Maggiore, September/October 1993; Rhein, December 1993 and January, 1995, and in the Oder catchment, July 1997 as well.

On the south of the Alps, an approximately stationary planetary trough over Western Europe caused an air stream from the south against the Alps during 8 days, in October 2000. The resulting rainfall generated big floods in the Lago Maggiore and later on down stream in the entire Po catchment (Grebner et al., 2000). Comparable air stream conditions on the north of the Alps proved to be of minor importance.

The importance of the antecedent period changes with increasing duration of precipitation episodes. For the increase of the precipitation amount with the altitude, individual precipitation events do not show a systematic correlation, neither on the north, nor on the south of the Alps. Vertical interpolations has to be performed with gradients determined for each event and for each local condition. In inner-Alpine basins or leeward of a narrow mountain ridge, however, a vertical increase of precipitation amount usually occur not only in the average but also during individual events due to a spreading of precipitation from the windward side (Fig. 6 b and 7 b-d).

As described above, a heavy to extreme precipitation power require a corresponding favourable combination of the contributing process components. Therefore, the number of different appropriate circulation conditions in the atmosphere is limited. The analysis of cyclonic events generating heavy precipitation in Switzerland shows that, on the north of the Alps, several circulation patterns can meet the requirements (Grebner et al., 1998). In addition to the northern circulation types, the north-eastern portion of the country can also be covered from precipitation systems whose circulation centre is located on the south of the Alps (Fig. 6 a). This type is an important reason for the higher frequency of heavy precipitation in the eastern zone north of the Alps (Zone 3) compared with Zones 2 and 1. The contribution of the orography through the barrier effect directly to the precipitation generation proved secondary for the analysed extreme events north of the Alps, .

On the south of the Alps, heavy cyclonic precipitation are, in contrast to the north, confined to one circulation pattern only, consisting of a cyclone or low pressure trough located to the west or south-west of Switzerland with a southern wind direction over the Mediterranean Sea against the Alps. For the high precipitation amounts, as known for this area, the water vapour content of the advected air as well as its stratification of both, the temperature and the wind speed, are responsible.

The thermal stratification is usually conditioned unstable. This instability can be released through the ascend of the air at the mountain slope and explains the strong convection like variability of the precipitation intensities with peaks exceeding 50 mm/h even at the end of a long lasting cyclonic event. The instability explains as well the strong gradients of areal precipitation between the two Zones 6 and 7 (Fig. 5) and it explains the typical field patterns of precipitation south of the Alps and in the inner Alpine basins (Figs. 6 b and 7 b-d). For the vertical profile of the wind speed, the intensity of heavy precipitation is correlated with the appearance of a secondary wind maximum in the layer below 2000 m a.s.l. (Buzzi et al. 1995; Buzzi and Tartaglione, 1995) and with the location and intensity of the upper air jet.

In particular, the wind direction is also the crucial parameter for the extension of precipitation fields from the southern slope of the Alps into the inner-Alpine catchments and across the mountain range to the north of the Alps (Figs. 6 a, b). The most intensive precipitation in the Rhone basin (Wallis) arise with a south-south-east air stream (Figs. 7 c, d).

CONCEPT OF SCENARIOS

For the fields of hydrology and civil engineering, the application of scenarios serves traditionally for design purposes. Today, it is an approach as well for the regional evaluation of the water balance and runoff in the case of a changing climate.

For the practical operation so far, point precipitation for specific return periods were used. They do not allow, however, the direct derivation of areal precipitation amounts for the return period concerned. Additionally, the properties and influences of antecedent periods as well as the areal and temporal structures of the precipitation and their seasonal variations remain unknown or unconsidered.

Therefore, scenarios composed by generalised and individual observed components of the rainfall runoff process suggest themself. The depth-area-duration relationships yield areal precipitation for required return periods. The knowledge about relevant precipitation systems - such as migration, typical duration, restrictions for transposition, influences of orography, patterns and locations of the precipitation fields and possible courses of precipitation intensities - can be derived from hydrometeorological analyses of heavy or extreme events of rainfall and runoff as is briefly outlined in the preceding chapters. For sensitivity tests and reference conditions, this approach covers the entire spectrum ranging from typical up to probable maximum conditions of meteorological causes for runoff.

REFERENCES

Buzzi, A.; Tartaglione, N.; Cacciamani, C.; Paccagnella, T.; Patruno, P. (1995 a) The Piedmont flood of November 1994. MAP Newsletter Nr. 2, Swiss Meteorological Institute Zürich (2-6).

Buzzi, A. and Tartaglione, N. (1995 b) Meteorological modelling aspects of the Piedmont 1994 flood. MAP Newsletter Nr. 3, Swiss Meteorological Institute Zürich (27-28).

BWG (2000) Hochwasser 1999; Analyse der Ereignisse. Bundesamt für Wasser und Geologie, Bern. Studienbericht 10 / 2000, 148 S. mit Anhang.

Grebner, D. und Roesch, T. (1998) Flächen-Mengen-Dauer-Beziehungen von Starkniederschlägen und mögliche Niederschlagsgrenzwerte in der Schweiz. vdf Hochschulverlag ETH Zürich (189 S.).

Grebner, D.; Roesch, T. und Schwarb, M. (1998) Extreme Gebietsniederschläge unterschiedlicher Dauer und Wiederkehrperioden. In: Hydrologischer Atlas der Schweiz, Landeshydrologie, Bundesamt für Wasser und Geologie, Bern, Kartenblatt 2.5.

Grebner, D. und Roesch, T. (1999) Zusammenhänge und Beurteilung der Hochwasserperiode vom 11. bis 15. Mai 1999. Wasser, Energie, Luft, 91. Jg., Heft 5/6, 127-132.

Grebner, D.; Aschwanden, H.; Steinegger, U.; Zimmermann, M. (2000) Charakteristik des Hochwassers vom 9. bis 16. Oktober 2000 auf der Alpensüdseite und im Wallis. Wasser, Energie, Luft, 92. Jg., Heft 11/12, 369-377.

Ihringer, J. (1992) Programmpaket zur Extremwertanalyse auf DOS_PC. Entwickelt am Institut für Hydrologie und Wasserwirtschaft an der Universität Karlsruhe (IHW).

Zeller, J.; Geiger, H. und Röthlisberger, G. (1976-1992) Starkniederschläge des schweizerischen Alpen- und Alpenrandgebietes. Eidg. Forschungsanstalt für Wald, Schnee und Landschaft, Birmensdorf, Bände 1-9.

Dr. Dietmar Grebner
Institute for Atmospheric and Climate Sciences ETH
Winterthurerstr. 190
CH 8057 Zürich
email grebner@geo.umnw.ethz.ch

grebner@geo.umnw.ethz.ch

Topic 2: Estimation and classification of spatial/temporal patterns of extreme precipitation events

Generation of hydrometeorological reference conditions for the assessment of flood hazard in large river basins (Proceedings of International Workshop, Koblenz, 6. and 7. March 2001). CHR-Report No. I-20

Spatio-Temporal Structure of Precipitation during Flood Events in the Moselle Basin

Alfred Helbig
Dept. Climatology, Fac. Geography/Geosciences, Univ. of Trier
Trier, Germany

Abstract Analysis of the temporal pattern, intensity and duration of precipitation in the various parts of the Moselle catchment area can contribute to the estimation of the occurrence probability of extreme flood events. In the worst possible case a particular sequence of rainfall leads to flood crests in the Moselle and its tributaries Sauer and Saar which superpose on each other and finally join the flood crest of the Rhine at the confluence of the rivers Moselle and the Rhine. The daily distributions of precipitation in the Moselle catchment area in the phases between the beginning and end of flood events in the period 1961 – 1968 are studied in order to find typical patterns when they are coupled with large-scale flow conditions. These patterns are then compared with the occurrence times of the flood crest at the gauges of the lower Moselle and its tributaries.

OBJECTIVES

The IRMA(SPONGE)-Project DEFLOOD was initiated to develop methodologies for the analysis of the efficiency of flood reduction measures in the Rhine Basin on the basis of reference floods. Flood reduction measures are e.g. modified soil cultivation, afforestation, creating of retention and overflow areas.

The kind and variability of spatio-temporal precipitation distribution is the main influence for the development of differing flood events with respect to their peak flow and duration. For the river basins of the larger tributaries of the River Moselle a semi-distributed precipitation runoff model will be calibrated. For the creation of reference floods meteorological input data are required. Within the project two approaches for generation of hydrometeorologial data sets: first: the derivation of reference hydrometeorological conditions from historic flood events and classification of the precipitation pattern in the 30 day interval before peak flow (this article) and second: the assessment of the maximum probable rain in the Rhine Basin using a rainfall generator. The Moselle is the largest of all tributaries to the Rhine; the catchment coming to 28230 km2 in total. The river has its source at the Vosges at 1365m asl. After 520 km both rivers meet in Koblenz. The French part of the Moselle and Saar catchments make up 58% of the entire area (Fig. 1).

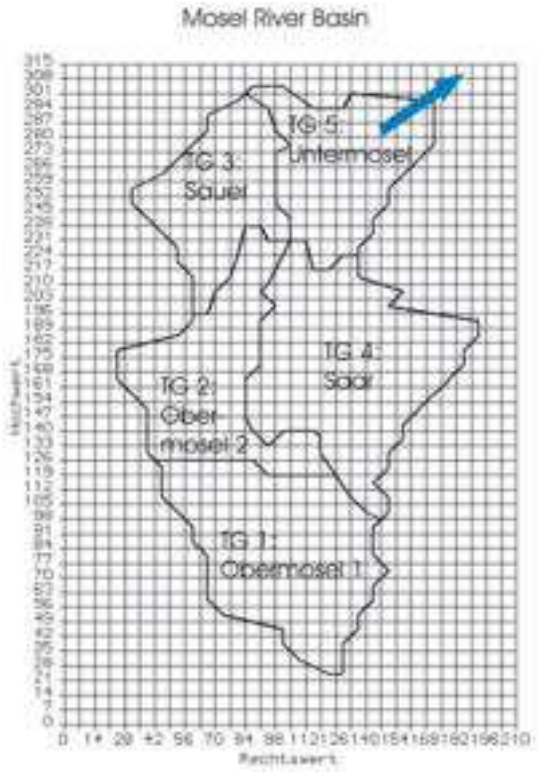

Fig. 1 Sub-catchments in the River Moselle Basin

PRECIPITATION, WIND FIELD PATTERN AND FLOODS

With regard to the general air-pressure distribution over Western Europe, the Moselle area is dominated by south-westerly and westerly winds. On average, about 50% of observed winds fall into these categories. Coming from these directions, the Atlantic air mass only has to pass over the 600 to 700 m asl. high central plateau of France and Morvan before arriving in the Moselle catchment as a wet and, in the winter months, comparatively warm air current.

Due to this relatively exposed situation, incoming air frequently meets the Vosges hills almost at a right angle, which induces it to generate or enhance rainfall (BfG 2001).

The first comprehensive study of the floods events in the Moselle Basin (TEIN 1905) has showed, that for generation of floods an area precipitation greater the 3 mm/d in the summer and greater then 1 mm/d is need. The difference is caused by greater evapotranspiration in summer. Very often the rising of water level was experienced at the same time in all sub-catchments approximately two days after the precipitation maximum. Finally, the effect of the River Saar was stronger as of River Sauer regarding the peak flow at Koblenz

From the in this study collected data, highest amounts of rainfall are to be found in the southern parts of the Vosges. The Sewen site (998m asl) recorded and average amount of over 2300 mm/a for the period 1961-1990. Further to the north of the Vosges amounts still reach values of over 1700mm/a (Grandefontaine 659m asl). Over 1000 mm/a have been measured at various stations in the Hochwald of the Hunsrück although the average value lies around 800mm/a, similar to the Ardennes and Eifel with averages around 700 to 800mm/a. Maximum values here though reach over 1200 m/a at Schneifelforsthaus (657m asl). Compared to -these fairly wet regions, the Moselle Valley itself, especially the lower part, stays relatively dry (Koblenz < 700 mm/a at 72m asl).

The spatial distribution of flood-inducing precipitation over the basin is decisive for the resulting discharge character. According to IKSMS (1998), partial rain cover only in the south leads to high discharge in the Upper Moselle (December 1947), which undergoes considerable reduction of its peak in the retention areas of Lorraine.

The same study claims that a concentration of extreme precipitation fields in the north half leads to fast climbing flow in the Moselle from Trier onwards due to shorter flow distances of the Sauer and Saar and fewer retention areas. Of this kind, the 'Weihnachtshochwasser' (Christmas Flood) of 1993/1994 and Jan-Feb 1995 Flood were the most memorable.

Homogeneous rainfall of the entire catchment can lead to a build-up of flow peaks from Upper Moselle, Sauer and Saar. This was the case for the Apr-May 1983 Flood, which did not reach the absolute values of the 1993-1995 floods as the inflow below Perl was not so pronounced. Hence, with this in mind the postulation is as follows: extreme floods can be expected when a intensive rain front comes from the Southwest, precipitates over the Upper Moselle, moves on to the Northeast and without being lessened by the catchment's orography precipitates over the Sauer and Saar (IKSMS 1998).

SUB-BASINS AND GRID

For further data analysis the catchment area of the Moselle is divided into sub-basins. Within a statistical approach, contrasts in sub-basin rainfall parameters can be expected due to the divergent topography of the area as well as other non-apparent controls to be explored. Hence the shape and layout of the sub-basins should in some way reflect the geography of the objects, more precisely, the tributaries to the Moselle or sections of the Moselle itself. With these prerequisites, the Moselle Basin as a whole was split into five sub-basins incorporating: 1. The Upper Moselle 1 (Obermosel 1, 6819 km^2), 2. The Upper Moselle 2 (Obermosel 2, 5204 km^2), 3. The Sauer (4338 km^2), 4. The Saar (7421 km^2) and 5. The Lower Moselle (Untermosel, 4448 km^2)

A rectangular grid with 45 cells in N-S direction (total length: 315 km) and 30 cells in W-E direction (210 km) was established, each grid cell being 7km x 7km surrounding a central grid point (Fig. 1). The co-ordinates of the grid points enter all calculations. The bottom-left corner of the grid has the following co-ordinates (Gauss-Krüger coordinates referring to the second reference meridian 6°E):

Hochwert: 5278937.0 Rechtswert: 2437648.0

PRECIPITATION DATA

The basis of all analyses in this project are the daily precipitation sums at sites within the Moselle Basin. The data was provided by the BfG, Koblenz. The data is composed of readings from the European countries France, Germany, Belgium and Luxembourg. The data was processed from a period ranging from 01.01.1961 to 31.12.1998, consisting of 174 climate and precipitation sites.

The precipitation data was not corrected for systematic errors which occur when using the Hellmann precipitation gauge in standard position. For this project the correction of the precipitation data is not vital as the precipitation data was not used for further balances. Systematic errors consist of wetting and evaporation losses and the wind error. RICHTER (1995) gives a detailed description of all systematic precipitation errors with regional differences for Germany.

The time series of daily precipitation sums had considerably large gaps. These were not spread out evenly over the complete catchment but rather amplified in the southern regions, i.e. the available sites in France. As a norm, only 100 to max. 155 sites provided precipitation data simultaneously. The missing data is particularly noticeable in the period 1961-1970, but also from 1990 onwards, especially in Sub-basins 1 and 2.

SPATIAL INTERPOLATION OF PRECIPITATION DATA

One task of the project was to calculate daily precipitation sums for every cell of the grid over the entire time interval 1961-1998, as well as to provide monthly averages over the same time span per grid cell.

Various approaches could be chosen from for the interpolation of the daily precipitation sums, such as several kriging methods (BARDOSSY 1983, KLEIN 1994) and the spatial interpolation for a specific point derived from a weighted average of precipitation of neighbouring sites. The latter came into use. The algorithm is slightly altered from ISAAKS & SRIVASTAVA (1989), from each more details on the inverse distance method can be taken. The necessary weights are determined from the squared inverse distances, r^2, between the adjacent sites and respective grid point. The orographic effects of precipitation lead to additional dependencies affecting the resulting interpolations. This height gradient is more pronounced during winter due to predominant frontal precipitation than during summer which witnesses more frequent convective precipitation. The consideration of this external drift (BARDOSSY 1983) enhances the interpolation result.

The site search is put into effect with the prerequisite that at least one site must be used in each quadrant surrounding the respective grid point to compute the average. The peripheral points can only be obtained by using the quadrants inside the research area. The FORTRAN- program 'NACHBAR' allows the selection of the number of neighbouring sites (generally n=5).

The calculation steps were as follows. Monthly and annual sums of precipitation were computed using the daily sums at sites, which had complete data sets. Long-term monthly and annual averages were then determined for the periods 1961-1990 and 1971-1990. Additionally, long-term averages for the same periods were devised for Winter (Oct-Mar) and summer (Apr-Sep) for later usage within the interpolation process. These data sets were then completed to 186 sites with aid of various interpolation methods und values obtained from climatological references (DWD, European climate data). These sites lie either inside the Moselle catchment or in its immediate surroundings.

In order to obtain the interpolated precipitation data, the daily precipitation sums are not interpolated but the daily quotients, which are created from the daily site sums and long-term daily average for the respective site and calendar day (see DÄLLENBACH 2000). After the spatial interpolation of the quotient to the grid point this is then multiplied with the already calculated respective long-term daily precipitation value. Hence, both the orographic induced variation and seasonal variation flow into the calculation by utilising different daily values for summer and Winter months (Fig.2).

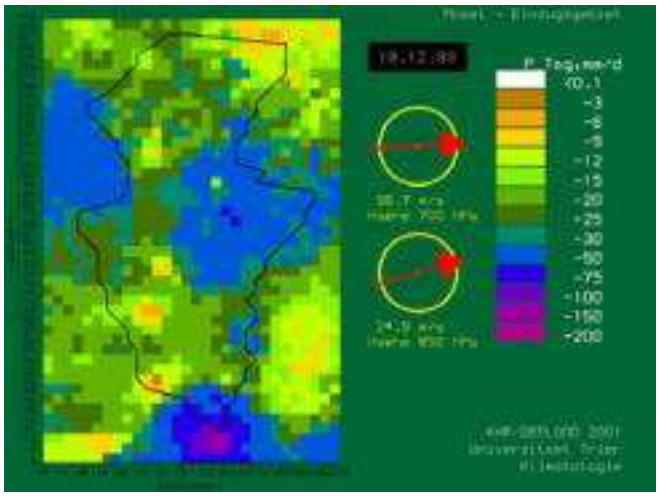

Fig. 2 Gridded daily precipitation sums and mean wind vector on 19th Dec 1993

WIND DATA AND ATMOSPHERIC CIRCULATION DATA

It is apparent that there is a close relationship between atmospheric circulation and precipitation. In the project was examined, whether the 'Grosswetterlagen' (after Hess and Brezowsky) are governed by specific wind directions in the troposphere and whether the distribution of' these wind directions change with differing rainfall situations.

Two pressure levels, those of the 850hPa (geopotential height ca. 1500 gpm) and 700hPa (ca. 3000 gpm) were chosen for comparative applications of horizontal wind vector. Reanalysis data from NCEP/ NCAR on a 2.5° grid provides a good basis for creating an average value per day for the area.

In order to calculate the value, the horizontal components (u and v) of four points were used to produce one horizontal wind vector average: 50.0° N/ 5.0°E, 50.0°N/ 7.5°E, 47.5°N/ 5.0°E and 47.5°N/7.5°E. The vectors which were calculated for each day can be seen, as an example, together with the daily precipitation sums in Fig. 2, the upper vector being the 700 hPa average for the area and the bottom one the 850 hPa horizontal vector.

The GWL (Großwetterlagen) data was supplied by the PIK-Potsdam in form of catalogue of general atmospheric circulation patterns, or GWLs. The different circulation patterns are given per day as a number ranging from 1 to 30 (GERSTENGARBE et al. 1999).

SPATIO – TEMPORAL STRUCTURE OF PRECIPITATION FIELD

For the spatial separation of rainfall amounts the sub-basin site averages of daily precipitation amounts were compared in order to obtain a picture of the regional differences of rainfall distribution. Depending on the day, the amount of sites per sub-basin which expose a reading may differ. lnterpretations on precipitation can also be made when regarding the occurrence of rain, i.e. relative portion of sites where rain falls over a specific threshold. This gives insight into the cover of rain for a given area, whether this is the entire catchment or a sub-basin. Figs. 3 to 5 show the rainfall amounts in the sub-basin 3. Deducing from the figures regarding the sub-basins 1, 2, 4 and 5 (here not presented) the highest average daily precipitation sums per sub-basin are always attained 2 to 4 days prior to peak flow, though the pattern of precipitation um development is different for each event. The May-June 1983 Flood (Fig. 3) reveals more or less consistent rainfall for the entire period up to the discharge peak with emphasis on the period from 23rd to 28th May and highest values on 24th (Sub-basin 1) and 25th May (other sub-basins). Average daily site values almost reach 50mm for Sub-basin 1, but only below 20 mm in Sub-basin 2.

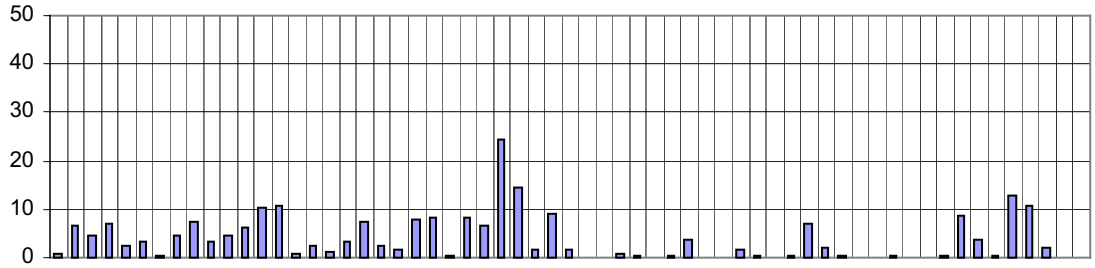

Fig. 3 Development of daily precipitation site averages (mm) during the May-June 1983 flood in the Sub-basin 3 (-30 to +30 days centred around peak flow at Trier)

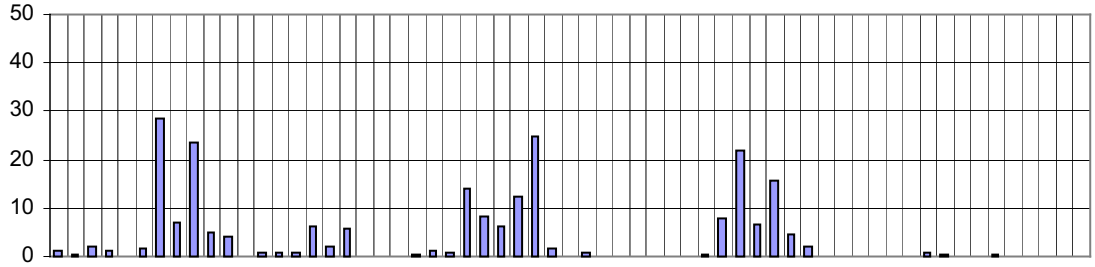

Fig. 4 Development of daily precipitation site averages (mm) during the Jan-Feb 1990 flood in the Sub-basin 3 (-30 to +30 days centred around peak flow at Trier)

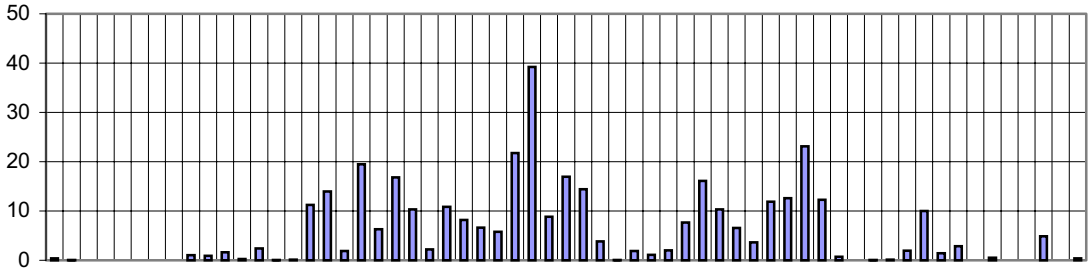

Fig. 5 Development of daily precipitation site averages (mm) during the Dec 1993-Jan 1994 flood in the Sub-basin 3 (-30 to +30 days centred around peak flow at Trier)

Looking at the time series in Fig. 4 the Jan-Feb 1990 flood does not show such a homogeneous distribution of precipitation. High amounts can be found on 23rd and 25th January gradually decreasing till 3rd February, with a second period commencing on 10th February ending with highest values on 14th February, two days before peak flow. Again, highest average sums are to be found in Sub-basin 1 and lowest in Sub-basin 2.

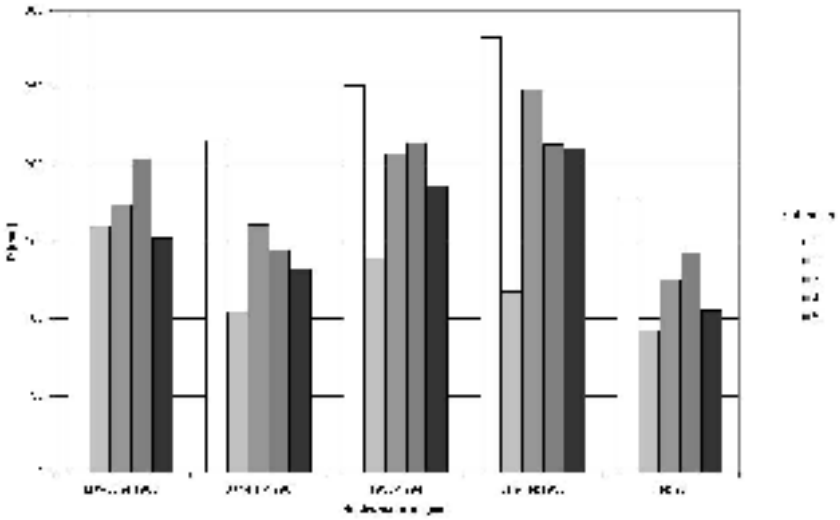

Fig. 6 Sums of daily precipitation for sub-basins 1 to 5 accumulated from -30 days to peak flow.

Observing the 30-day preceding period for the extreme 1993-1994 Flood (Fig. 5), elevated amounts of rainfall do not start until 7th December with pursuing abundant precipitation past peak flow on 22nd December. The absolute daily maximum of all areas is to be found in Sub-basin 4 (>45mm), followed by 3 and 5.

The Fig. 6 shows the precipitation sums of the 30-day preceding period in all five sub-catchments for five extreme flood events between 1983 and 1997. The highest amounts were observed in the sub-basins Upper Moselle (TG 1) followed by sub-basin Saar (TG 4).

ANALYSIS OF THE GRIDDED INTERPOLATED DATA

The analysis of the interpolated data runs alongside that of the original site data. The great advantage of the data at grid points is that it is spatially homogenous, without differences of site density playing a role in later interpretation of the analysis.

For this task six parameters were devised to describe the precipitation field at the grid points for day i, referring to a) the sub-basins and b) the entire catchment. The parameters are as follows:

1. **PM** average precipitation mm/d
2. **R2** relative amount of sites with P≥2 mm
3. **R3** relative amount of sites with P≥5 mm

4. **R4** relative amount of sites with P≥l0 mm
5. **PMX** maximum precipitation at a grid-point
6. **PMD** precipitation median of the area

The least favourable case for flood-threat sets in when the duration of precipitation inducing general atmospheric circulation forms is extremely long, coupled with a corresponding continuous transport of water vapour. For the evaluation of this phenomenon the following steps should be considered:

- Linkage of precipitation in the catchment with the general atmospheric circulation pattern (GWL)

The relative frequency distributions of the general atmospheric circulation patterns (GWLs), depending on precipitation characteristics of complying days show the obvious result increasing occurrence of zonal circulation forms when examining days with PM≥2 mm, 5 mm and 10 mm. This behaviour is even more evident when summer days are excluded. Zonal-form participation climbs from just over 30% relative frequency for all winter days to over 70% when regarding days with PM 10 mm! Zonal forms are generally more common for the winter months and this perception would support the idea that precipitation in the Moselle Basin is more frequent during periods of sustained propagation of Atlantic air masses from the west. This recognition is useful but here attention is directed to the discrimination of individual atmospheric circulation patterns, i.e. the GWLs 1 to 29 (30).

Generally speaking, increased precipitation in the Moselle Basin (PM> 2, 5, 10 mm and R2, R3 and R4≥90%) generates a redistribution of atmospheric circulation forms (ZFs) and, consequently, patterns (GWLs). 'Zonal forms' increase (28% for all days, 55% for PM≥l0_mm), 'mixed' and 'meridional' forms decrease. Marked relative increases of the individual GWLs are found in 'WZ', 'WS', and 'WW' (zonal), 'SWZ' and 'NWZ' (mixed) and 'TRM', 'SZ', 'TB' and 'TRW (meridional). These differences are more prominent when only regarding winter days due to amplified relative occurrence of frontal precipitation.

- Connection between precipitation in the catchment and wind direction in 850hPa and 700hPa-levels

The same precipitation parameters reveal supporting results when considering 850 hPa / 700 hPa wind characteristics. Above all, westerly wind sectors are more frequented during days with more intense rainfall. Sectors 226°-255° and 256° 285° witness the stronger favouring.

- Duration behaviour of the regarded GWLs and wind directions

Zonal GWLs encompass the most extreme duration periods of up to 23 days ('West Cycionic') in the time series. The generally more right-orientated distributions provide the prerequisite for continuous abundant flood inducing rainfall. Zonal GWLs also reveal the most right-orientated distributions concerning duration of days with PM ≥1.0 mm. 'WZ' again has the longest time span exceeding the limit (up to 18 days). Duration behaviour of wind sectors underline the aforementioned findings. Westerly directions prevail longest (Fig. 7).

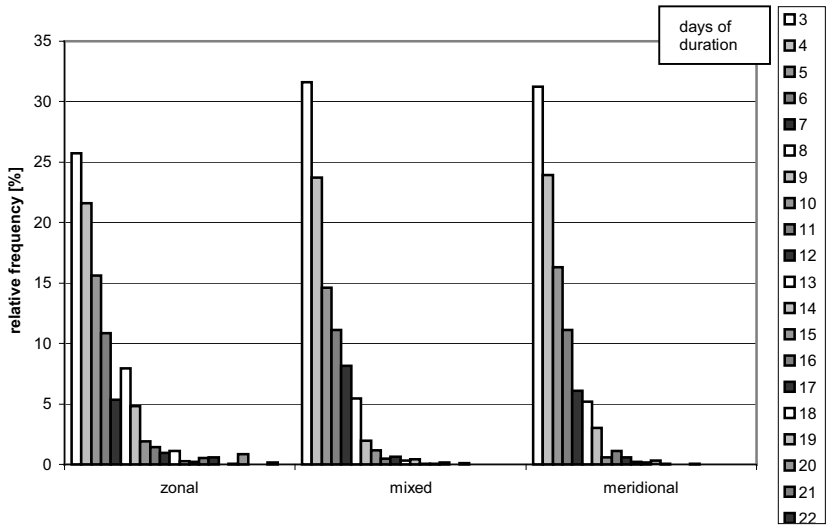

Fig. 7 Average relative frequency of GWL duration periods (days) for all 'circulation forms' – 1961-1998

- Investigation of the linkage between GWL and wind direction

Analysis of GWL against wind direction verifies the claimed origin of the specific GWLS. The comparison between the two with respect to the precipitation parameters once more reveals a turn to westerly directions during days of developed precipitation.

The possibility to identify movement of precipitation fields with daily data was checked with the aid of the qualitative measure of consecutive daily maps. Although first glances did not exhibit any identifiable drift of a field the footprint of a general precipitation movement could be recognised in the characteristics of the correlation fields. A W-E, or more a WSW-ENE preferred direction found in the iso-correlates for correlation pairs of precipitation and in the distance-decay curves imply a preferred direction of precipitation movement in exactly this direction.

HYDROMETEOROLOGICAL REFERENCE CONDITIONS

From the analysis of the daily sums of area precipitation in the period –30 days to peak flow at Trier and Cochem three typical models were extracted. The models based on normalized precipitation sums allow the estimation of synthetic daily area precipitation sums for each sub-basin as input in hydrological catchment models.

A detailed representation of the project results can be find in WHITE (2001).

REFERENCES

Bardossy, A. (1983) Stochastische Modelle zur Beschreibung der raum-zeitlichen Variabilität des Niederschlags, IHW Mitteilungen, H. 44, Univ. Karlsruhe.

BfG (2001) www.bafg.de.

IKSMS (eds.) (1998) Hochwasserschutz im Einzugsgebiet von Mosel und Saar: Bestandsaufnahme/ ed.: Internationale Kommissionen zum Schutze von Mosel und Saar. Trier.

Dällenbach, F. (2000) Gebietsniederschlag Schweiz. Interpolation und Berechnung der Niederschlagsdaten. Gutachten METEOTEST, Bem.

Gerstengarbe. F.-W. & WERNER, P. C. (1999) Katalog der Großwetterlagen Europas (1881- 1998). 5th Edition. Potsdam, Offenbach a. M.

Isaaks, E. H. & Srivastava, R. M. (1989) Applied Geostatistics, Oxford Univ. Press. NewYork.

Klein, G. (1994) Regionalisierung von Niederschlag mit Hilfe digitaler Gelände-informationen – Entwicklung eines geo8kologischen Modells zur routinemäßigen Ableitung hochauflösender Niederschlagskarten. Freiburger Geographische Hefte. H. 44 112p, Freiburg.

Richter, D. (1995) Ergebnisse methodischer Untersuchungen zur Korrektur des systematischen Meßfehlers des Hellmann-Niederschlagsmessers. Berichte des Deutschen Wetterdienstes, H. 194. Offenbach a.M.

Schafmeister, M.-T. (1999) Geostatistik für die hydrogeologische Praxis. Springer, Berlin, Heidelberg, New York.

Schönwiese, C.-D. (1992) Praktische Statistik für Meteorologen und Geowissenschaftler. 2nd Edition, Bornträger, Berlin and Stuttgart.

Tein, M.v. (1905) Ergebnisse der Untersuchung der Hochwasserverhältnisse im Deutschen Rheingebiet, VII. Heft Das Moselgebiet.

White, W. (2001) Spatio-Temporal Structure of Precipitation in the Moselle Basin with Particular Regard to Flood Events. Diploma Thesis, Dept. Climatology, FB VI, Univ. of Trier.

Univ.-Prof. Dr. Alfred Helbig
Dept. Climatology
Fac. Geography/Geosciences
University of Trier
D – 54286 Trier

helbig@uni-trier.de
helbig.meteo@t-online.de

Generation of hydrometeorological reference conditions for the assessment of flood hazard in large river basins (Proceedings of International Workshop, Koblenz, 6. and 7. March 2001).
CHR-Report No. I-20

InterNied - A geostatistical interpolation procedure for hourly measured precipitation data

Angela Hinterding
Institute for Geoinformatics, Westfälische Wilhelms-Universität Münster
Münster, Germany

Abstract The spatial variability of short-term precipitation is an important input parameter for flood forecasting models. Without the use of radar data interpolation methods are required for the estimation of area-wide spatial distributions of precipitation from pointwise measured data. The paper presents an interpolation procedure for hourly measured precipitation data. The procedure estimates spatial distributions of precipitation with regard to the actual weather situation. For this purpose, spatial precipitation patterns related to general weather conditions were identified from historical data. The patterns are used as a first approximation of an actual precipitation distribution. The geostatistical method kriging is used as mathematical basis of the interpolation procedure.

INTRODUCTION

The quality of flood forecasting models depends crucially on the quality of their input parameters. Therefore, data preprocessing is an important issue in this context. The paper focuses the interpolation of pointwise measured precipitation as part of the data preprocessing for hydrologic models. The interpolation of precipitation data is necessary because normally precipitation is measured pointwise but flood forecasting models work with area-wide spatial distributions. Radar as a way to measure area-wide spatial distributions is often not available for operational tasks.
Due to the high variability of precipitation in space and time modelling and interpolation of short-term precipitation is a difficult task. In order to estimate spatial distributions of precipitation adequately, the joint influence of atmospherical and orographical factors should be considered. Often simple interpolation procedures as the Thiessen polygon or inverse-distance method are used in flood forecasting models. They provoke large errors (Goovaerts 2000), and hence decrease the quality of a forecast. Johansson (2000) and Goovaerts (2000) present an interpolation procedures that integrate the influence of orographical factors.
Knowledge about general spatial and temporal characteristics of precipitation processes exists as result of an intensive research. Knowledge about characteristics of a precipitation process in a specific area is obtained by an analysis of the historical precipitation time series in this area. For this purpose, automatic techniques are required to cope with the huge amount of data.
The paper presents an interpolation procedure for hourly measured precipitation data that integrates knowledge from historical precipitation data. Spatial distributions of precipitation are estimated by use of historical precipitation patterns. In order to illustrate the main ideas of the procedure the paper is organized as follows. The next section (section 2) describes the mathematical basis of the procedure. The geostatistical method kriging is described in section 2.1; the technique of soft overlapping of different kriging models is described in section 2.2. Section 3 introduces a procedure for the identification of typical precipitation patterns that are integrated in the interpolation. Sections 2 and 3 are the basis for the geostatistical model used in the interpolation procedure. This model is presented in section 4. Section 5 contains technical aspects of the interpolation procedure. The paper closes with some conclusions in section 6.

MATHEMATICAL BASIS

The interpolation procedure for precipitation data presented in section 4 is based on the geostatistical interpolation method kriging. The first part 2.1 of this section summarizes this method. The second part 2.2 presents a fuzzy-based approach for overlay of different kriging models. This approach is part of the interpolation procedure for precipitation.

The underlying theory and several applications of geostatistical methods are presented in detail e.g. in (Goovaerts 1997, Cressie 1991).

Kriging

Kriging is a family of geostatistical interpolation methods, which are based on a geostatistical model and which estimate an area-wide distribution by a best linear unbiased estimator (BLUE). In contrast to simple interpolation methods as inverse-distance or Thiessen polygon method it can be suited to the parameter under investigation.

Within kriging a spatial parameter is modelled as a spatial stochastic process Z = (Z(x)) (Kitanidis 1997). Z(x) denotes the probability variable of the process at location x. Measured values of the parameter of interest at location x are assumed to be realisations of the probability variable Z(x). By means of interpolation a realisation of the whole process is estimated from the well known pointwise realisations.

The stochastic process Z is decomposed in processes of different scale; in general a macro-scale and a micro-scale are assumed:

$$Z(x) = Z_{macro}(x) + Z_{micro}(x)$$

The macro-scale process is assumed to be deterministic. Different kriging variants are distinguished according to the definition of the macro-scale process, for example ordinary kriging (macro-scale process constant but unknown) or universal kriging (macro-scale process is a trend function).

The micro-scale process models the deviation of process Z from the macro-scale process Z_{macro}. Systematical components aren't allowed for deviations. Therefore the mean of the micro-scale process is regarded as zero $E[Z_{micro}(x)] = 0$. The micro-scale process is assumed to be autocorrelative. A variogram is used for modelling autocorrelation:

$$\gamma(h) = Var(Z(x) - Z(x+h))$$

The krige-estimator is given by the two conditions of unbiasedness and of minimization of the error variance.

When interpolating a spatial parameter by kriging a suitable model and the model parameters have to be specified. The adequate variant depends on the spatial characteristics of the parameter under investigation.

Soft combination of different kriging models

The spatial distribution of short-term precipitation is highly variable in space. In the interpolation procedure presented in section 4 a soft combination of different kriging models is used for describing this variability. In the following the mathematical basis for such a combination is described.

There is a standard way to build a combined model Z for different geostatistical approaches in one area. The area under investigation is partitioned by a tessellation. For each subarea a geostatistical model Z_i is defined. Spatial indicator variables I_i describe the shapes of the subareas. The whole model is then defined as:

$$Z(x) = \Sigma\, Z_i(x)\, I_i(x)$$

However, this model isn't appropriate for describing the spatial distribution of precipitation. Hard boundaries can cause discontinuities within spatial distributions. Therefore this model is generalized replacing the spatial indicator variables by spatial fuzzy sets to

$$Z(x) = \Sigma\, Zi\,(x)\, Ri(x)$$

R_i denotes the membership function of the fuzzy set of the ith subarea. A definition and meaning of fuzzy sets is given e.g. in (Kruse 1993).

The interpolation procedure described in section 4 uses this approach to model homogeneous areas of precipitation intensities.

IDENTIFICATION OF TYPICAL PRECIPITATION PATTERNS

Precipitation has been measured in the investigated regions on a time-scale of an hour since circa 1990. The historical time series contain knowledge not only about the temporal but also about the spatial characteristics of precipitation. In order to take advantage of this knowledge within the interpolation historical data are analysed with special regard to the spatial characteristics of precipitation.

From a wide range of research in this field it is well established that the spatial distribution of precipitation is influenced by a complex set of different external parameters, such as atmospherical patterns, seasonal variation and, of course, orography. The goal of this analysis is to specify the influence of these factors on the spatial variability of precipitation registered in the investigated areas. Typical spatial patterns depending on extern weather conditions are identified. As described in the next section these patterns are used for interpolating an actual data set of precipitation measurements.

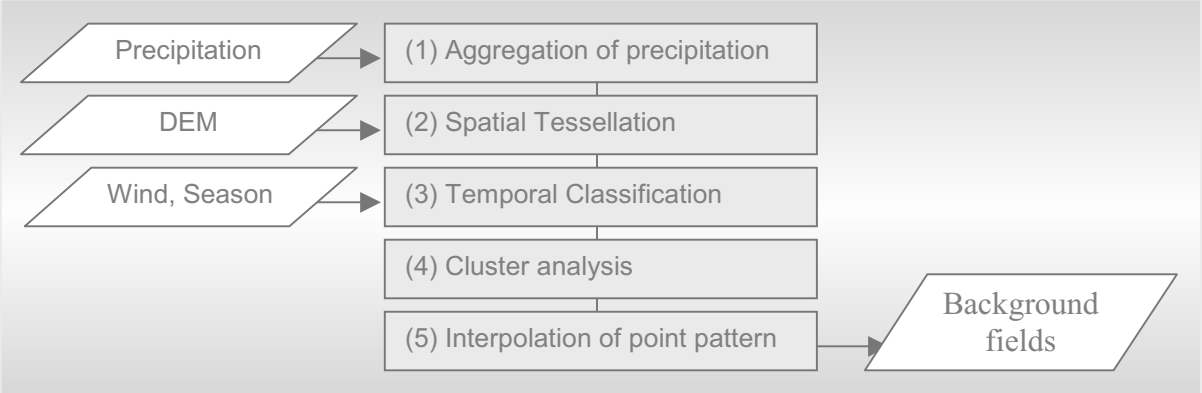

Fig. 1 Identification of typical precipitation patterns

The identification of typical spatial precipitation patterns is performed in a procedure of five steps (figure 1). The set of time series of precipitation in the area under investigation forms the main base of this analysis. In addition, wind direction and season were chosen as potential factors of influence. They are described by parameters available in the operational use of the interpolation method. A combination of parameters of the Objective Weather Classification (Dittmann 1995) and the weather classification after Hess and Brezowsky (Gerstengarbe 1993) is used for the classification of the eight main wind directions. Orography is specified by a digital elevation model (DEM).

Because hourly measured data does not match to the natural characteristics of precipitation – precipitation appears in events with duration between some minutes and some hours - the hourly measured data have been aggregated to so-called complete events (step 1). Events are defined by local minima of the averaged intensity of precipitation in the area under investigation and take a time of one to some hours. These are the main elements of interest for further analysis. The next two steps classify these events in homogeneous classes in space and time.

In order to analyse the influence of orography the area under investigation is partitioned in subareas with specific orographic characteristics (step 2). An example of such a tessellation is shown in figure 2. Each subarea is analysed separately.

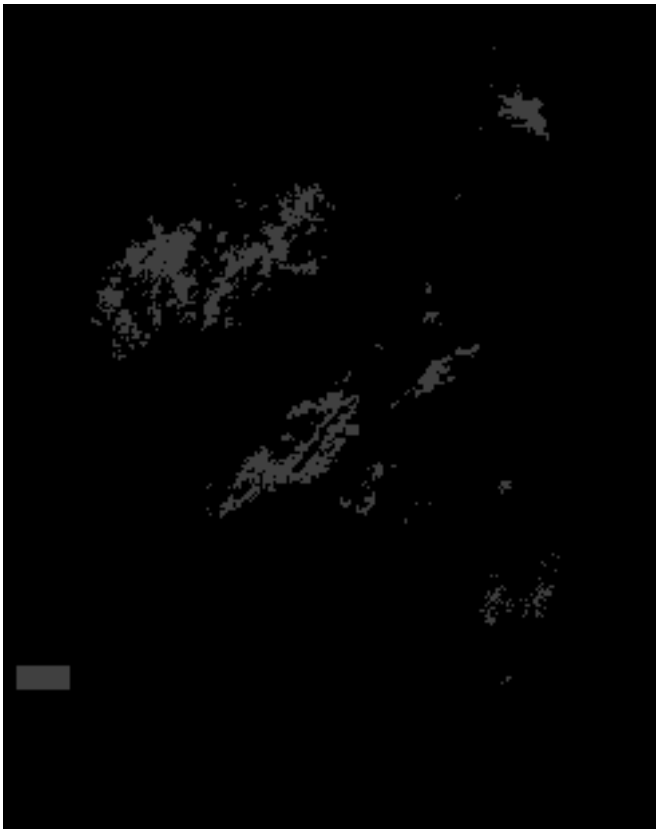

The complete events are divided in time into homogeneous classes according to the time-variant factors wind direction and season (step 3).

The inner structure of the spatially and temporally classified data are analysed using cluster analyses (step 4). A cluster analysis method offered by the data analysis tool SPSS was used. The result is a set of typical spatial point patterns for each spatial and temporal class of precipitation events.

These typical patterns are interpolated with regard to the interpolation procedure (step5). Here additional information about the correlation of elevation and precipitation and disaggregated daily measurements for densing the measurement net are used. The interpolation method kriging serves as the mathematical basis.

For each class of spatially and temporally classified data between 5 and 10 typical patterns have been chosen. This is in accordance with the high spatial and temporal change of characteristics.

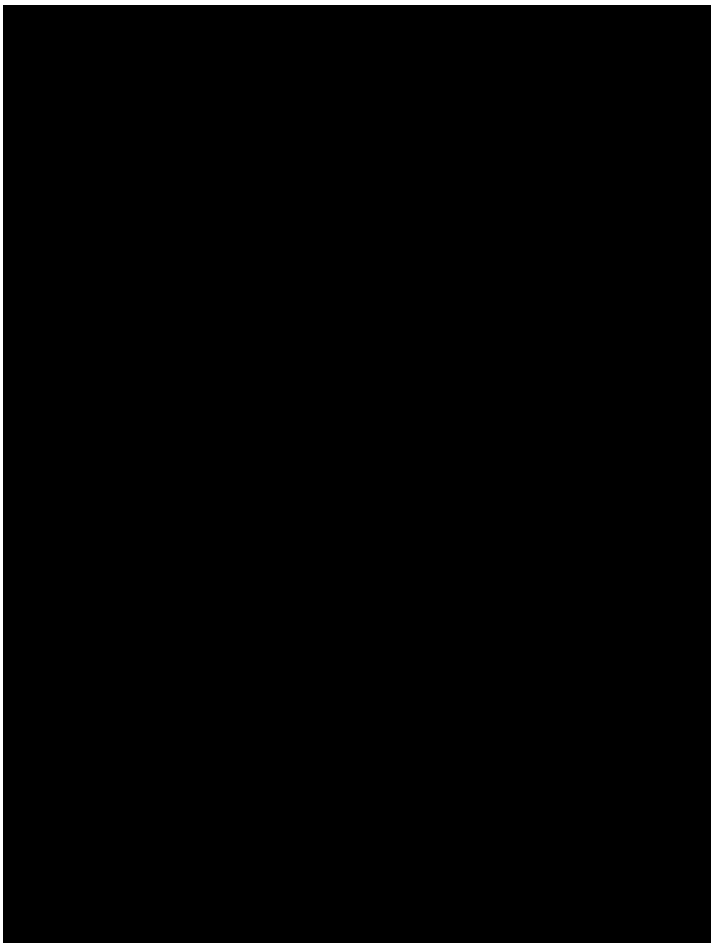

INTERNIED – THE INTERPOLATION PROCEDURE

This section presents the overall mathematical model of the interpolation procedure. The results of the previous sections are reflected in this formal description. For a good motivation and understanding of the model it is described in a constructive way.

When modelling the spatial distribution of precipitation on a time scale of one hour precipitation cells with a range smaller than the area under investigation have to be taken into account. A basic model suiting these conditions is given by the approach described in section 3.2:

$$N(x) = N_o(x)\, R_o(x) + \Sigma_{i=1,\ldots,n}\, N_i(x)\, R_i(x), \text{ where}$$

$N(x)$ spatial stochastic process of precipitation
$N_o(x) = 0$ spatial stochastic process of zero precipitation
$R_o(x)$ spatial membership function of the subarea with zero precipitation
$N_i(x)$ spatial stochastic process of the i-th subarea with non-zero precipitation
$R_i(x)$ spatial membership function of the of the i-th separate subarea with non-zero precipitation

The estimator $\underline{n}(x_0)$ of an unknown precipitation value at a location x_0 is given by

$$\underline{n}(x_0) = \begin{cases} 0 & \text{if } R_o(x_o) > 0.6 \\ \Sigma\, \underline{n}_i(x_0)\, \underline{r}_i(x_0) & \text{otherwise} \end{cases}$$

$\underline{n}_i(x_0)$ non-zero component estimator of the i-th separate subarea at loc. x_0
$\underline{r}_i(x_0)$ normalized membership grade at location x_0
$= (R_i(x_0)/ \Sigma_{i=0,\ldots,n}\, R_i(x_0)) * R_0(x_0)$

The threshold value 0.6 was found adequate after some experimental work. An example of a division of the area into subareas of zero precipitation and subareas of positive precipitation by this approach is shown in figure 3.

The internal spatial structure of a precipitation cell is described by use of the typical precipitation patterns described in section 4:

$$N_i(x) = \Sigma N_{ji}(x)\, R_{ji}(x), \text{ where}$$

$N_{ji}(x)$ spatial stochastic process of the j-th subarea of the i-th cell
$R_{ji}(x)$spatial membership function of the of the j-th convex subarea of i-th c.

When ever there is a wide range of precipitation intensities or non-convex cells these are divided into further convex subareas with a homogenous precipitation intensity.

At this stage, a typical precipitation pattern (called background field) is used to achieve a first approximation of the actual precipitation pattern in this area:

$$N_{ji}(x) = HG_{ji}(x) + res_{ji}(x), \text{ where}$$

$HG_{ji}(x)$ background field of the j-th subarea of the i-th cell
$res_{ji}(x)$ residuals between the background field and the actual data

An optimal background field is determined by a least-square method considering all background fields of the actual wind direction and the actual season. The residuals are estimated by ordinary kriging.

One example of a spatial distribution interpolated by the described procedure is shown in figure 4.

Different validations were performed. Precipitation measured at a gauge was compared to the estimated precipitation ignoring this gauge within the interpolation. Figure 5 shows this on the basis of gauge Odenbach situated in the investigated area Rheinland-Pfalz. Larger variations between the estimated and the measured values are observed. These variations are partly a result of the sparse measurement net.

Particularly with regard to the use of the interpolation procedure within flood forecasting the estimated precipitation of subareas was analysed. In figure 6 a good match between the estimated precipitation in area Eschenau including gauge Odenbach and excluding a gauge is shown. This result is representative for other subareas in the area of Rheinland-Pfalz. It indicates that precipitation within subareas is estimated adequately by means of the interpolation procedure.

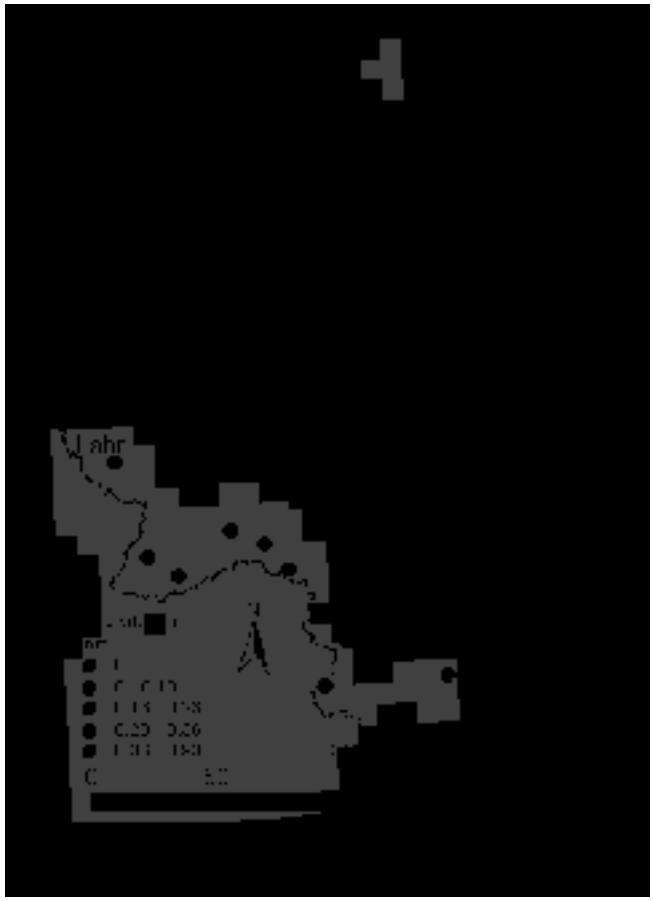

Technical aspects

The interpolation model presented in section 4 has been implemented in the interpolation procedure *InterNied* (*Int*erpolation von stundenbasierten *Nie*derschlagsdaten). The procedure is raster-independent and independent of the spatial constellation of the gauges too. It has been developed for operational use and is suited for batch processing. It takes a few minutes to interpolate a data set. InterNied is implemented in the c programming language and runs on Windows platforms.

The interpolation procedure has been applied to the catchments of river Mosel and Nahe and to the area of Rheinland-Pfalz, a federal state of Germany. For transferring the interpolation method to other areas of interest the background fields have to be renewed.

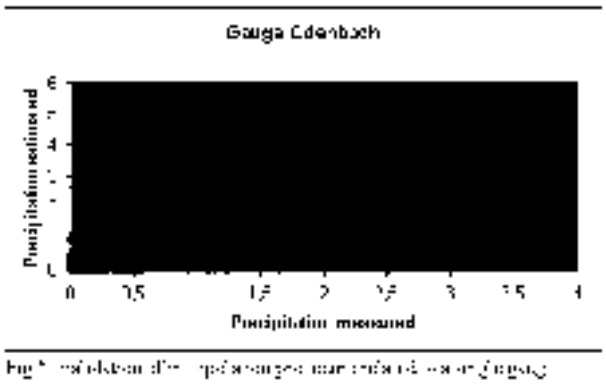

CONCLUSIONS

In this paper InterNied, an interpolation procedure for precipitation data on a time scale of one hour is described. The procedure determines spatial distributions according to the actual weather situation. For this goal so-called background fields are used. A fuzzy-based combination of geostatistical models was chosen as the mathematical basis.

The interpolation procedure estimates the spatial variability of hourly measured precipitation data with regard to the use in flood

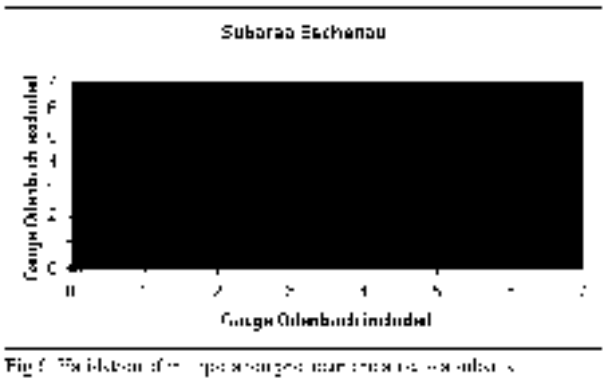

forecasting models adequately. With a runtime of a few minutes the procedure is optimised for operational and real-time use.

However, more accurate knowledge about the spatial structure of short-term precipitation may improve the outcome of interpolation. Radar data could help to come to a better understanding of it. Furthermore, a densification of the operational measurement net is recommended with regard to a better quality of interpolation outcomes.

REFERENCES

Cressie, N. (1991) Statistics for Spatial Data.- John Wiley & Sons, New York.

Dittmann, E., S. Barth , J. Lang, G. Müller-Westermeier (1995) Objektive Wetterlagenklassifikation. Berichte des Deutschen Wetterdienstes, 197, Selbstverlag des DWD.

Gerstengarbe, F.-W., P. Werner (1993) Katalog der Großwetterlagen Europas nach Paul Hess und Helmuth Brezowski (1881-1992) Berichte des Deutschen Wetterdienstes, 113, Selbstverlage des DWD.

Goovaerts, P. (2000) Geostatistical approaches for incorporating elevation into the spatial interpolation of rainfall. Journal of Hydrology, 228, pp. 113-129.

Goovaerts, P. (1997) Geostatistics for Natural Resources Evaluation. Oxford University Press, New York.

Johansson, B. (2000) Precipitation and Temperature in the HBV Model. SMHI Reports Hydrology, 15.

Kitanidis, P.K. (1997) Introduction to Geostatistics. Cambridge University Press.

Kruse, R., J. Gebhardt, F. Klawonn (1993) Fuzzy-Systeme. B.G.Teubner, Stuttgart.

A. Hinterding
Institute for Geoinformatics
Westfälische Wilhelms-Universität Münster
Robert-Koch-Str. 26-28
48149 Münster
Germany

hinterd@ifgi.uni-muenster.de

Topic 3: Modelling of extreme precipitation events of long duration (mesoscale meteorological modelling and stochastic precipitation generators)

Generation of hydrometeorological reference conditions for the assessment of flood hazard in large river basins (Proceedings of International Workshop, Koblenz, 6. and 7. March 2001). CHR-Report No. I-20

How to use meso-meteorological models to predict cases of extreme precipitation

Georg Skoda
Institute of Meteorology and Geophysics of the University of Vienna
Vienna, Austria

Abstract In order to get as close as possible to the actual *extreme precipitation value of a region*, it is vital to know about the detailed structures of the basic precipitation fields. These patterns can be derived from high resolution meteorological models available today. These take into consideration the interaction between the process of precipitation and orography. Numerical experiments pursued under suitable starting conditions and boundary values create climatological results of precipitation fields, which are used amongst other things to increase the network of observed values. The latter is particularly significant in mountaineous areas.

The methodical *combination of observation and modelling* proves its worth with re-processing of average precipitation conditions, calculation of design values within catchment areas, and the construction of heavy precipitation maps for short durations. It also appears to be possible to estimate maximized values of areal precipitation.
There are, however, two significant *limitations*:

1. We have to bear in mind that results derived from meso-meteorological models are only valid within those atmosphereic starting assumptions for which the respective model has been conceived. It is possible that when assuming starting assumptions that are too extreme, some fundamental laws of model physics are broken.

2. Due to the rapid decrease in forecast quality after some time with meso-scale models (the predictability ranges between two and three days), prognoses over several days may be useless in some particular cases.

INTRODUCTION

Hydrological models need meteorological input. In the long run, our goal is to improve coupling of meteorological and hydrological models. Fine scale precipitation forecast fields are necessary in flash flood prediction because of non-linear runoff response to precipitation. Grid-scales of high-resolution operational NWP models are about 10 km. Therefore, spatial resolution of meteorological forecasts has to be improved and these fine-scale forecast systems have to be validated. We will give two examples to prove our point:

QUANTITATIVE PRECIPITATION FORECASTS WITH ALADIN

AHRENS et al., (2001) performed simulations with different configurations of ALADIN (cycle 11.2.; please have a look at http://www.cnrm.meteo.fr/aladin/). The first configuration is the hydrostatic ALADIN/VIENNA, actually operational at ZAMG, with 9.6 km gridspacing. ALADIN/VIENNA uses the „classic method“ of moisture convergence modulation in the deep convection schmeme. The second configuration (4 km / V1) is non-hydrostatic with 4 km gridspacing. Moisture convergence modulation is done with the more physical and less tunable „smarter method“. The third configuration

(4 km / V2) is identical with the version 4 km / V1, but again uses the „classic method“ for moisture convergence modulation. Target area of the reported investigation is the „Ticino-Verzasca-Maggia“ (TVM) watershed (total area: 2 627 km ²) upstream of Lago Maggiore. With each model configuration the authors have performed a sequence of 7 forecasts (June 26, 12UTC, to June 30, 12UTC, 1997), each over 18 hours. Intercomparison of the simulation results and of observational data is shown in F i g. 1. Estimation of precipitation fields with rain gauge data is difficult because of low station density and measurement errors. The interpretation of radar data is difficult because of, e.g., ground reflectivity or shielding by mountains.

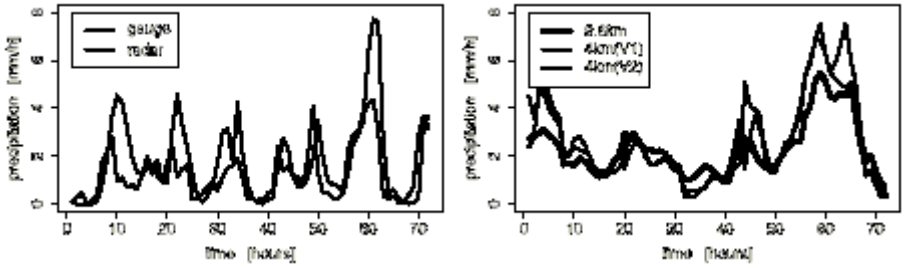

Fig. 1 TVM catchment mean time series of precipitation estimated from rain gauge, radar data, and simulated with ALADIN.

The sequences of hourly accumulated precipitation fields are used as input to the distributed hydrological model WaSiM-ETH. All meteorological input is interpolated to the hydrological grid (500 m gridspacing). Fig. 2 shows observed and simulated runoffs at the TVM catchment outlet. The temporal structure of simulated runoff with observed (gauge or radar data) input outperforms the runoff structure with simulated input. Obviously, there is a wrong increase of simulated runoff in the beginning of the flood period because of the erroneously forecasted precipitation peak. But the total runoff amount is underestimated with observational input.

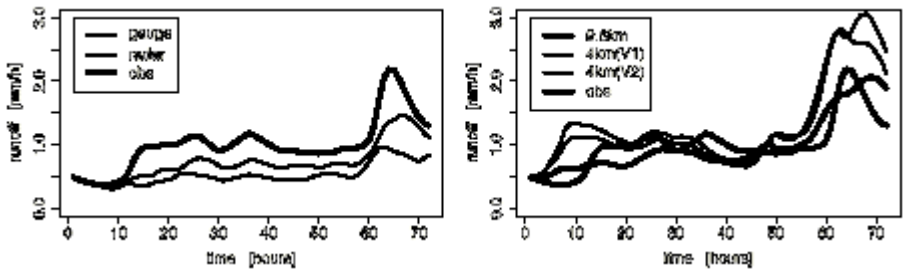

Fig. 2 Observed runoff time series at TVM catchment outlet and simulated runoffs with different precipitation inputs.

From that we can conclude: Simulated precipitation amounts are larger than observed precipitation amounts.

MODELLING OF DESIGN VALUES FOR HEAVY PRECIPITATION

The depicted *extreme precipitation values* have been taken from studies on design values on the area for short durations (less than or equal to 12 hours) or can be derived from those studies (LORENZ and SKODA, 2000, 2001). The studies on design values for heavy precipitation mentioned above follow the deliberations and prerequisites of the proceedings worked out in the course of the ÖKOSTRA project (ÖKOSTRA-93, 1992; HAIDEN, 1994; HAMMER, 1993; SKODA, 1993).

Generally, it is required to first check all the possibilities, and to use measured data, processed material or digitalised precipitation values which have already been put in the data bank from the respective catchment area. When the requirements have been fulfilled, the amount of a certain design value of precipitation *hN* for the requested duration *D* and the return period *T* can be investigated according to the ÖKOSTRA guidelines.

When dealing with small catchment areas or alpine areas, required observation data will be missing. In non-mountainous areas there are regional gaps in the field of high resolution data. Thus in practice we are commonly confronted with inadequate data. Under these circumstances we deem it necessary to take the required precipitation values from areal high resolution meteorological models, e.g. LAMs.

Modelling of convective precipitation

This model was developed between 1991 and 1997 within the framework of the programme IDNDR and it was implemented at the ZAMG in Vienna from April 1997 onwards for the use of predicting convective precipitation. The calculations have been done with this model (HAIDEN and PICHLER, 1997). Since in the warm season the main interest focuses on short durations (*D < 12 hours*) a non-stationary, orographic-convective model performs the calculations in this particular case („OKM“). The essential factor when calculating convective precipitation is to grasp the formation of clusters in the precipitation fields, as well as the knowledge of altitude dependency as precisely as possible. In order to achieve an explicit calculation, the suitable resolution of digital area data in a high resolution is necessary. Not a single point value from a certain slope and altitude, but their mean values over a larger area is decisive for orographical enhancement of precipitation. The area altitudes which are used in the model OKM in a resolution of about 1.5 km were obtained by a mean value of the data from a digital area model with a very high resolution. The actual model domain for calculation spans from 9 - 18 degrees E and 40 – 50.5 degrees N. Generally, the resolution of OKM is 1/80 degree meridional (about 1.38 km) and 1/48 degree longitudinal (1.55 km).

The OKM model is time dependent, and it calculates the local orographical-thermal forcing of convective formation of clouds and precipitation over complex landscapes, interacting with the synoptic fields. It can be applied on topography of any steepness and height, since the model topography is separated into a “basic topography” and a “relative topography”. The “basic topography” corresponds to the main mountain body and can be seen as an imaginary connection area between the valley grounds and bigger valleys, or as a lower boundary surface of topography.

The maximum inclinations of basis topography are considerably lower than those of the total topography. This fact makes possible the use of a local, one-dimensional mixing layer formula to obtain a model of the boundary layer construction. The volume effect of relative topography in the boundary layer has got consequences, and it is actively taken into consideration.

For practical reasons, we chose 00 UTC as a starting point for our daily model calculation, since radio sondes data (from Vienna, Budapest, Budejovice, Prague, Munich , Payerne, Udine and Zagreb) is available for this time. For initialisation, we use the radio sounding observations and the synop stations from the domain. At first, the 00 UTC radio sounding profiles of temperature and dewpoint are horizontally interpolated. The next step is to process the temperature and dew point values observed at 00 UTC of those stations at valley level. They are interpolated, their altitude is taken into consideration and they are used for a suitable correction of temperature and humidity conditions close to the ground. In a third step, we calculate which values are supplied by the three-dimensional initiation fields of temperature and humidity of mountainous stations. From the difference to the actual measured values, we produce three-dimensional correcting fields. Synoptic scale advection processes have to be taken into consideration in free atmosphere during the forecast period, so we include additional forecasts of the ECMWF model (European Centre for Medium-Range Weather Forecasts) or wind, temperature, humidity and vertical wind velocity. These horizontally interpolated values of temperature and dew point form the initial state of the model atmosphere. The time period between 00 UTC and sunrise is treated separately, since the nightly cooling off of the boundary layer is explicitly taken into consideration. The effective long wave emission in this time period is parametrised as a function of values of temperature and dew point close to the ground. Combined with the observed morning minimum temperatures in the synoptic stations, the thickness of the cooled-off layer can be

estimated. The original vertical temperature profile thus can be modified correspondingly in the lower level of the energy balance.
As soon as the radiation balance turns positive, the growth of the convective boundary layer and the warming up of the valley atmosphere starts. The pre-defined values of the Bowen ratio (depending on the surface type) direct the split into flows of sensible and latent heat. Height and exposition are explicitly taken into consideration in the course of these calculations.

We calculate the growth of the convective boundary layer by means of mixing layer formula, and entrainment on the upper level of the layer caused by thermal and shear-induced turbulence will be taken into consideration in a simple form. To achieve integration in time, a time step of half an hour is sufficient, since a semi-analytic procedure is being used. Sensible flow of heat, starting from parts of slopes above the upper limit of the convective boundary layer, warms the corresponding layer in the valley atmosphere. If this causes an over-adiabatic lapse rate, the warming on higher layers will be redistributed in a way that the dry adiabatic lapse-rate will not be surpassed. The meso-scale distributions of the following entities will be calculated in half hour steps, according to the method mentioned above: altitude of the mixing layer, temperature within the mixing layer, power of inversion on the upper boundary of the mixing layer, water vapour mixing ratio in the mixed layer, and the cumulative heating rate of the valley atmosphere above the mixed layer. From these entities we calculate parameters necessary for the forecast of convective activity, such as the altitude of the "cumulus condensation level" or the orographically modified Showalter index as a field distribution.

The actual calculation of convective precipitation is based on a superposition of precipitation from individual, locally started, idealised convective cells. There is an explicit modelling of the dependency of the isoline distribution on translation velocity and direction of the cell, and its duration of life. It is assumed that each recently developed cell produces, in a relation to the system surrounding it, a precipitation distribution characteristic for it in space and time. This cell is guided by several parameters, which are calculated individually for each individual cell in the OKM: starting time of precipitation, altitude zLCL of starting of precipitation, maximum updraft, maximum precipitation rate, life duration parameter of a convective precipitation complex, translation velocity, translation direction. The precipitation rate of a cell is assumed to be radially symmetric, normally distributed and exponentially decreasing with time. The cell movement is calculated from the mass weighted mean wind vector in an altitude area of one to six km. The wind field used for this purpose results from a linear spatial and time interpolation of the prognosis field of the ECMWF model. In order to maintain cumulative precipitation in static systems, we have to integrate in time, taking the cell movement into consideration. Calculation of the different parameter guiding the cell precipitation is individually calculated for each cell in OKM. The time of precipitation release is estimated from the temperature of the cumulus tops on the altitude zTOP, and the vertical extension of cumulus clouds. It is assumed that the formation of precipitation in a cumulus cloud or cumulus cluster happens when it grows above the level of the - 10° isotherm, and at the same time extends over at least 2000 m vertically.

The maximum precipitation rate Pmax is dominant in the centre of the cell at the time of cell formation. It is estimated by the vertical integration of the moist-adiabatic condensation rate.

$$P_{\max} = \sum_{z=z_{LCL}}^{z=z_{TOP}} w(z)_z \cdot \rho(z)_z \cdot \left(-\frac{\delta r_s}{\delta z} \right)_z , \qquad (1)$$

w(z) is the profile of vertical velocity calculated in the "open parcel" model, ρ(z) is a mean density profile, and δrs(z)/δz is the decrease of the saturation mixing ratio with increasing altitude in case of humid-adiabatic lifting.

Determining life duration of a convective precipitation complex is extremely difficult, since it is determined by several factors working in a non-linear way. Results from numerical thunderstorm models indicate a correlation between the type of a thunderstorm and its duration, as well as a suitably selected Richardson number (the ratio of instability energy to kinetic energy of windshear). Therefore, if long life thunderstorms occur, a certain balance of the energy forms mentioned above is necessary. The life expectancy can be several hours under suitable conditions: If there is little average wind, correspondingly high point values of precipitation occur.

In case of locally limited heavy precipitation from thunderstorm cells, the combination of time in the day and synoptic forcing must not be neglected: The change in time of temperature and humidity

in the free atmosphere on a synoptic scale is taken from the corresponding prognosis fields of ECMWF by means of linear interpolation in space and time. The differences of temperature and humidity in the ECMWF field occurring between two OKM time steps are added as three-dimensional fields to the values calculated in OKM.

When interpreting observed and modelled convective precipitation, it is useful to distinguish maximum point values and areal mean values. OKM provides two precipitation fields for each date, which are to be interpreted in this way. In the following, we only focus on the field of maximum precipitation (P_{max}): For each point, it indicates what amount of precipitation is to be expected in case of thunderstorm cells moving above exactly that point with their core. This P_{max} represents a sort of maximum estimation of precipitation on the model area with a pixel size of 1.5 km x 1.5km.

A simulation of convective precipitation with a pre-defined return period

Initially, we picked any convective heavy precipitation events from the summer of 1997 and we determined their synoptic causes. In order to create a meteorological classification, we particularly used observations from radio sounding profiles on a certain date, and checked thermal instability, potential energy release, and temperature as well as humidity conditions.

To calculate typical convective precipitation in a synoptic way, we pursued a great number of test runs with the OKM model version valid since the beginning of 1998. We took care to simulate events close to the highest, still observable intensity. Starting and boundary values acceptable in model physics, such as high thermal instability, high insolation, high humidity, suitable time tendencies of these entities etc., were assumed to be „extreme“ and they produced model precipitation of various high intensities and long durations. We concluded that there would be no point in further increasing the intensities, since the model physics on which these deliberations are based are not made for this kind of procedure. The model results were adapted to the evaluation results of regions with long observation series via modified starting assumptions. This way, we made sure that the meteorological model and the observations provide adequate results. Wrong values at the observation points, caused by measurement errors were taken into consideration by a general rise of about 5 %. The physical starting conditions took shape, and eventually they supply an assumed precipitation P_{max} at a duration D of 2 and 4 hours in the OKM for Austria, once in 30 years and once in 75 years.

The precipitation P_{max} calculated at the grid point under the prerequisites above is compared to the known topography data: The results of the correlation calculation between convective precipitation and topography comprise the same area as in LORENZ and SKODA (1997, 1998, 1999). The coefficients (c_o, c_1, c_2, c_3) of a polynom regression $F(z)$, which describes the dependency of the convective precipitation amount with altitude as well as the field z_{min}, are saved.

$$F(z) = c_0 + c_1 z + c_2 z^2 + c_3 z^3 , \qquad (2)$$

z is the altitude in km, and z_{min} is the minimum altitude of all correlations within a square of 50 km length.

To produce a useful areal smoothing in the coefficient fields, we tried to recreate the initial precipitation field by regression (2). We looked for an optimum areal moving average which best describes the original fields by means of analysis of variance: The average value usable for Austria is a square of 50 km of length. The calculated precipitation values serve as initial values in equation (3).

In the following, we assume that the relations between the amount of precipitation, duration and probability of occurrence found in the framework of ÖKOSTRA –93 (1992) for partial series, are valid in their simplest mathematical form for the whole of Austria: In the programme DRA (Digitalisierung und Regenauswertung) the amount of precipitation hN is expressed as a function of the duration D and the return period T for partial series like that

$$hN(D,T) = u(D) + w(D)\ln T . \qquad (3)$$

For the simple logarithmic form of $u(D)$ and $w(D)$ in the form of

$$u(D) = a_u + b_u \ln D \qquad and \qquad w(D) = a_w + b_w \ln D \,, \tag{4.1}$$

we calculate the parameters of fitting $\boldsymbol{a_u}$, $\boldsymbol{b_u}$, $\boldsymbol{a_w}$ and $\boldsymbol{b_w}$ at the grid (1.5 km x 1.5 km) with given several realisations of precipitation fields from OKM. We smooth them overlapping in space and save them at the co-ordinates of the calculating grid (mesh width approximately 5 km x 5 km). Thus, all calculation results are transferred to the larger depiction grid (1/2 degrees longitudinally, 1/20 degrees meridionally), firstly to make links to deliberations made there easier, and secondly to dampen high frequency fluctuations. **The adaptation constants characterise the convective precipitation behaviour, and they replace measurements of precipitation**.

The double logarithmic formula for u and w, which has to be calculated in the suggestion DRA can also be easily calculated. The dependency of u and w on the duration D was mentioned in great detail in another paper (HAMMER, 1993). To avoid the weaknesses mentioned there, we tried an additional power variant:

$$u(D) = a_u D^{b_u} \qquad and \qquad w(D) = a_w D^{b_w} \,. \tag{4.2}$$

Both (4.1) and (4.2) produce results of similar quality.

That way, we can calculate the desired amount of precipitation (3). We have to take into consideration that the derived coefficients are only valid within the time spans in which the conditions of the OKM are valid. For the duration *D*, that was half a day at most, and for the return period *T* it was hundred years at most. In relevant literature, we find several indications that the exceeding probability *P* of very extreme precipitation, i.e. above the validity of common GEV formulae, can be depicted by a power function with the exponent q_s. Q_s is a parameter of an event commonly referred to as SOC-event (self-organised critical event; BAK et al., 1988). This phenomenon takes place in time series with diverging moments of a higher order, which is a direct consequence of the multi-fractality of the precipitation process (SCHERTZER et al., 1997; SCHERTZER et al., 1998). The determination of such supposedly universal entities can only be obtained after studying very long series of observations with a high resolution. Changes in the precipitation climate increase the range of insecurity. Currently, a value of around *5.2* appears to be reasonable for q_s (HUBERT, 1996; PANDEY et al., 1998; TESSIER et al., 1993; 1996). Since the inverse of the studied characteristic value - annual exceedance probability $P\ [a^{-1}]$ - can be expressed by the return period *T [years]*, we easily obtain a proportionality between extreme precipitation *hN* and the return period *T,* i.e. $hN \propto T^{1/qs} \propto T^{0.19}$.

Should you wish a calculation of design values with a return period of T > 100 [years], calculate hN(D,T=100) according to equation (3) and for T > 100 years optionally from

$$hN(D, T > 100) = \frac{hN(D, T = 100)}{4.6} \cdot \ln T \tag{5.1}$$

or

$$hN(D, T > 100) = \frac{hN(D, T = 100)}{2.4} \cdot T^{0.19} \,. \tag{5.2}$$

Finally, compare the result with the wrapping record curve (JENNINGS, 1950; MARX, 1969; WIESNER, 1970; HUBERT, 1996; STADELBACHER, 1998; SCHINDLER, 2000)

$$hN_{RECORD} = 50.54 D^{0.5} \,, \tag{6}$$

with *hN [mm], D [minutes],* $T \to \infty$, and take care that the condition (7)

$$hN(D, T > 100) \quad \leq \quad hN_{RECORD} \tag{7}$$

is always fulfilled.

Thus we can determine a value relevant for design purposes ***hN(D,T)*** as an **area-related maximum amount of convective precipitation**. The amount of precipitation *[mm]*, calculated for the duration *D [hours]*, and the selected return period *T [years]* represents the lower limit of maximum convective precipitation, which occurs at least once within a pre-defined average area of about 25 km^2, and during a time span of *T* years.

The results range *between* the measured values obtained by the common procedures (see for example ÖKOSTRA - 93, 1992) and the theoretically biggest amounts of precipitation (PMP) and the precipitation "world records".

The heavy precipitation maps for selected duration and return periods show the maximum intensity of convective precipitation in area-related evaluation (F i g s. 3 and 4).

The procedure of indicating intensities of convective precipitation in an area-related way, and not from a measuring site punctually, has worked well in hydrology (DINGMAN, 1994; Huff 1994). A precipitation value taken from a map thus is not a punctual value. Generally, it does not correspond to the searched registered value at the precipitation measurement point chosen from a pixel. It is a function of D and T, and represents an estimation of maximum convective amounts of rain, that has been smoothed in space within an area of about 5 km x 5km. It is implicitly influenced by the surrounding topography up to a radial distance of 25 km.

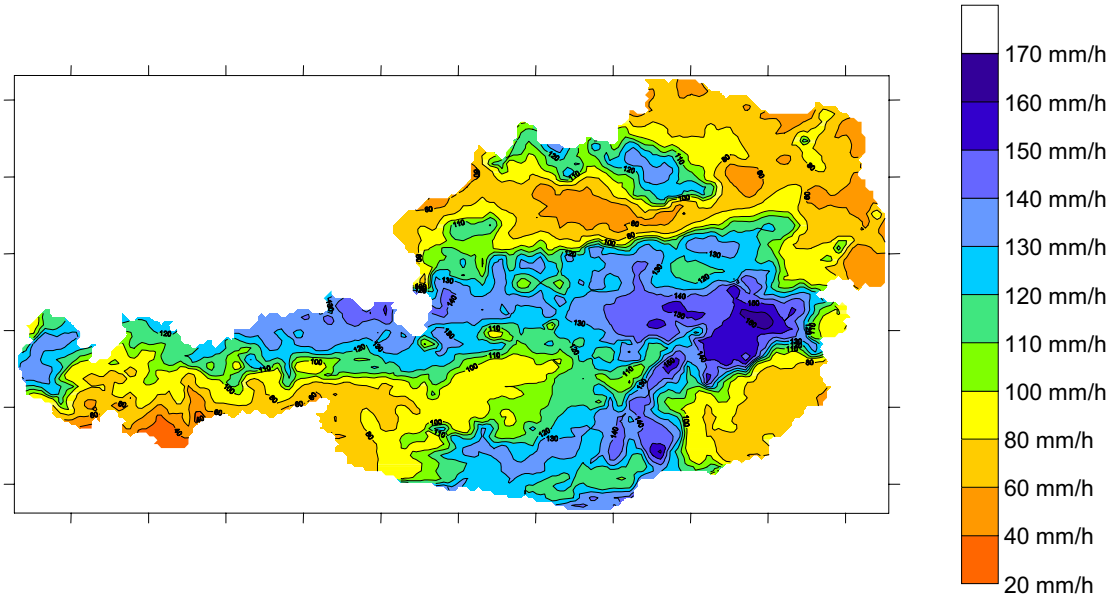

Fig. 3 Design values of maximum precipitation in Austria for D = 1 h and T = 100 a.

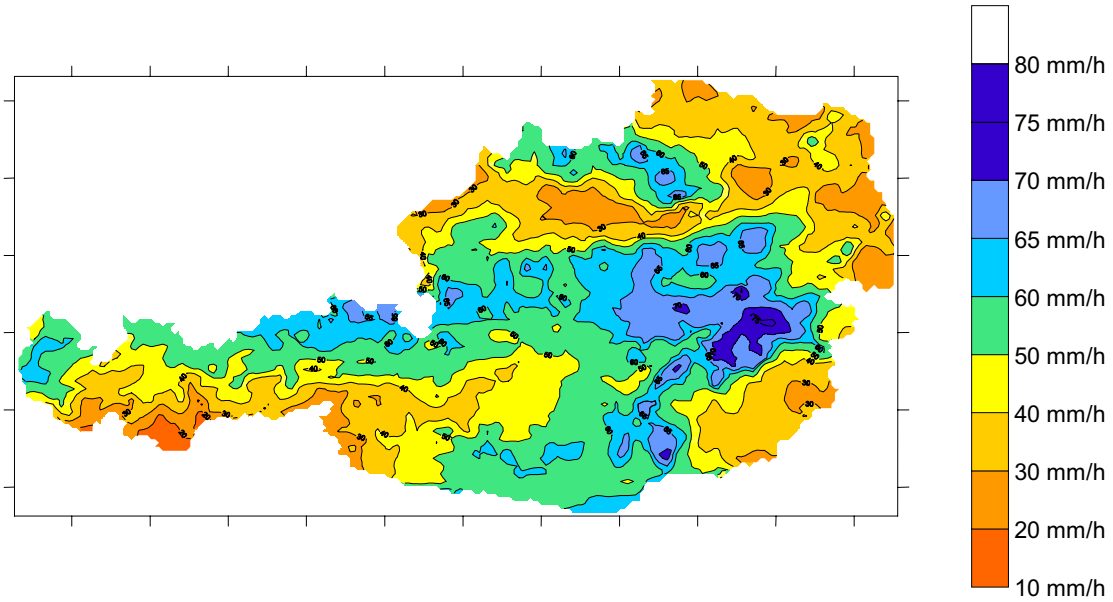

Fig. 4 Design values of maximum precipitation in Austria for D = 3 h and T = 100 a.

When applying this in practice, it is necessary to take the following into consideration: The read value represents a lower limit in time of maximum convective precipitation. It also represents an envelope surface for extreme convective precipitation within an area of 25km² – valid on a wrapping area which smoothes over all subscale maximum amounts of rain.

Since extreme precipitation events are generally insufficiently well grasped with conventional station networks, this area-relevant approach can lead to regionally higher values than usual when comparing the data with selected precipitation measurement stations.

Some caution is necessary: Meteorological forecast skill generally shows strong dependencies on spectral aspects of the atmospheric flow. The larger the scale of an atmospheric system is, the more predictable it normally is. The decrease in predictive skill starts to affect small baroclinic systems or fronts around D+2, whole cyclonic systems around D+4 and finally the long planetary waves around D +6. These large scale systems relate to the general weather type and the systems skill in predicting them means that the forecaster will be able to make useful forecasts up to a week ahead most of the time, although the timing of cyclones or fronts might be in error (ECMWF, 1999). The deterministic predictability of atmospheric structures (BOER, 1984) is strongly dependent on the spectral wavenumber „n“: The higher „n“ is, the more details are described by the model but the lesser is the overall precision of the calculated results (DALCHER and KALNAY, 1987). Therefore meso-scale modelling usually crashes after a time span of approximately 48 hours.

CONCLUSION

There are three different concepts of how to treat the complexity of the physical system „water cycle“ (MÖLDERS, 2001):

- parameterization of subsurface and surface hydrological processes in the atmospheric model,
- one-way or two-way coupling of hydrological and atmospheric models by data exchange, and
- direct coupling of hydrological and atmospheric models by use of a common intersection.

The latter seems to be the most advantageous way to realize the coupling between hydrological and meteorological models, because such a realization provides i.a. an optimized physical consistency between the models. Meteorological modelling of all kinds is a rapidly developing field and possibly this development will also be a significant stage in the progress of hydrology.

REFERENCES

Ahrens, B., Y. Wang, and K. Jasper (2001) On ALADIN quantitative precipitation forecasts in Vienna. ALADIN newsletter.

Ahrens, B. and K. Jasper (2001) Precipitation modelling in an Alpine catchment. Poster, presented at EGS, XXVI General Assembly, session OA16, Nice France, 25-30.

Boer, G.J. (1984) A spectral analysis of predictability and error in an operational forecasting system. Mon. Weather Rev. 112, 1183-1197.

Dalcher, A. and E. Kalnay (1987) Error growth and predictability in operational ECMWF forecasts. Tellus 39A, 474-491.

Dingman, s. L. (1994) Physical Hydrology. Prentice-Hall Inc., New Jersey 07458, USA.

ECMWF (1999) User guide to ECMWF forecast products, § 3.1. Reading.

Haiden, T. (1994) Eine optimierte Starkniederschlagsauswertung. Teil IV: Niederschlagsinterpolation unter Berücksichtigung orographischer Effekte. Mitt. Hydr. Dienst in Österr. 72, 47-62.

Haiden, T. und R. Pichler: IDNDR - Mesoskaliges Kurzfrist-Vorhersagemodell.

Projektteil: Analytisch-numerische Simulation extremer Niederschlagsereignisse im mesoskaligen Bereich. Aus: SKODA, G. (Ed.): IDNDR-Tätigkeitsberichte zu den Phasen I bis VII (1991 bis 1997), Abschließender Bericht zu Phase VII. IMG der Universität, Wien1997.

Hammer, N.((1993) Eine optimierte Starkniederschlagsauswertung. Teil III: Optimierung - Erstellung von Regenhöhenlinien und Regenspendenlinien. Mitt. Hydr. Dienst in Österr. 69, 43-58.

HUFF, F. A. (1994) Record-breaking microstorm system supports new rainfall frequency estimates in Illinois. Bull. AMS, 75, 7, 1223 - 1226.

Lorenz, P. und G. SKODA (1997) Ermittlung von Flächenmitteln des Niederschlags aus punktuellen Messungen. Forschungsbericht beim BMLF, Abt. IV A 3, Wien.

Lorenz, P. and G. SKODA (1998) Aerea means of precipitation calculated from isolated measurements. 2nd European Conference On Applied Climatology (ECAC 98), 19 to 23 Oct. 1998, Vienna. Österr. Beiträge zu Meteorologie und Geophysik, Heft 19, CD-ROM, Wien.

Lorenz, P. und G. SKODA (1999) Ermittlung von Flächenmitteln des Niederschlages aus punktuellen Messungen. Mitt. Bl. d. Hydrographischen Dienstes in Österr. 78, 47-65.

Lorenz, P. und G. Skoda (2000) Bemessungsniederschläge kurzer Dauerstufen (D ≤ 12 Stunden) mit inadäquaten Daten. Mitt. Bl. d. Hydrographischen Dienstes in Österr. 80, 1-24.

Lorenz, P. und G. Skoda (2001) Bemessungsniederschläge auf der Fläche für kurze Dauerstufen (D ≤ 12 Stunden) mit inadäquaten Daten. ÖWAV-Seminar-2000. „Wiener Mitteilungen; Wasser-Abwasser-Gewässer“, Technische Universität Wien.

Mölders, N. (2001) Concepts for coupling hydrological and meteorologcal models. Wiss. Mitt. Inst. für Meteorologie, Univ. Leipzig (VI), 22, 1-15, Leipzig.

ÖKOSTRA-93 (1992) Österreichische koordinierte Starkniederschlagsregionalisierung und Auswertung. Heft 3 (Ed. G. SKODA): Eine optimierte Starkniederschlagsauswertung. Forschungsbericht, BMLF, Wien.

Skoda, G. (1993a) Eine opimierte Starkniederschlagsauswertung. Projektbericht. Mitt. Hydr. Dienst in Österr. 69, 26 - 28.

Skoda, G. (1993b) Eine optimierte Starkniederschlagsauswertung. I: Erste Erfahrungen mit ÖKOSTRA-93. Mitt. Hydr. Dienst in Österr. 69, 29 - 32.

Skoda, G. (1993c) Eine optimierte Starkniederschlagsauswertung. II: Digitalisierung und Regenauswertung. Das Programmpaket DRA. Mitt. Hydr. Dienst in Österr. 69, 33 - 42.

Univ.-Prof. Dr. Georg Skoda
Institute of Meteorology and Geophysics of the University of Vienna
U Z A II
Althanstraße 14
1090 Wien
Austria

georg.skoda@univie.ac.at

Generation of hydrometeorological reference conditions for the assessment of flood hazard in large river basins (Proceedings of International Workshop, Koblenz, 6. and 7. March 2001). CHR-Report No. I-20

Precipitation scenarios from expanded downscaling

G. Bürger
Potsdam Institute for Climate Impact Research (PIK)
Potsdam, Germany

Abstract It is well known that climate models are incapable of simulating the small scale effects that lead to extreme precipitation events. On the other hand, each local weather record is strongly conditioned upon the state of the large-scale, atmospheric circulation. This enables the use of statistical models such as linear regression to simulate local weather from the circulation, i.e., define a 'downscaling'. However, limited correlations between the large and the small scales render all such deterministic approaches useless as the simulation of local variability and, related to that, extreme events is unrealistic. A modification of the classical regression scheme of unconditional error minimization leads to the so-called expanded downscaling' (EDS). EDS results from relaxing that scheme to allow for the preservation of local covariance, and thus enables the realistic simulation of local variability from the observed circulation, including extreme precipitation. If the circulation characteristic changes, for example in a modified climate, the EDS-simulated local characteristics will change accordingly. Prior to any EDS application all variables have to be normalized to Gaussian quantities. This is achieved using the **prob**ability **i**ntegral **t**ransformation (probit). The probit is an optimized form of the transformation techniques commonly applied in weather generators. For each process x it renders, on the one hand, a set of parameters defining the climatology of x (which for Gaussian x is just the the classical mean and variance). On the other hand it defines, in a 1-1 fashion, a N(0,1)-distributed process which serves as input to the EDS module. The statistics of extreme events is mainly determined by the probit parameters and therefore heavily depends on their correct estimation. Climatic change is treated as an anomaly in the normalized series. We will show precipitation scenarios for the Saar derived from the 'business-as-usual' simulation of the Hamburg climate model
Keywords: precipitation scenario, statistical downscaling, extreme events, flooding.

INTRODUCTION

The modified radiative balance of a CO_2-enriched atmosphere warms the ocean surface and intensifies the global hydrological cycle through increased evaporation. But since highly nonlinear, turbulent effects dominate the formation of clouds and precipitation it is not very likely that this happens spatially homogeneous. It will instead show marked regional differences, with a tendency to dryer conditions in some regions and wetter conditions in others.

Global warming scenarios of current climate models (General Circulation Models, GCMs), being unable to resolve the small, turbulent scales, are not particularly unique in defining those regions (cf. *http://ipccddc. uea.ac.uk*); even undisturbed ('control-') model climates of precipitation tend to show large errors (relative to observations). These facts do not contribute very much to model credibility, nor do they allow for a thorough assessment of climatic change under hydrological terms. To fill the gap between large-scale GCM dynamics and local observations of small scale weather features, the method of *downscaling* can be applied. Numerous forms of downscaling exist which can be

by, for example, whether they are dynamically or empirically based, whether they use daily or monthly time steps, or whether they generate point or areal scenarios. Here we will focus on, and briefly describe, expanded downscaling which is an empirical method that generates point scenarios on a daily time scale.

Although considerable progress has been obtained during the last decade in applying downscaled GCM simulations to river catchments, the problem of extreme and rare events is still a matter of ongoing research. Floods and droughts are such events, and they are the visible consequences of what can be called the *non-Gaussian* and *intermittent* behavior of precipitation. The global atmospheric fields, on the other hand, are neither non-Gaussian nor intermittent, a fact which complicates the downscaling problem considerably.

Midway between deterministic, regressional techniques and stochastic, weather generating schemes lies the method of expanded downscaling (EDS, Bürger 1996). EDS modifies the classical regression principle by relaxing the condition of *absolute error minimization* to allow for a side condition to be satisfied, which for EDS is the preservation of local variability. In this way, a *constraint minimization problem* is defined that has a unique solution model to which we refer as expanded downscaling (a better name would be 'expanded regression').

EDS has been applied in a number of studies as a method to derive daily weather from large-scale atmospheric fields (Bürger 1996, Dehn et.al. 2000, Müller-Wohlfeil et.al. 2000). In this article we describe an example of the simulations that were undertaken for the European project EUROTAS (**EUR**opean River Flood **O**ccurrence and **T**otal Risk **A**ssessment **S**ystem). EUROTAS was aimed at assessing flood risk across Europe, including the effects of environmental change. It included 5 case studies (catchments) for which runoff models were driven by EDS-simulated climate scenarios; see Bronstert et.al. (2000). The model requirements for the simulation of extreme precipitation statistics are significantly stronger compared to average statistics, so that EDS had to be adapted and fine-tuned quite a bit.

Extreme precipitation involves so many local and strongly nonlinear phenomena that no one can infer with certainty how their statistics will be affected by climatic change. Any projection of extreme precipitation derived from a global climate scenarios, like ours, is therefore loaded with considerable uncertainty.

EXPANDED DOWNSCALING

For brevity, we merely describe those EDS ingredients which differ from the standard regression model. In modification of the classical regression scheme, the EDS model is determined as a statistical linear relationship **L** between the large-scale atmospheric input, **g**, and the small-scale weather output, **l**, in the following way:

$$\min\left\{\left\langle \left|\mathbf{l}-\mathbf{L}\mathbf{g}\right|^2\right\rangle\right\}$$
$$S=\left\{L\middle|\, LC_g\,L^T=C_l\right\} \tag{1}$$

where $\mathbf{C_g}$ and $\mathbf{C_l}$ denote the respective covariances. This defines a linear model that minimizes the expected model error - like regression, but only under the side condition that the modeled covariance be identical to the observed. Note that the preservation of covariance only applies to the observed forcing fields (from the calibrating set); when driven by a GCM, for example, or in a modified climate, the simulated covariance may change accordingly. For details please consult Bürger (1996).

As for any linear model, EDS applies to *anomalies* only. In the normalization step, observed and simulated precipitation series are scaled in a 1-1 fashion using a nonlinear transformation. A generic form of this is the **prob**ability **i**ntegral **t**ransformation (probit, Ledermann 1984). The probit is basically identical to the cumulative distribution function (*cdf*) of the quantity combined with the normal *cdf*. For discrete quantities the probit is discrete as well, and the main difficulty is to find a smooth fit (to which we refer equally as the 'probit'). For this purpose we have used special classes of nonlinear functions (power and exponential) allowing for 3 parameters. The probit renders, for each

local variable, a small set of parameters that completely (up to the second moment) describe the climatology of that variable, along with a time series of a N(0,1) distributed variable that is in 1-1 correspondence to the original variable. This also includes the annual cycle, since we determined the probit for each month separately. EDS solely operates on the normalized series, and climatic change is modeled as an *anomaly* about the fixed seasonal climatology. Drastic changes of climate are therefore beyond the scope of EDS.

Please note that we present here an updated version of the EUROTAS results. It is beyond the scope of this article to describe in detail the modifications of the down-scaling scheme since the start of EUROTAS. Besides several minor technical details a major improvement was achieved through a refined treatment of the annual cycle. More importantly, we have now included atmospheric humidity as a forcing field, as described in the next section.

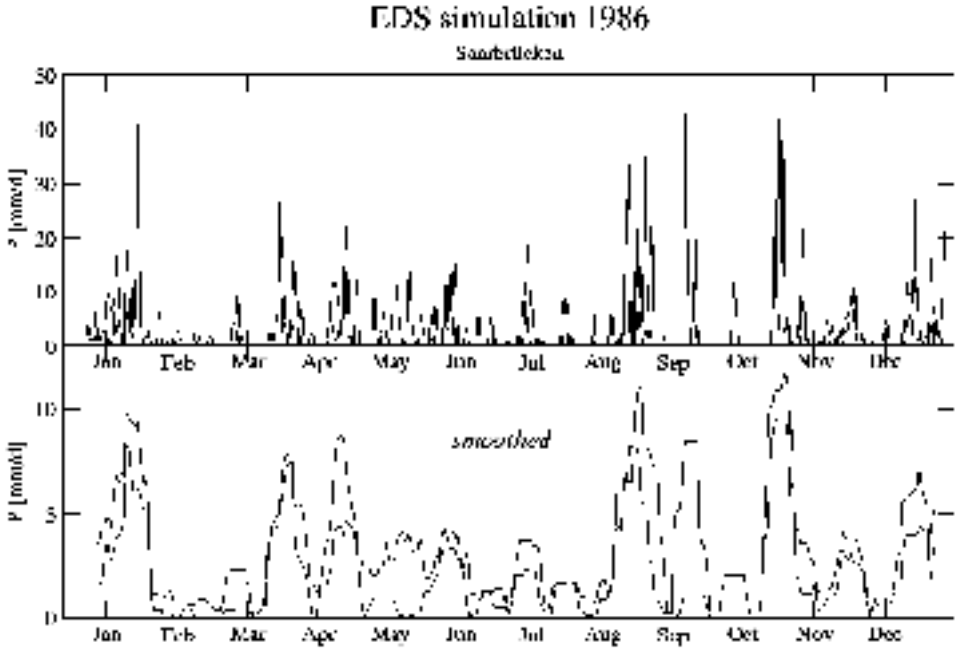

Fig. 1 Upper panel: Observations vs. simulation for daily precipitation at Saarbrücken, for the year 1986. Scale and variability appear realistic. From the extraordinary double event in September/October, with an intermediate dry spell of one month, the second is simulated with good accuracy. The first is not simulated at all, and during the dry spell a short period of rain is simulated. From the filtered curve (lower panel), using a moving average of 11 days, it appears that rainfall clusters are reproduced quite well.

AN APPLICATION FOR THE SAAR

From the EUROTAS catchments we report results for the Saar river catchment here in more detail. The river belongs to the Rhine tributaries that in the 1990s experienced many extraordinary floods, like those of 1993 and 1995 which are among the three largest floods of the entire record. As EDS respects covariability it is desirable to include as much from the catchment observations as the computational complexity (mainly Eq. (1)) allows. Accordingly, we simultaneously modeled daily values of temperature, relative humidity, insolation, and wind, along with the record of 11 precipitation stations.

Calibration and validation of EDS

If not indicated otherwise, EDS was calibrated using the WMO base period of 1961-90. This applies to the calculation of the annual cycle and its anomalies, the subsequent EOF calculation, the

normalization step of the local variables, and the EDS parameters. Any simulated climate change must be regarded relative to this base climate.

Observed circulation The global atmospheric fields were taken from the NCEP reanalysis from which we selected the sections defined by the rectangle between the edges (10W,40N) and (20E,60N). As predictors we chose a field mix of

- 500hPa geopotential height (HGT)
- 850hPa temperature (TMP)
- 700hPa specific humidity (SPH)

Both fields were projected onto the major principal components so that they hold 99% of the variance, respectively 90% for SPH. The components (40 as a whole) were scaled to ensure that each field contributes equally to the final predictor variance.

To illustrate the working of EDS we depict simulation results for the precipitation record of Saarbrücken. For this purpose, EDS was calibrated for the period 1961-75, and Figure 1 shows daily values of observations vs. simulations for the year 1986. This year reflects typical features of the local climate together with its simulation. Moreover, it contains a remarkable sequence of events in September/October: A heavy double-event is followed by a month-long dry spell that is ended by another heavy event. The second event and the dry spell are reproduced quite well by the EDS model, while the first is simulated only with half the scale. Generally, precipitation clusters are reproduced satisfactory, as can be seen from the moving average using a window of 11 days.

Application to simulated circulation (climate scenarios)

The IPCC emission scenario IS95a, usually termed 'business as usual', is taken as the basic forcing for the climate change scenarios. The Max-Planck Institute (MPI) at Hamburg, Germany, conducted a climate simulation for the years 1860-2100, where the emissions were chosen from historic measurements for the period 1860-1990 and from IS95a for the remaining period, respectively. Evolutions of aerosols were not included. The simulation was done by the global atmosphere-ocean model ECHAM4/OPYC3, which represents the current version of the MPI climate model development. With this model, an additional 300-year control simulation without any extra forcing was conducted. A simulation of this kind is particularly valuable as it is the major, perhaps the only, source of information about the natural variability of the climate system. Fluctuations associated with longer time scales and how they are transformed to the local weather will be reflected by this simulation. A comprehensive description of the ECHAM4/OPYC3 is given by Roeckner et.al. (1996).

To apply the downscaling we select from the daily model grid the same North Atlantic/European section that was used for calibration with the NCEP fields, and interpolated them onto the same grid. Finally we projected the GCM fields onto the leading EOFs of the NCEP fields. The model climatology relative to which we calculate anomalies is determined from the period 1961-90 in the IS95a case and from an arbitrary 30-year period in the control case. These anomalies are fed into the EDS, which outputs a weather scenario that is consistent with the global climate scenario.

In Figure 2 we see annual values of 4 different precipitation series: **OBS** denotes direct observations, while the other denote downscaled values from the following global fields: observations (analyses) (**ANA**); simulated fields from the GCM control run without extra forcing (**CTL**), and the scenario A simulation IS95a of the GCM (**SCA**). Of course, the GCM-induced scenarios are completely decoupled of any actual observations, so only the simulated scale and variability are relevant. A clear signal can be observed in the annual averages (lower panel), which varies about 2.5 to 3 mm/d and in creases by about 1 mm/d until the end of the century. Scale and variability of the other simulations appear realistic. For the annual extremes (upper panel) there is no obvious trend. But note that extremes in the range 30-50 mm/d seem to become rare in the next century, and are being replaced by larger amounts (see below). The maximum simulated extremes above 100 mm/d (in **ANA** and **CTL**) do not show a significant trend, nor do they have any counterpart in observations.

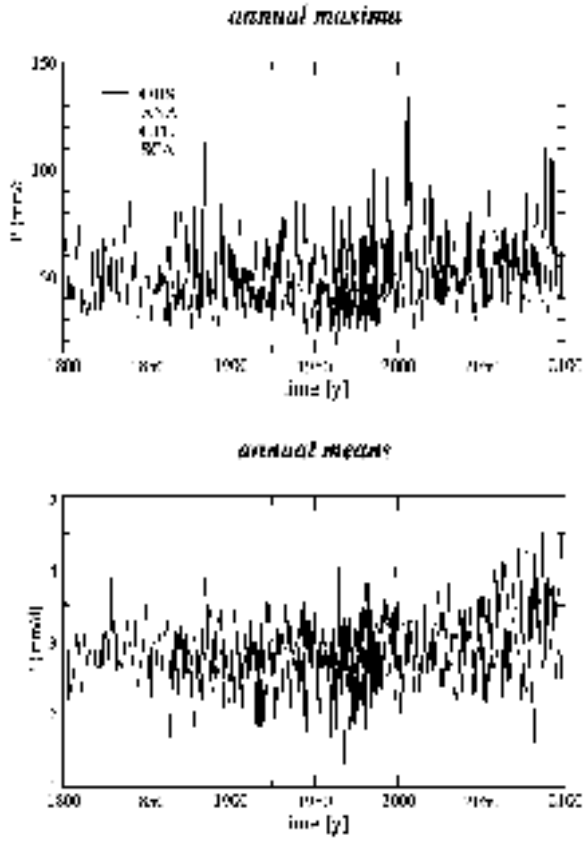

Fig. 2 Annual values of daily precipitation for **OBS, ANA, CTL** and **SCA**. Annual means (lower panel) show a clear positive trend for the 21 st century. Maxima (upper panel) appear more stationary, with a slight increase after 2050 for medium scales.

Summary statistics

In the assessment of climate change it is important to know if one can distinguish, for a given climate scenario, a significant change in the statistics. The term 'significant' relates the scenario to what can be called the 'background noise', which is composed of natural climate variations and model errors. In our case, this noise is made up of the 3 ingredients **OBS, ANA**, and **CTL**. We used 3 parameters summarizing the daily precipitation statistics: The mean precipitation, *m*, the wet day probability, *p*, and the intensity, *i*. We estimate them for the winter (October - March) and summer (April - September) season separately. The significance analysis requires a comparison of **OBS**, **ANA**, and **CTL** statistics on the one hand and those of **SCA** on the other. For **SCA**, we calculate statistics of the period 2061-2090, to which we equally refer to as **SCA**. The underlying uncertainty comes from an accumulation of *internal* variances in **OBS**, **ANA**, and **CTL**, along with the differences *between* **OBS**, **ANA**, and **CTL**. We have estimated this uncertainty in a rather simplified fashion by forming the enlarged sample **OBS+ANA+CTL** and comparing its properties, mainly *m, p,* and i, against the **SCA** sample.

Specifically, we formed annual values of *m, p*, and *i* and tested if their sample distributions are significantly equal or not, using the Kolmogorov-Smirnov test. The result is shown in Table 1, separately for the winter and summer season. We highlight those **SCA** values which have significantly changed, using a 1% significance level. Basically, the scenario simulates wetter conditions for both seasons. Rainfall intensity is significantly higher in both seasons, while mean rainfall is higher in winter. Rainfall probability does not change significantly. But again, recall that test design and significance analysis are rather simplistic and open to critique.

Table 1 Summary statistics (see text) of the EDS simulations. Bold blue numbers indicate significant departure of the scenario **SCA** from the joint distribution of **OBS+ANA+CTL**, after Kolmogorov-Smirnov. For winter, this is the case for the mean as well as the intensity, which are both increasing. For summer, rainfall intensity is significantly increasing.

winter	**OBS**	**ANA**	**CTL**	**SCA**
m	2.9	3.2	3.1	4.1
p	52.2	51.0	52.9	54.2
i	5.5	6.3	5.8	7.4
summer				
m	2.5	2.7	2.6	3.1
p	45.1	47.6	47.2	48.3
i	5.6	5.8	5.5	6.5

Extreme value statistics

The cumulative distribution function (*cdf*) of a quantity *q* empirically combines scale and probability of *q*, the latter conveniently being measured in terms of return periods. In our study we have generally refrained from estimating return periods exceeding the length of the base period of 30 years. For example, from the 300 year period of the downscaled control run we are formally able to estimate return periods of comparable length. However, those scenarios depend on the probit estimate and, consequently, on the base period. Likewise, one can formally extrapolate 30-year return periods to longer ones by using certain smoothness assumptions on the *cdf*. While estimates of extreme value statistics are quite uncertain anyway, such techniques expand the uncertainty level into *unknown* magnitudes.

By employing long simulations like the 300 year control run for smaller return periods it is possible to give more precise estimates of the corresponding uncertainty level. Subdividing the 300-year period of the con trol run into 10 30-year sections renders an entire sample of empirical *cdf's*. This sample of *cdf's* represents the natural fluctuations as they are simulated by the GCM.

The analysis is again conducted for the winter (October - March) and summer (April - September) season separately. Figure 3 shows the empirical *cdf's* of **OBS**, **ANA**, **CTL**, and **SCA**. This amounts to 13 datasets, each representing 30 years of daily precipitation. The prominent impression of both figures is the wide spread of the **CTL** *cdf's*, in particular with respect to the large scales. This marks the major source of uncertainty for signal detection. However, for moderate scales with return periods of less than 3 years one can distinguish a clear signal for both seasons. In particular for winter an intensification of rainfall is projected by **SCA** (see former section). For example, the 1-year event increases by about 10 mm.

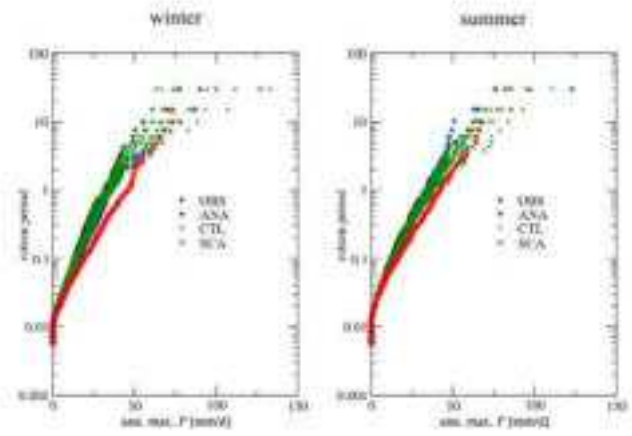

Fig. 3 Return periods for extreme precipitation. The large spread for the strong events, i.e. the major source of uncertainty, arises from natural fluctuations - as simulate by **CTL**. The model error (= difference between **OBS** and **ANA/CTL**) is relatively small. A significant increase exists for moderate return periods of about 1 y, especially for winter (left panel).

CONCLUSIONS

We have presented contributions to a recent 3-year European project on flood risk assessment, called EUROTAS. They consisted of scenarios of daily precipitation for the next 100 years, based on the IS95a emissions scenario of the IPCC and the corresponding simulation of the climate model ECHAM4/OPYC3. This global climate scenario was regionalized using the method of expanded downscaling (EDS) and applied to a number of river catchments across Europe that served as case studies for EUROTAS. For the purpose of this article we repeated the applications for the Saar river, applying several refinements that were added since the end of the project, most notably the inclusion of atmospheric humidity as a driving force. This improved the downscaling considerably, and because atmospheric humidity bears a strong and independent climate change information the overall uncertainties could be reduced as well, relative to EUROTAS.

The Saar case showed EDS to be capable of reproducing precipitation clusters satisfactory when driven by observed atmospheric fields. When driven by simulated fields, the EDS-weather had realistic scale and variability. There was a clear positive trend in mean annual precipitation for the downscaled version of the IS95a climate scenario. A rather basic significance analysis using daily summary statistics supports this view. It reveals a significant shift to more intense rainfall, accompanied with enhanced mean precipitation for winter. This is reflected in the extreme value statistics. The rare events show a large spread across all scales. It turned out that natural fluctuations, as they are simulated by the GCM control run, are the major source of uncertainty for those events. For more frequent ones, such as a 2- or 3-year event, an intensification is projected, in particular for winter.

We emphasize again that the climate projections depend in a cumulative manner on a cascade of imperfect models. Therefore, they have to be taken with great caution. Simulations of other global climate models will improve the significance of the results. But one should always keep in mind that the estimated uncertainty level represents a lower bound for the true uncertainty.

REFERENCES

Bardossy, A., and E. Plate (1992) Space-Time Model for Daily Rainfall using Atmospheric Circulation Patterns. Wat. Resources Res. 28, 1247-59.

Bronstert, A., C. Bismuth, L. Menzel (eds.) (2000) European Conference on Advances in Flood Research, Proceedings (Vol. 1 - Vol. 2). Summary Report 65. Potsdam-Institute for Climate Impact Research, Potsdam, Germany.

Bürger, G. (1996) Expanded downscaling for generating local weather scenarios. Clim. Res. 7, 111-28.

Dehn, M., G. Bürger, J. Buma, and P. Gasparetto (2000) Impact of climate change on slope stability using expanded downscaling. Engineering Geology 55, 193-204.

Giorgi, F., and L. O. Mearns, C. Shields, and L. McDaniel (1998) Regional nested model simulations of present day and 2 x CO_2 climate over the central plains of the US. Climatic Change 40, 457-93.

Ledermann, W. (Ch. Ed.) (1984) Handbook of Applicable Mathematics A, VI. Wiley & Sons, Chichester.

Müller-Wohlfeil, D. I., G. Bürger, W. Lahmer (2000) Response of a River Catchment to Climatic Change: Application of Expanded downscaling to Northern Germany. Climatic Change 47, 61-89.

Roeckner, E., Oberhuber, J.M., Bacher, A., Christoph, M. and Kirchner, I. (1996) ENSO variability and atmospheric response in a global coupled atmosphere-ocean GCM. Climate Dynamics, 12: 737-754.

Dr. G. Bürger
Potsdam Institut für Klimafolgenforschung (PIK)
Telegrafenberg C4
Postfach 60 12 03
D-14412 Potsdam
Gerd.Buerger@pik-potsdam.de

Generation of hydrometeorological reference conditions for the assessment of flood hazard in large river basins (Proceedings of International Workshop, Koblenz, 6. and 7. March 2001). CHR-Report No. I-20

Rainfall generator for the Rhine basin: multi-site simulation of daily weather variables by nearest-neighbour resampling

Jules J. Beersma, T. Adri Buishand and Rafał Wójcik
Royal Netherlands Meteorological Institute (KMNI)
DE Bilt, The Netherlands

Abstract Nearest-neighbour resampling is used here for the joint simulation of daily rainfall and temperature at 36 stations in Germany, Luxemburg, France and Switzerland all situated in the Rhine basin. The daily temperatures are used to determine snow accumulation and melt in winter. A major advantage of a non-parametric resampling technique is that it preserves both the spatial association of daily rainfall over the drainage area and the dependence between daily rainfall and temperature without making assumptions about the underlying joint distributions. Both unconditional simulation of daily rainfall and temperature and conditional simulations of these variables on the atmospheric flow are discussed. In particular the unconditional simulations reproduce the standard deviations and autocorrelation coefficients and properties of extreme 10-day rainfall and snowmelt well. The largest 10-day rainfall amounts in 1000-year simulations are up to 40% larger than those in the historical record (1961-1995).

INTRODUCTION

The Rhine is the most important river in the Netherlands. Large parts of the river, which originates in the Swiss Alps, are situated in Switzerland, Germany, France and the Netherlands. Small parts of Austria, Belgium and almost the whole country of Luxemburg also drain to the river. Protection against flooding is a point of continuous concern. According to safety standards, laid down in the Flood Protection Act, measures against flooding in the non-tidal part of the Rhine in the Netherlands have to withstand a discharge that is exceeded on average once in 1250 years. Traditionally this design discharge has been obtained from a statistical analysis of peak discharges at Lobith, where the river enters the country. Several probability distributions have been fitted to the discharge maxima of that record. The long return period requires an extrapolation far beyond the length of the observed discharge record. Different distributions then usually lead to quite different design discharges.

During a re-evaluation of the design discharge at Lobith, there was a strong feeling that the uncertainties of extrapolation could be reduced by taking the physical properties of the river basin into account. It was suggested to develop a hydrological/hydraulic model for the whole basin. The development of a stochastic rainfall generator was also required in order to produce long-duration rainfall series over the basin. The use of synthetic rainfall series in combination with a hydrological/hydraulic model does not only provide the peak discharges but also the durations of these extreme events. This may lead to a better insight into the profile of the design flood.

In this paper nearest-neighbour resampling models are considered for simulation of multi-site daily precipitation and temperature time series in the Rhine basin. Temperature is needed to account for the effects of snow(melt) and frozen soils on large river discharges. The reproduction of second-order moment statistics of temperature and precipitation and properties of extreme winter precipitation and snowmelt are examined. Results of 1000-year simulations with these models are presented. In these simulations much larger multi-day precipitation maxima occur than the historical ones. More details,

including several alternative nearest-neighbour resampling models, can be found in Wójcik *et al.* (2000).

NEAREST-NEIGHBOUR RESAMPLING

Nearest-neighbour resampling was originally proposed by Young (1994) to simulate daily minimum and maximum temperatures and precipitation. Independently, Lall and Sharma (1996) discussed a nearest-neighbour bootstrap to generate hydrological time series. Rajagopalan and Lall (1999) presented an application to daily precipitation and five other weather variables. Basically the same method is used for generating daily precipitation and temperature in the Rhine basin. Especially for multi-site simulations summary statistics are needed to avoid problems with the high dimensional data space (Buishand and Brandsma, 2000).

In the nearest-neighbour method weather variables like precipitation and temperature are sampled simultaneously with replacement from the historical data. To incorporate autocorrelation, resampling depends on the simulated values for the previous day in the works of Young (1994) and Rajagopalan and Lall (1999). Therefore, one first searches the days in the historical record that have similar characteristics as those of the previously simulated day. One of these nearest neighbours is randomly selected and the observed values for the day subsequent to that nearest neighbour are adopted as the simulated values for the next day t. A feature vector (or state vector) $\mathbf{D}_t$ is used to find the nearest neighbours in the historical record. In Rajagopalan and Lall (1999) $\mathbf{D}_t$ was formed out of the standardized weather variables generated for day t - 1. The k nearest neighbours of $\mathbf{D}_t$ were selected in terms of a weighted Euclidean distance. For two q-dimensional vectors $\mathbf{D}_t$ and $\mathbf{D}_u$ the latter is defined as:

$$\delta(\mathbf{D}_t, \mathbf{D}_u) = \left(\sum_{j=1}^{q} w_j \left(v_{tj} - v_{uj} \right)^2 \right)^{1/2} \tag{1}$$

where v_{tj} and v_{uj} are the jth components of $\mathbf{D}_t$ and $\mathbf{D}_u$ respectively and the w_j's are scaling weights.

A discrete probability distribution or kernel is required to select one of the k nearest neighbours. Lall and Sharma (1996) recommended a kernel that gives higher weight to the closer neighbours. For this decreasing kernel the probability p_n that the nth closest neighbour is resampled is given by:

$$p_n = \frac{1/n}{\sum_{i=1}^{k} 1/i}, \qquad n = 1, \ldots, k \tag{2}$$

From the above description it is clear that apart from creating a feature vector (see Section 5), the user has to set the values of the number k of nearest neighbours and the weights w_j. A sensitivity analysis in Brandsma and Buishand (1999) showed that k = 5 usually works well. In this study we also use this value of k. A more difficult issue is the choice of the weights w_j. Tuning the weights can be very time consuming especially if the dimension of the feature vector is high. In Wójcik *et al.* (2000) an alternative approach is introduced that avoids specification of the weights by using the *Mahalanobis distance*.

DATA DESCRIPTION

Daily temperature and precipitation data from 36 stations were used. The stations are distributed all over the Rhine basin: 25 stations in Germany, 1 station in Luxemburg, 4 stations in France and 6 stations in Switzerland (see Fig. 1). For the 35-year study period (1961-1995) the data were provided by the "International Commission for the Hydrology of the Rhine Basin".

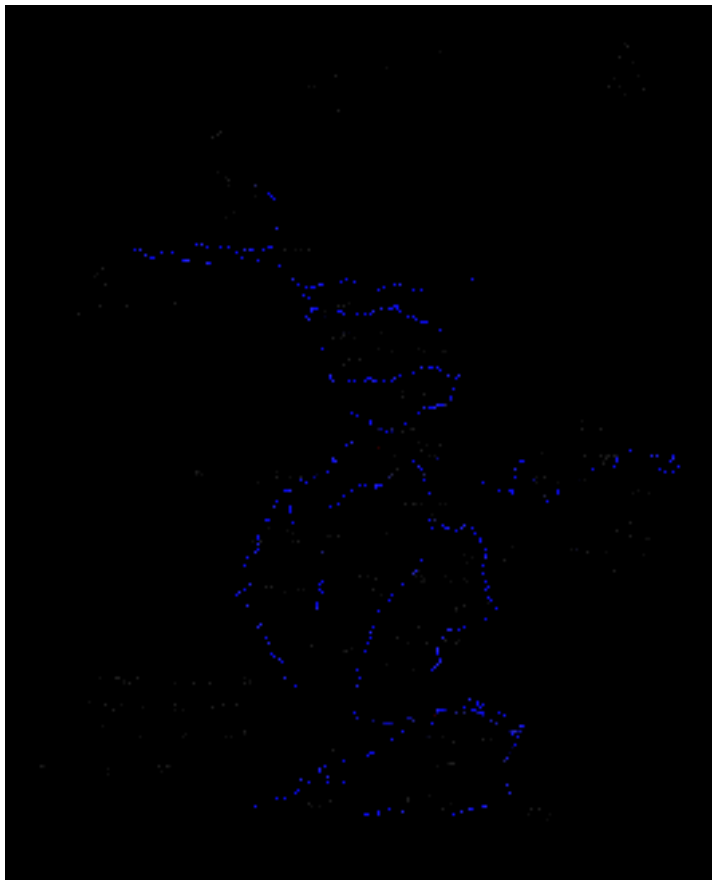

Fig. 1 Location of Lobith in the Netherlands and the 36 stations in the drainage area of the river Rhine used in this study.

Most stations in Germany, Luxemburg and France are lowland stations with annual mean rainfall ranging from 500 to 900 mm. However, two stations in Germany, Kahler Asten and Freudenstadt, have a much larger annual mean rainfall (≈1500 mm). For the Swiss stations mean annual rainfall ranges from about 800 mm for Basel to almost 2400 mm for Säntis. The latter is an exceptional station lying at an altitude of 2500 m.

Because precipitation P and temperature T depend on the atmospheric flow, three daily circulation indices are also considered: (i) relative vorticity Z, (ii) strength of the westerly flow W and (iii) strength of the southerly flow S. These circulation indices were computed from daily mean sea-level pressure data on a regular 5° latitude and 10° longitude grid. The derivation of the circulation indices is similar to that in Jones *et al*. (1993), except that the grid was centered at the Rhine basin instead of the British Isles.

STANDARDIZATION PROCEDURE

Before resampling the data were deseasonalized through standardization. The daily temperatures and circulation indices were standardized by subtracting an estimate m_d of the mean and dividing by an estimate s_d of the standard deviation for the calendar day d of interest:

$$\tilde{x}_t = (x_t - m_d)/s_d, \qquad t = 1,\ldots,365J; \quad d = (t-1) \bmod 365 + 1 \tag{3}$$

where x_t and $\tilde{x}_t$ are the original and standardized variables for day t, respectively, and J is the total number of years in the record. The estimates m_d and s_d were obtained by smoothing the sample mean and standard deviation of the successive calendar days.

Daily precipitation was standardized by dividing by a smooth estimate $m_{d,wet}$ of the mean wet-day precipitation amount:

$$\tilde{x}_t = x_t / m_{d,wet}, \qquad t = 1,\ldots,365J; \quad d = (t-1) \bmod 365 + 1 \tag{4}$$

A wet day was defined here as a day with $P \geq 0.1$ mm.

To reduce the effect of seasonal variation further, the search for nearest neighbours was restricted to days within a moving window, centered on the calendar day of interest. The width of this window was 61 days as in Brandsma and Buishand (1999).

MODEL IDENTIFICATION

The feature vector

Daily P and T observations were available for the 36 climatological stations in Fig.1 Because of their rather extreme weather characteristics, the two Swiss mountain stations Davos and Säntis are not included in the feature vector. It is, however, still possible to simulate values for these stations passively (i.e. the simulated values for the passive stations have equal historical dates as those simulated for the stations used in the feature vector). To keep the dimension of the feature vector low, a small number of summary statistics was calculated for the remaining 34 stations. Both for P and T the arithmetic mean of the standardized daily values was used. In addition, the fraction F of stations with $P \geq 0.1$ mm was considered. F helps to distinguish between large-scale and convective precipitation. To keep the notation compact, the above components of the feature vector will be referred to as a sub-vector $\mathbf{V} = \left[\tilde{P}, F, \tilde{T}\right]^T$ where the tilde indicates standardized values. In some cases, the feature vector also contains the standardized circulation indices $\tilde{\mathbf{C}} = \left[\tilde{Z}, \tilde{W}, \tilde{S}\right]^T$.

Three simulation models

Basically two different kinds of simulations can be distinguished: *unconditional* simulations and *conditional* simulations on the atmospheric flow indices.

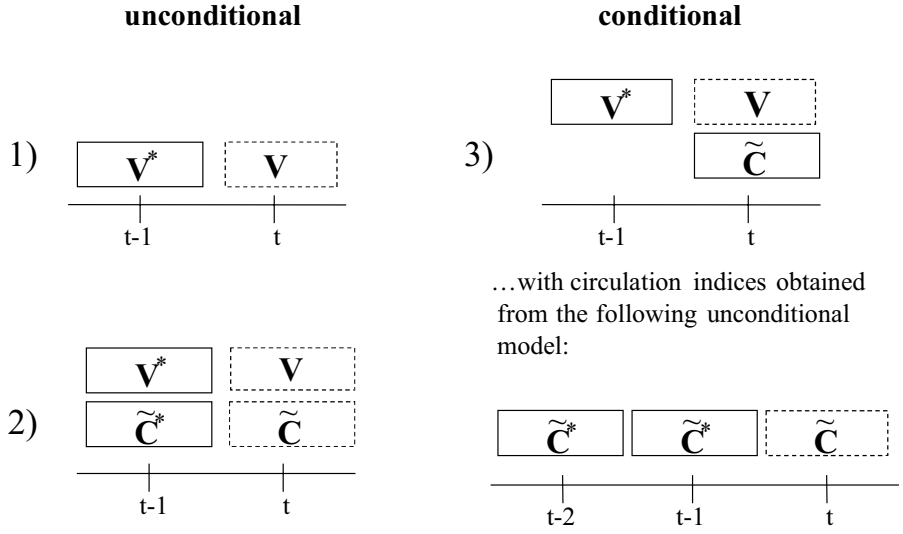

Fig. 2 Components of the feature vector (solid boxes) for unconditional simulations 1), 2) and conditional simulation 3). The dashed boxes relate to variables to be resampled. The asterisks indicate that the corresponding variables are resampled values of the previous time steps.

In the unconditional simulations the feature $\mathbf{D}_t$ comprises generated variables for the previous day as shown in Fig. 2 (cases 1 and 2). Conditional simulation on the atmospheric flow requires that the circulation indices for day *t* are included in the feature vector as schematically represented in the upper panel of case 3 in Fig. 2. The conditional model presented here uses *simulated* circulation indices obtained with a second-order model (circ2.5) described in Beersma and Buishand (1999) (see Fig. 2 lower panel of case 3). Conditional nearest-neighbour resampling is closely related to the analogue method used in climate change studies (Zorita and von Storch, 1999). Details of the three models are given in Table 1.

Table 1 Definition of models for unconditional and conditional simulation. The weights for the circulation indices apply to all three components of $\widetilde{\mathbf{C}}$. $\widetilde{P}$ and $\widetilde{T}$ denote respectively the standardized precipitation and temperature averaged over 34 stations, and *F* denotes the fraction of these stations with $P \geq 0.1$ mm. An asterisk indicates that a value was resampled in a previous time step.

Model	Elements of $\mathbf{D}_t$	Weights
unconditional		
UE	$\widetilde{P}^*_{t-1}, F^*_{t-1}, \widetilde{T}^*_{t-1}$	2,4,1
UEc	$\widetilde{\mathbf{C}}^*_{t-1}, \widetilde{P}^*_{t-1}, F^*_{t-1}, \widetilde{T}^*_{t-1}$	**1**,3,5,2
conditional		
CE	$\widetilde{\mathbf{C}}_t, \widetilde{P}^*_{t-1}, F^*_{t-1}, \widetilde{T}^*_{t-1}$	**1**,3,5,2

REPRODUCTION OF STANDARD DEVIATIONS AND AUTOCORRELATION

Extreme river discharges in the lower part of the Rhine basin are mostly caused by prolonged heavy rainfall in winter. The reproduction of the standard deviations of daily temperature and precipitation, the standard deviations of the monthly average temperature and the monthly precipitation totals, and the autocorrelation coefficients is therefore only presented for the winter half-year (October - March). To reduce the influence of the annual cycle these statistics were first calculated for each calendar month separately. For each of the 34 stations the winter estimates were obtained by taking the arithmetic mean of the six winter months (October, ..., March).

Twenty-eight runs of 35 years were generated to investigate the performance of the resampling procedure. For each station *i*, the standard deviations and autocorrelation coefficients were first estimated for each simulation run separately and then averaged over the 28 runs. The average estimates $\bar{s}_{\mathrm{D}_i}^*$, $\bar{s}_{\mathrm{M}_i}^*$, $\bar{r}_i^*(l)$ for the daily and monthly standard deviations and the lag *l* autocorrelation coefficient respectively, were compared with the estimates $\bar{s}_{\mathrm{D}_i}$, $\bar{s}_{\mathrm{M}_i}$, $\bar{r}_i\ (l)$ for the historical data. The average relative difference $\langle \Delta \bar{s}_{\mathrm{D}} \rangle$ between the observed and simulated daily standard deviation is calculated using:

$$\langle \Delta \bar{s}_{\mathrm{D}} \rangle = 1/34 \sum_{i=1}^{34} (\bar{s}_{\mathrm{D}_i}^* - \bar{s}_{\mathrm{D}_i}) / \bar{s}_{\mathrm{D}_i}\ 100\%, \tag{5}$$

with a similar equation for the average relative difference $\langle \Delta \bar{s}_{\mathrm{M}} \rangle$ of the monthly standard deviation, and:

$$\langle \Delta \bar{r}(l) \rangle = 1/34 \sum_{i=1}^{34} [\bar{r}_i^*(l) - \bar{r}_i(l)] \tag{6}$$

for the average difference $\langle \Delta \bar{r}(l) \rangle$ of the lag *l* autocorrelation coefficient.

In order to evaluate the statistical significance of $\langle \Delta \bar{s}_{\mathrm{D}} \rangle$, $\langle \Delta \bar{s}_{\mathrm{M}} \rangle$ and $\langle \Delta \bar{r}(l) \rangle$ standard errors *se* were calculated for the historical record. A criterion of 2 × *se* was used to indicate significant

differences between the historical and simulated values. Table 2 presents $\langle \Delta\bar{s}_{D} \rangle$, $\langle \Delta\bar{s}_{M} \rangle$ and $\langle \Delta\bar{r}(l) \rangle$ for the models defined in Table 1.

Table 2 Percentage differences between the mean winter standard deviations of monthly and daily values, and absolute differences between the mean lag 1 and 2 autocorrelation coefficients in the simulated time series (twenty-eight runs of 35 years) and the historical records (1961-1995), averaged over 34 stations. Bottom lines: average historical estimates (standard deviations in mm for precipitation and in °C for temperature; standard errors of standard deviations in %). Values in bold refer to differences more than 2 × *se* from the historical estimate.

	$\langle \Delta\bar{s}_{M} \rangle$		$\langle \Delta\bar{s}_{D} \rangle$		$\langle \Delta\bar{r}(1) \rangle$		$\langle \Delta\bar{r}(2) \rangle$	
Model	*P*	*T*	*P*	*T*	*P*	*T*	*P*	*T*
UE	0.3	-1.1	0.2	0.2	**-0.019**	**-0.032**	-0.001	0.006
UEc	-1.7	-8.2	-1.2	-1.9	**-0.018**	**-0.036**	0.001	-0.020
CE	-6.4	**-18.8**	-2.3	**-7.0**	**-0.052**	**-0.087**	**-0.022**	**-0.050**
Historical	35.7	2.1	4.2	4.2	0.283	0.826	0.144	0.639
se	4.53	6.16	2.45	2.49	0.008	0.007	0.009	0.015

For the unconditional model which incorporates only the large-scale features of the *P* and *T* fields (model UE) the precipitation and temperature statistics are well reproduced. A slight, though statistically significant, bias is present in the lag 1 autocorrelation coefficients. Incorporation of the circulation indices into the feature vector (model UEc) generally worsens the reproduction of daily temperature statistics. The results for precipitation are, however, similar to those obtained in the unconditional model without circulation indices. The latter insensitivity is in line with the results in Buishand and Brandsma (2000).

Conditional resampling of *P* and *T* on simulated circulation indices (model CE) lags behind. In Beersma and Buishand (1999) it was also shown that this occurs for simulations conditional on historical circulation indices. All temperature statistics and the lag 1 and 2 autocorrelation coefficients for precipitation are significantly underestimated.

REPRODUCTION OF 10-DAY WINTER MAXIMUM PRECIPITATION

Three quantities are considered to verify the reproduction of the 10-day winter maximum precipitation amounts: (i) the maximum *MAX* of the 10-day winter maxima (highest 10-day precipitation amount in the record), (ii) the upper quintile mean *QM*5 of the 10-day winter maxima and (iii) the median *M* of the 10-day winter maxima. *QM*5 refers to the mean of the data beyond the highest quintile (upper 20%).

Analogous to equation (5), we calculated for each of the three quantities the percentage differences between the values for the simulated and historical data averaged over the 34 stations. Table 3 presents the results for the three models.

There is always an underestimation of the extreme-value properties, which is, however, not more than 2% for the unconditional models. Conditioning the resampling procedure on circulation indices (model CE), results in a bit larger underestimation of the extreme-value statistics than in the unconditional cases. This is in agreement with the poorer reproduction of second-order moment statistics for conditional simulations as observed in Table 2.

Table 3 Percentage differences between the maxima (*MAX*), upper quintile means (*QM*5) and medians (*M*) of the 10-day winter (October-March) precipitation maxima in the simulated data (twenty-eight runs of 35 years) and the historical records (1961-1995), averaged over 34 stations. Bottom line: average historical estimates (mm).

Model	*MAX (%)*	*QM5 (%)*	*M (%)*
UE	-1.4	-0.6	-0.2
UEc	-0.9	-2.0	-1.9
CE	-5.5	-5.3	-4.5
Historical	138.5	111.1	75.2

REPRODUCTION OF 10-DAY MAXIMUM SNOWMELT AMOUNTS

Snowmelt generally, contributes to extreme river discharges in the lower part of the Rhine basin. It is, however, only for the highest stations Kahler Asten, Freudenstadt, Kl. Feldberg , Disentis, Davos and Säntis that a considerable part of the winter precipitation falls in the form of snow. For these six stations the reproduction of extreme-value properties of 10-day snowmelt has been analysed.

Historical estimates and simulated values of snowmelt were derived from the historical and generated daily precipitation and temperature, respectively. It was assumed that precipitation accumulates as snow if $T \leq 0$ °C. For $T > 0$ °C snowmelt is proportional to T (using a constant of 4 mm/°C). The 10-day winter maxima were taken from the calculated snowmelt amounts. As in the previous section, the statistics *MAX*, *QM*5 and *M* of these extremes were used to assess the reproduction of these maxima.

Table 4 presents the average percentage differences between the values of *MAX*, *QM*5 and *M* for the three models and the values of these statistics for the historical data for the six stations of interest. The extremes are satisfactorily reproduced by model UE. The largest discrepancies here are found for Kahler Asten and Davos (overestimation of the median of the 10-day maxima). A similar overestimation is found for model UEc. Conditional simulation (model CE) results, for most stations, in a relatively large underprediction of the extreme-value properties of 10-day snowmelt. This phenomenon can partly be explained by the considerable negative bias in the daily temperature autocorrelation coefficients, which reduces the likelihood that snow accumulates over long periods and thus the probability of extreme multi-day snowmelt.

The historical winter snowmelt maxima at the Swiss stations are not higher than those at Kahler Asten and Freudenstadt. In particular for Säntis there is, however, a lot of snowmelt outside the winter period. For example, the maximum 10-day snowmelt amount (*MAX*) calculated for the whole year at this station is as high as 444.8 mm, while for the winter period it is only 198.0 mm.

Table 4 Percentage differences between the maxima (*MAX*), upper quintile means (*QM*5) and medians (*M*) of the 10-day snowmelt extremes for the simulated data (twenty-eight runs of 35 years) and the historical records (1961-1995) for six stations in the Rhine basin. The columns denoted with Hist. give the historical values (mm).

	MAX (%)				*QM5 (%)*				*M (%)*			
Station	UE	UEc	CE	Hist.	UE	UEc	CE	Hist.	UE	UEc	CE	Hist.
Kahler Asten	-12.1	-12.8	-20.9	287.2	2.6	2.8	-7.3	184.6	20.7	20.3	9.2	86.6
Freudenstadt	-10.0	-6.4	-31.6	234.7	-11.2	-10.5	-30.2	180.4	-6.7	-8.8	-22.5	93.7
Kl. Feldberg	5.6	2.2	-18.4	151.6	-1.7	-6.0	-22.3	121.7	-6.5	-11.0	-23.0	71.3
Disentis	-13.6	-3.4	-34.2	171.8	-7.0	-3.3	-35.2	119.1	-7.6	-8.6	-23.0	67.8
Davos	-6.7	-4.9	-15.1	176.4	-4.8	-3.7	-12.8	137.8	11.0	14.5	8.7	63.6
Säntis	1.1	-5.8	-22.0	198.0	-13.6	-16.2	-29.2	157.0	-0.5	-1.9	-11.7	63.9

LONG-DURATION SIMULATIONS

For three 1000-year simulations Fig. 3 shows Gumbel plots of the 10-day winter maxima of area averaged precipitation (i.e. the average of the 34 stations used in the feature vector).

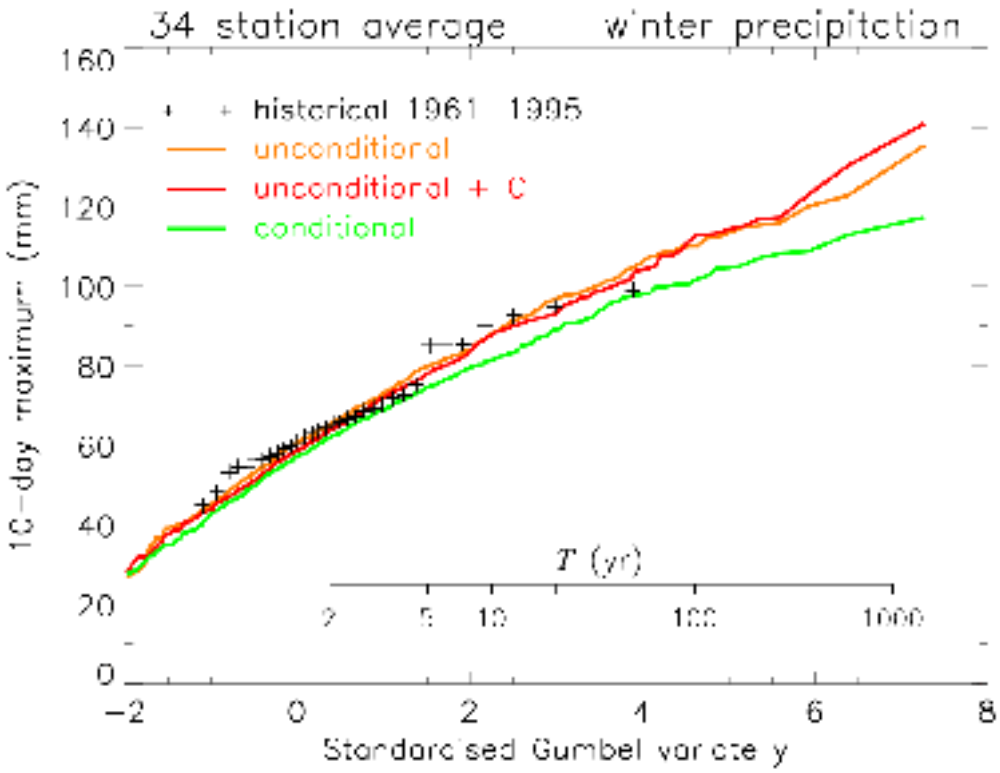

Fig. 3 Gumbel plots of 10-day winter precipitation maxima for observed and simulated data (runs of 1000 years)

There is a reasonable correspondence between the historical and simulated distributions. The figure clearly shows the underestimation of the extreme-value properties for the conditional model CE, discussed in Section 7. Furthermore, a large part of the curve for the conditional 1000-year simulation lies below the curves for the unconditional 1000-year simulations. Realistic 10-day precipitation amounts much larger than the largest historical ones are generated in all three simulation experiments.

CONCLUSIONS

The unconditional simulations preserved the second-order moment statistics of daily and monthly precipitation and 10-day maximum precipitation well. The lag 1 autocorrelation coefficients for daily precipitation and temperature were, however, significantly underestimated. The reproduction of the second order moments of temperature became worse in simulations where atmospheric circulation indices were added to the feature vector. Despite this deficiency the reproduction of 10-day maximum snowmelt was satisfactory.

Multi-site simulation of P and T conditional on simulated atmospheric circulation indices performed somewhat poorer than the unconditional simulations. Especially for temperature the reproduction of second-order moment statistics became worse. As a result a significant underestimation (up to 20-30%) of the median and the upper quintile mean of 10-day snowmelt amounts was observed for four high-elevation stations (Freudenstadt, Kl. Feldberg, Disentis, Säntis).
The ability of both unconditional and conditional models to generate realistic unprecedented multi-day rainfall events was demonstrated with simulation runs of 1000 years. Especially those extreme events may cause large peak discharges of the river Rhine in the Netherlands. A single simulation run of 1000 years does not provide, however, an accurate estimate of a 1000-year event. More simulations are

needed for that purpose and even then a considerable uncertainty remains due to the use of a relatively short 35-year historical record for resampling.

ACKNOWLEDGEMENTS

The UK Meteorological Office gridded MSLP data were kindly provided by P.D. Jones (Climatic Research Unit, University of East Anglia, Norwich). The daily precipitation and temperature data for the German, Luxemburgian, French and Swiss stations were made available by the following institutions: Deutscher Wetterdienst, Service de la météorologie et de l 'hydrologie de Luxembourg, Météo France and the Swiss Meteorological Institute via the International Commission for the Hydrology of the Rhine Basin (CHR/KHR). The work was performed in co-operation with the Institute for Inland Water Management and Waste Water Treatment (RIZA).

REFERENCES

J.J. Beersma and T.A. Buishand (1999) Rainfall generator for the Rhine basin: Nearest-neighbour resampling of daily circulation indices and conditional generation of weather variables. KNMI-publication 186-III, KNMI, De Bilt.

T. Brandsma and T.A. Buishand (1999) Rainfall generator for the Rhine basin: Multi-site generation of weather variables by nearest-neighbour resampling. KNMI-publication 186-II, KNMI, De Bilt.

T.A. Buishand and T. Brandsma (2000) Multi-site simulation of daily precipitation and temperature in the Rhine basin by nearest-neighbour resampling. Preprint 2000-14, KNMI, De Bilt (Submitted to Water Resour. Res.).

P.D. Jones, M. Hulme, and K.R. Briffa (1993) A comparison of Lamb circulation types with an objective classification scheme. *Int. J. Climatol.*, 13: 655-663.

U. Lall and A. Sharma (1996) A nearest neighbor bootstrap for resampling hydrologic time series. *Water Resour. Res.*, 32: 679-693.

B. Rajagopalan and U. Lall (1999) A k-nearest-neighbor simulator for daily precipitation and other variables. *Water Resour. Res.*, 35: 3089-3101.

R. Wójcik, J.J. Beersma, and T.A. Buishand (2000) Rainfall generator for the Rhine basin: Multi-site generation of weather variables for the entire drainage area. KNMI-publication 186-IV, KNMI, De Bilt.

K.C. Young (1994) A multivariate chain model for simulating climatic parameters from daily data. *J. Appl. Meteorol.*, 33: 661-671.

E. Zorita and H. von Storch (1999) The analog method as a simple statistical downscaling technique: Comparison with more complicated models. *J. Climate*, 12: 2474-2488.

Jules J. Beersma, T. Adri Buishand, Rafał Wójcik
Royal Netherlands Meteorological Institute (KNMI)
PO Box 201
NL-3730 AE DE Bilt

Jules.Beersma@knmi.nl
Adri.Buishand@knmi.nl

Topic 4: Temporal trends of precipitation series, especially with regard to extreme behaviour and spatial development

Generation of hydrometeorological reference conditions for the assessment of flood hazard in large river basins (Proceedings of International Workshop, Koblenz, 6. and 7. March 2001). CHR-Report No. I-20

Observed long-term precipitation trends in Central Europe and some preliminary remarks on change in extremes

Christian-D. Schönwiese
J.W. Goethe University, Institute for Meteorology and Geophysics
Frankfurt a.M., Germany

Abstract Time series, which are based on the measurement of climate elements at certain stations or are also consolidated to area-related data, can be statistically separated into different components. These include linear and/or non-linear trends, polynomial and cyclical structures, and extreme values. An analysis of the precipitation variations observed in Europe during the last century and the last decades show that the long-term trends vary a great deal, both regionally and seasonally, so that it is important to record this with the help of spatial interpolation techniques in precipitation fields (trend maps). In Central Europe there is an obvious increase in winter precipitation as against a less pronounced decrease in summer precipitation.

Extreme behaviour should be studied not only on the basis of the exceedence or shortfall frequency of certain threshold values, but also in the form of a residuum analysis in which, following separation and subtraction of trends and other time series components, values possibly appear, that are not appropriate for a random distribution. It is then evident from monthly data that the above-mentioned winter precipitation increase is accompanied by an increase in frequency of such "extreme events". As yet there are only a few such studies based on daily data; these, however, produce similar results.

INTRODUCTION

Climate has changed in the past and will do so in the future, due to various reasons, both natural and anthropogenic (IPCC, Houghton et al., 1996, 2001). Even without a causal interpretation, the observed or reconstructed, respectively, patterns of climate change reveal to be very complicated in time and space. In this context, in most countries of the world, there exists a special interest in the behaviour of precipitation, because this behavioiur has considerable effects on river runoff, water management, agriculture etc. and may lead to problems or even disasters in the form of flooding or droughts. Unfortuntely, in contrast to e.g. temperature or air pressure, just in case of precipitation there exist serious problems concerning reliability (due to measurement errors; see e.g. Sevruk, 1989; Legates, 1993; Schönwiese and Rapp, 1997) and representativeness of data. If one looks, for example, on the represenativeness of seasonal precipitation data in terms of time series correlation coefficients in relation to station distance one finds that these correlations drop below a value of 0.7 at a station distance of roughly > 50 - 100 km (lower value in summer) whereas a similar analysis in case of temperature leads to a station distance of roughly > 500 - 1000 km (again lower value in summer; details see Rapp and Schönwiese, 1996; Schönwiese and Rapp, 1997).

On the other hand, the availablity of observational precipitation data covering a decadal to centiennual time scale and concerning the Central European region is relatively satisfactory. In Germany, since 1891, the data from more than 250 stations can be used where, however, roughly 50 % of the related time series reveal to be probably non-homogeneous (Rapp and Schönwiese, 1996; for the homogeneity tests applied see Schönwiese and Rapp, 1997). In the following, using this data base and the precipitation records from some adjacent European stations, first, the technique of time

series separation is explained and demonstrated. Subsequently, one component of time series variability is considered separately: the trend behaviour, with a special focus on the trend patterns in space within different seasons. Finally, before some conclusions are drawn, an additional aspect of time series separation is addressed: the evaluation of extreme event detection where some preliminary results are presented.

TIME SERIES SEPARATION TECHNIQUE AND APPLICATIONS

Climate variability in time can be considered, analysed and quantified by the technique of time series separation (Schlittgen und Streitberg, 1992; Grieser et al., 2000, 2001). The basic idea is that any observed (or modelled) time series y(t) can be seen as a superposition

$$y(t) = \bar{y} + tr(t) + s(t) + c_m(t) + l(t) + e_k(t) + N$$

where y is any climate element (e.g. precipitation), t = time, $\bar{y}$ = average, tr = trend, s = seasonal component (annual cycle), $c_m(t)$ = other cyclical components, l = residual low-frequent component, $e_k(t)$ = extremes, and N = residuum noise. Furthermore, in case of a time series, y(t) is known in time steps Δt leading to the data $y_i(t_i)$, i=1,...,n, n = number of time steps = sample size. The trend may be linear or non-linear of order k, $tr = a + bt^k$, where k = 1 in case of linearity (often supposed).

As an example, Fig. 1 shows the time series of winter (December-February) precipitation at station Trier, North Western Germany (49.8° N, 6.8° E; Δt = 1 year). As indicated in this Figure, a long-term linear trend is detectable which amounts to a 170.6 mm precipitation increase during the 1891-1990 period. If this linear trend is computed related to the 1971-2000 subperiod, it amounts even to 240 mm increase. In the next step, the long-term trend may be subtracted from this time series and one may look for other time series components. Indeed, a weak low-frequent variability component is existent (within the low-frequent residuum of the variance spectrum, Figure not shown). More important, in this case, is that spectral variance analysis (Schönwiese, 2000) points to some cyclical variability components of interest which can be characterized by periods of c. 2.5 and 5 years (latter peak significant at the 90 % confidence level), see Fig. 2 (in summer, plot not shown, cycles of 2.4, 4.4, 6.7 and 12.5 years prevail). Using the numerical low-pass filter technique, the decadal oscillations become visible, see again Fig. 1.

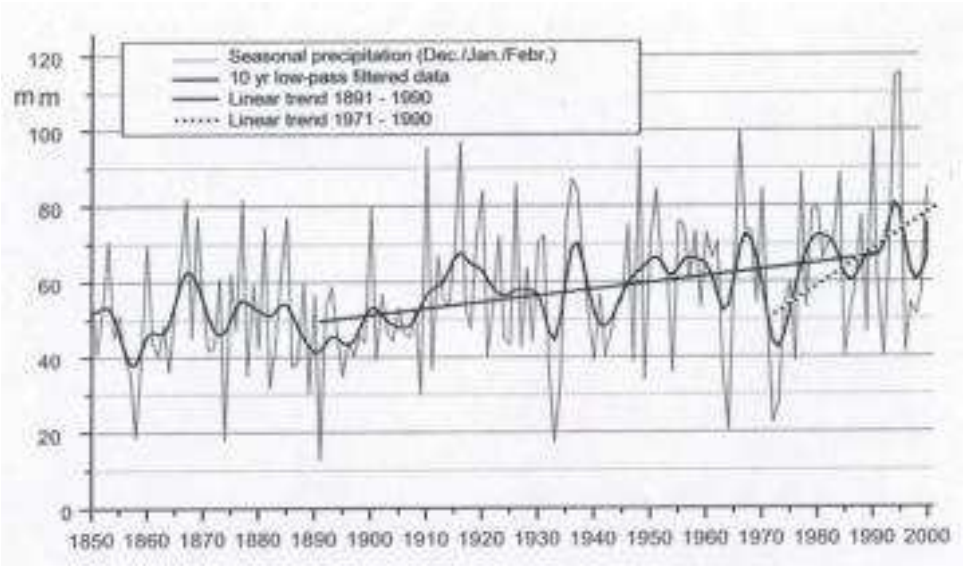

Fig. 1 Winter (Dec.- Febr.) precipitation time series 1850 - 2000 at station Trier (Germany), 10 yr low-pass filtered data and linear trends 1891 - 1990 (heavy solid line) or 1971-2000 (dotted line), respectively.

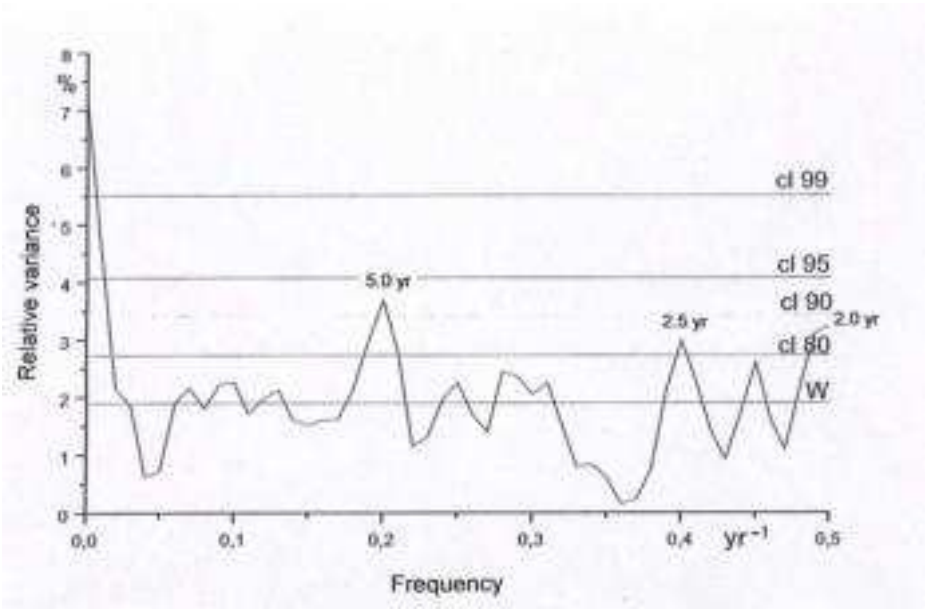

Fig. 2 Variance spectrum (autocorrelation spectral analysis, ordinate scale specifying relative variance in percent) of the time series shown in Fig. 1. W means white background spectrum, cl confidence levels.

If not only the long-term trend but also the cyclical and the low-frequent components are subtracted from this special original time series under consideration, the residuum reveals to be Gaussian-distributed so that this residuum variability may be random. (In other cases also other frequency distribution types have to be taken into account). From this point of view, in this case no extreme events can be detected if such extreme events are defined to appear as significant deviations from a Gaussian or any other random residuum distribution (see Grieser et al., 2000, 2001). If, however, as usual from a conventional point of view, extremes are defined to be values exceeding certain thresholds above or below the average, the 1994/1995 events (leading to extreme flooding) are evidently extreme (maximum of the whole time series since 1850). However, from the point of view of time series separation, these events are a consequence of both a superposition of cyclical variability (note that these events are in phase with a relative maximum of the low-pass filtered time series representing the decadal oscillations) and the recent 30 yr trend which has amplified compared to the more long-term centiennual trend.

SPATIAL-SEASONAL PRECIPITATION TREND PATTERNS IN CENTRAL EUROPE

Now, we should have a somewhat closer look on trends, implying the analysis of their structure in space. The research group of the author, especially Jörg Rapp, has done some work concerning such climate trend analysis. The outcome of this work is the ‘Climate Trend Atlas of Europe’ (Schönwiese and Rapp, 1997), the ‘Atlas of Precipitation and Temperature Trends in Germany’ (in German, Rapp and Schönwiese, 1996) and the report ‘Concept, Problems, and Results of Climate Trend Analyses in Respect to Europe and Germany’ (again in German, Rapp, 2000). In the following, a few results of this work are summarized.

Based on a 117 stations network of (probably) homogeneous precipitation time series in Europe, the trend pattern of annual totals 1891-1990 reveals the most outstanding trends in Southern Scandinavia (increase, highly significant) and most parts of the Mediterranean region (decrease, weakly significant). With a focus on Germany and related to the more recent time interval 1896-1995, see Fig. 3, it can be seen that the precipitation increase occurred mainly in autumn and especially in winter (up to 40% increase in some Western and South Western parts of Germany) whereas in summer a weak decrease prevails. Table 1 summarizes the seasonal and annual precipitation trends for the whole country of Germany where it arises that the winter increase and the summer decrease (latter one, however, at an considerably lower rate of magnitude) have amplified in

recent decades whereas the autumn trend has weakened and the spring trend has changed its sign (from increase to decrease).

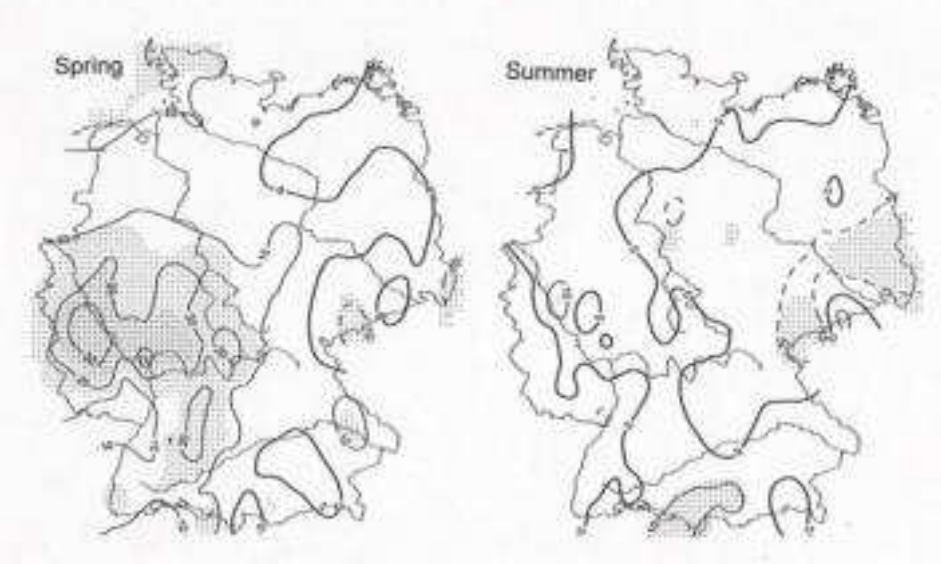

Fig. 3a Linear precipitation trends 1896 - 1995, Germany, spring (March-May) and summer (June-Aug.), in percent; dashed lines indicate negative values, light shading 70%, heavy shading 95 % confidence; from Rapp, 2001

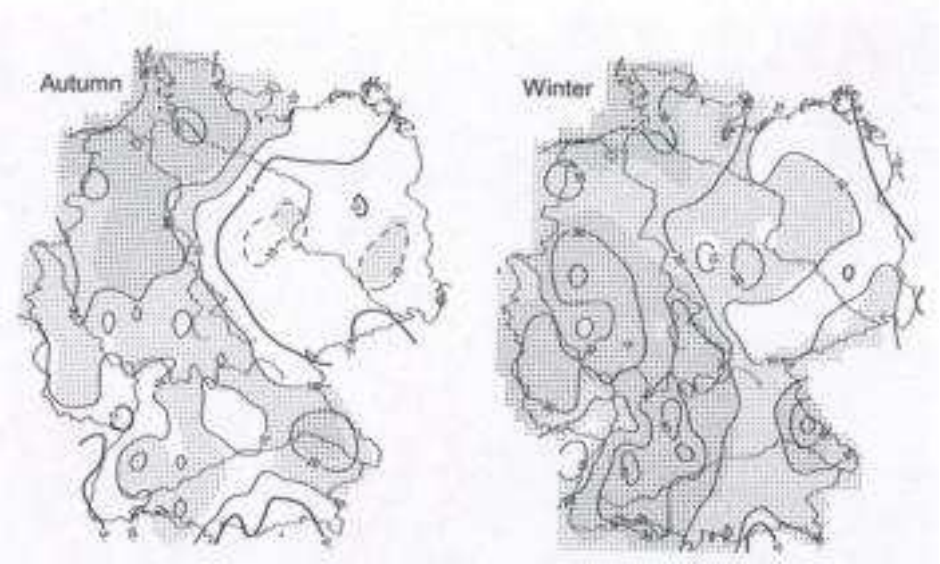

Fig. 3b Linear precipitation trends 1896 - 1995, Germany, autumn (Sept.-Nov.) and winter (Dec.-Febr.), in percent; symbols and source as in Fig. 3a

Table 1 Observed seasonal and annual total precipitation trends in percent, Germany, related to different time intervals (where 1961-1990 is the recent climate normal (CLINO) period; combined from Rapp and Schönwiese, 1996; Rapp, 2001)

Period	Spring	Summer	Autumn	Winter	Annual
1891 - 1990	+ 11 %	0 %	+ 16 %	+ 19%	+ 9 %
1896 - 1995	+ 8 %	- 1 %	+ 20 %	+ 21 %	+ 8 %
1961 - 1990	- 9 %	- 8 %	+ 10 %	+ 20 %	+3 %
1966 - 1995	- 3 %	- 7 %	0 %	+ 26 %	+ 3 %

Coming back to an European point of view, Fig. 4 illustrates that the recent winter precipitation increase in Central Europe coincides with a temperature increase and a systematic change of the atmospheric air pressure pattern: pressure decrease both at mean sea level and within the troposphere

(represented by the 500 hPa pressure level, c. 5 km altitude) in Northern and corresponding increase in Southern parts of Europe leading to an intensification of the Icelandic low and Azores high pressure systems (see related textbooks, e.g. Schönwiese, 1994) and, in turn, of the zonal (West to East) air flow component in the North Atlantic and adjacent European region (see also analysis of 'Grosswetterlagen', e.g. Werner et al., 2000). Note that the most pronounced precipitation decrease in the Mediterranean region coincides with the most pronounced mean sea level pressure increase. The intensification of the zonal air flow component is reflected in the behaviour of the North Atlantic Oscillation (NAO) and may be – although uncertain – a consequence of the human impact on climate (IPCC, Houghton et al., 2001; Paeth et al., 1999).

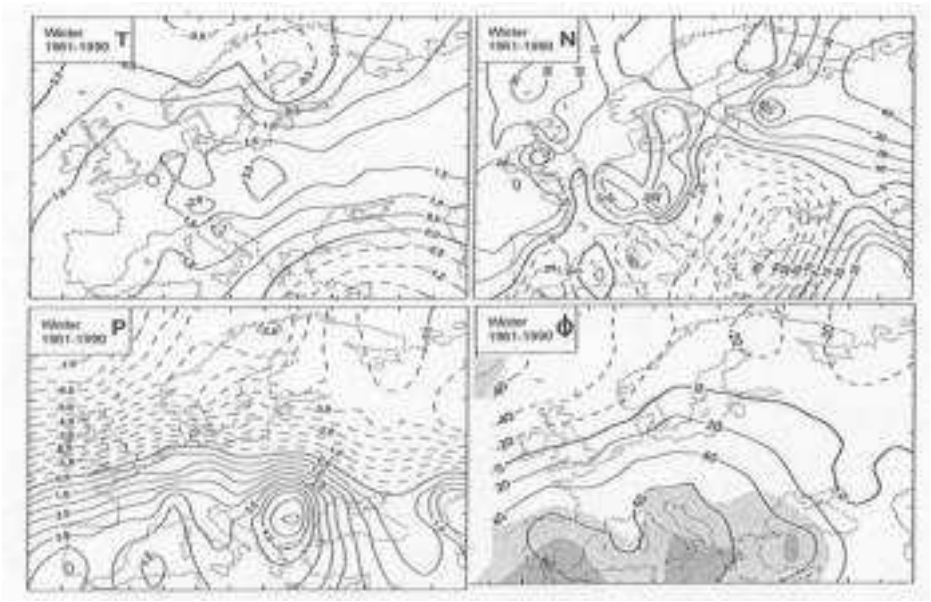

Fig. 4 Linear winter trends 1961-1990 in Europe, surface air temperature T (K), precipitation N (percent), mean sea level pressure P (hPa), and 500 hPa geopotential height Φ (gpm, representing the air pressure in c. 5.5 km height); combined from Schönwiese and Rapp, 1997.

CHANGE IN EXTREMES

It is often speculated that the recent climate change (global warming since c. 1850/60) is associated with more extremes. The actual IPCC Report (Houghton et al., 2001) states that within the second half of the 20th century the occurrence of more intense precipitation events is very likely over many of northern hemisphere mid- to high latitude land areas. Furthermore, it is assumed that increased summer drying is likely in a few areas of mid-latitude continental interiors. However, going in detail, it seems that the situation is very complicated and one has to discern between the phenomena within different regions, seasons, and time subintervals so that comprehensive further research is necessary (will be done in the context of the new German Climate Research Programme (DEKLIM)).

Here, focussed on Central Europe, only a few preliminary results can be presented based on a study by Grieser et al. (2000). Although the detection of anthropogenic climate change in observational climate data was the main topic of this study, the authors looked also on the time series behaviour in respect to variability, especially in terms of standard deviation and number of extremes. First, based on 100 yr annual data time series of surface air temperature (T), precipitation (R) and mean sea level pressure (P), the standard deviation of the related running 30 yr subinterval time series was computed and it was asked wether there is a significant trend (of variability) or not. The outcome of this analysis is listed in Table 2 and it can be seen that in case of pressure no trends, in case of temperature negative trends and in case of precipitation positive trends prevail. That means, there is some indication that precipitation variability has actually amplified. A similar result (no negative trends, some positive trends, however, no trends prevailing) is obtained by a correspondung analysis of a German precipitation data set (see again Table 2).

Table 2 Trends (95 % confidence level) of 30 yr running standard deviations of European climate observational annual time series, gridded data, surface air temperature 1899-1998 (52 grid points), precipitation 1899-1998 (83 grid points), and mean sea level pressure 1896-1995 (44 grid points), in addition precipitation time series 1896-1995 from (81) German stations; from Grieser et al (2000), simplified.

Data set	negative trend	no significant trend	positive trend
Europe, temperature	29	21	2
Europe, pressure	3	36	5
Europe, precipitation	10	34	39
Germany, precipitation	0	50	31

The next step is the identification of the number of extreme events following the definition as outlined in section 2 (time series separation; method from Grieser et al., 2000, 2001). Table 3, using the same data sets as in Table 2, specifies the number of extremes detected in this way, their sign (minimum or maximum, respectively) and their number in the first and the second half of the secular time interval considered. Similar to the results of the running time series standard deviation analysis it arises that temperature seems to have become less extreme (decrease of extreme events) and precipitation more extreme (increase of extreme events). This holds also for the German precipitation data set where, moreover, all detected extremes are maxima. In contrast to Table 2, also in case of pressure there seems to exist a trend to more extreme events. More important, in case of precipitation now not only the European but also the German data set clearly indicates an increase of extreme events.

Table 3 Extreme events (definition and detection technique see section 2) of European climate observational monthly time series, data base same as in Table 2, total number and minima such as maxima within the first and second time subinterval (from Grieser et al., 2000).

Data set	Total number	Minima		Maxima	
		First half	Second half	First half	Second half
Europe, temperature	231	116	74	32	9
Europe, pressure	137	13	31	37	56
Europe, precipitation	405	1	4	137	263
Germany, precipitat.	444	0	0	186	258

Finally, a closer look just on the German precipitation data set adding a seasonal analysis, see Table 4, reveals that the increase of extreme precipitation events is restricted to the spring and – much more pronounced and significant – the winter season. There may be a relationship to the winter trends and the related change of atmospheric circulation (see section 3: change of pressure pattern, NAO). Implying similar results from other parts of the world, the IPCC Report (Houghton et al., 2001) states that increasing precipitation trends which are observed in some mid-latitude regions in winter, may be due to an increase in extreme events. This assumption was confirmed also by a study related to the South West Part of Germany (Baden-Wuerttemberg; Sanchez Penzo et al., 1998) where it was found that increasing winter precipitation trends are connected with an increasing number of extreme events (but not with an increasing magnitude of these events).

Table 4 Precipitation extreme events, Germany, 1896-1995 (subset from Table 3, note that all these events are maxima), in different seasons and over the year, total number and numbers in respect to the first or second time subinterval, respectively; furthermore, the change of these numbers in percent and the related confidence levels are specified (from Grieser et al., 2000).

Season	Total number	First half	Second half	Change	Confidence
Winter	53	8	45	+ 462.5 %	> 99.99 %
Spring	45	14	34	+ 121.4 %	> 99 %
Summer	255	129	126	- 2.3 %	-
Autumn	91	48	43	-10.4 %	-
Year	444	199	245	+ 23.1 %	> 95 %

CONCLUSIONS

The availability of observational climate data from the Central European region, over a centiennual time scale, and the empirical-statistical analyses in respect to precipitation data done so far provide considerable information about long-term trends and some other aspects of variability. On the other hand, the analysis of both regional-seasonal trend patterns and especially extreme events need further research, including climate model simulations in order to understand the underlying processes, especially if one is confronted with the question whether any past or future climate change may be natural or anthropogenic. However, just in case of precipitation there are serious shortcomings of modelling in respect to both a reliable and accurate reproduction of climate change and prediction which is, of course, even much more problematical. So, empirical-statistical methods will continue to be important. All together, not only the very climatic phenomena but also their implications in ecological, economic, and social affairs are important.

REFERENCES

Grieser, J., Staeger, T., Schönwiese, C.-D. (2000) Statistische Analyse zur Früherkennung globaler und regionaler Klimaänderungen aufgrund des anthropogenen Treibhauseffektes. Bericht Nr. 103, Inst. Meteorol. Univ. Frankfurt a.M. (brief English version Report No. 103).

Grieser, J., Trömel, S., Schönwiese, C.-D. (2001) Statistical time series decomposition into significant components and applucation to European temperature, Submitted to Theor. Appl. Climatol.

Houghton, J.T., et al. (eds.) (1996) Climate Change (1995) The Science of Climate Change. Contribution of WGI to the Second Assessment report of the Intergovernmental Panel on Climate Change (IPCC). Univ. Press, Cambridge.

Houghton, J.T., et al. (eds.) (2001) Climate Change (2001) The Scientific Basis. A Report of Working Group I of the Intergovernmental Panel on Climate Change (IPCC) (Third Assessment Report). Univ. Press, Cambridge.

Legates, D.R. (1993) Biases in precipitation gauge measurements. In World Climate Research Programme, 'Global Observations, Analyses and Simulation of Precipitation', WMO Td-No. 544, 31-34.

Paeth, H., Hense, A., Glowienka-Hense, R., Voss, R., Cubasch, U. (1999) The North Atlantic Oscillation as an indicator for greenhose-gas induced regional climate change. Clim. Dynamics, 15, 953-960.

Rapp, J. (2000) Konzeption, Problematik und Ergebnisse klimatologischer Trendanalysen für Europa und Deutschland. Breiucht Nr. 212, Deut. Wetterdienst, Selbstverlag, Offembach.

Rapp, J., Schönwiese, C.-D. (1996) Atlas der Niederschlags- und Temperaturtrends in Deutschland 1891-1990 (2. Aufl.). Band 5, Serie B, Frankfurter Geowiss. Mitt., Frankfurt a.M.

Sánchez Penzo, S., Rapp, J., Schönwiese, C.-D. Luft, G. (1998) Räumliche Strukturen aktueller Trends des Gesamt- und des Extremniederscghlages in Baden-Württemberg. Deut. Hewässerkundl. Mitt., 42, 157-163.

Schlittgen, R., Streitberg, B.H.J. (1994) Zeitreihenanalyse (5. Aufl.). Oldenbourg, München.

Schönwiese, C.-D. (1994) Klimatologie. Ulmer (UTB), Stuttgart.

Schönwiese, C.-D. (2000) Praktische Statistik für Meteorologen und Geowissens chaftler (3. Aufl.). Borntraeger, Stuttgart.

Schönwiese, C.-D., Rapp, J. (1997) Climate Trend Atlas of Europe - Based on Observations 1891-1990. Kluwer, Dordrecht.

Sevruk, B. (1989) Reliability of precipitation measurement. In Sevruk, B. (ed.): Precipitation Measurement. WMO/IAHS/ETH, Zürich, 13-19.

Werner, P.C., Gerstengarbe, F.-W., Fraedrich, K., Oesterle, H. (2000) Recent climate change in the North Atlantic/European sector. Internat. J. Climatol., 20, 463-471.

Prof. Dr. Christian-D. Schönwiese
J.W. Goethe University, Institute for Meteorology and Geophysics
P.O. Box 11 19 32,
D-60054 Frankfurt a.M.
Germany

schoenwiese@meteor.uni-frankfurt.de

Generation of hydrometeorological reference conditions for the assessment of flood hazard in large river basins (Proceedings of International Workshop, Koblenz, 6. and 7. March 2001). CHR-Report No. I-20

Evidence of a climate-induced change in maximum streamflow of the Alzette river (Grand-Duchy of Luxembourg)

Laurent Pfister and Lucien Hoffmann
Centre de Recherche Public - Gabriel Lippmann, Cellule de Recherche en Environnement et Biotechnologies (CREBS)
Luxembourg, Luxembourg

Abstract The combined influence of climate variability and/or climatic change and changes in landuse makes it very difficult to detect the main origins of changes in the rainfall-runoff relationship. These problems are commonly investigated through the analysis of long hydro-climatological time-series and/or by the use of hydrological models.

In the Alzette experimental basin (Grand-Duchy of Luxembourg) both approaches are currently used in order to get a better understanding of the rainfall-runoff relationship.

So far, the analysis of long hydro-climatological time-series in the Alzette river basin has shown that the temporal variability of rainfall had a strong impact on streamflow over the last decades. The local-scale sensitivity of the Alzette river to large-scale changes in atmospheric circulation patterns has been detected. Since the 1950s, there has indeed been a marked increase in the contribution of the westerly component of atmospheric circulation to rainfall. These changes in atmospheric circulation are on a par with an increase in rainfall intensity and duration, which has induced a significant increase in winter maximum daily stormflow in the Alzette river since the 1970s.

Rainfall and streamflow data of high spatio-temporal density, measured since 1995 in the Alzette basin, have revealed so far that anthropogenic effects, such as changes in landuse, only have a very local impact on maximum streamflow values. Preliminary hydrological modelling results tend to confirm these observations.

The increase in major floods, observed throughout the 1990s, could thus be clearly related to a change in winter rainfall distribution, the latter being induced by a significant increase in westerly atmospheric circulation patterns.

INTRODUCTION

Since the end of the 1980s, several large-scale floods have caused severe damage on multiple occasions in Europe. These events have rised concern about the possible impacts of a climatic change on the hydrological regimes of our rivers. In northern Europe, an increase in rainfall over the last decades has been detected for example in Scotland (Mansell, 1997) and in Denmark (Nicholls et al., 1996). No significant trends towards an inrease of rainfall have been observed in Central Europe over the last century, while in southern Europe decreasing trends in rainfall appear to dominate (Nicholls et al., 1996).

Studies on the impact of changes in the structure and the typology of rainfall on streamflow are rather scarce. In the USA, the increase of autumn rainfall is accompanied by an increase in streamflow. Lins and Michaels (1996) have detected significant increases of streamflow during autumn and winter months in almost all regions over the period 1948-1988. In four basins of western Scotland, Mansell (1997) has detected trends towards an increase of rainfall and streamflow for the period 1964-1994. The increase is more than proportional regarding rainfall and is essentially linked to changes in the distribution and the typology of rainfall events.

Due to its central position in western Europe, the Alzette river basin is located between two very different hydro-climatological regions: northern Europe, where rainfall is supposed to increase and southern Europe, where climate is expected to become drier in the future. Rainfall and streamflow data recorded between 1954 and 1996 were used for this study in order to investigate the long-term evolution of the rainfall-runoff relationship in the Alzette basin. Given the fact that the Alzette basin is rather small (1175 km^2), the results that were obtained can only have a very local validity.

RESULTS AND DISCUSSION

Between 1954 and 1997, four pluviometric stations (Belvaux, Koerich, Roeser and Luxembourg-city) have been subject to comparable variations of winter rainfall. The highest annual rainfall heights were measured in 1967 (1095 mm in Belvaux) and in 1982 (1104 mm in Belvaux). No positive or negative trend was observed on annual totals (fig. 1A). The ratio between summer rainfall and winter rainfall however indicates a negative trend, with a decrease of 30% between the end of the 1950s and the beginning of the 1990s (fig. 1B). Thus, there has been a significant increase of winter rainfall versus a decrease of summer rainfall.

The analysis of monthly rainfall totals over the period 1860-1995 in Luxembourg-city has also shown important fluctuations of rainfall. Around 1885, as well as in the 1940s and the 1970s, the 5-year moving average of annual rainfall only reached 550 and 680 mm respectively, while in the 1900s, 1920s and the 1990s maximum values of 960, 980 and 940 mm were recorded. The maximum annual rainfall totals over the whole study period were observed at the end of the 1980s, with a mean 5-year moving average of 1050 mm. Since then, this average has decreased to less than 800 mm. No general trend could be detected on an annual scale.

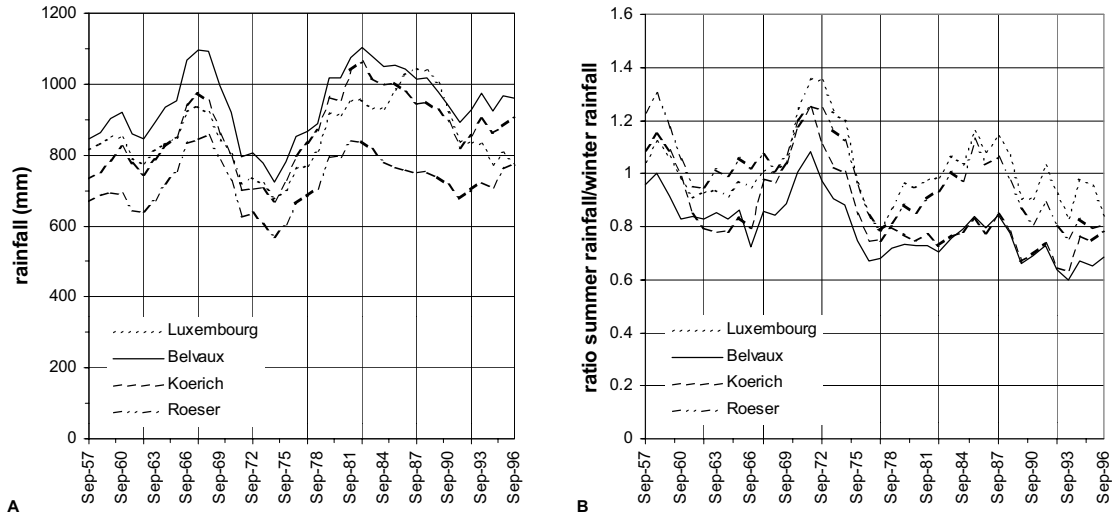

Fig. 1 5-year moving average of annual rainfall (A) and 5-year moving average ratio of summer rainfall/winter rainfall between 1957 and 1995 (B).

In western Europe, winter rainfall is strongly influenced by the westerly atmospheric fluxes that bring humid air masses from the Atlantic Ocean (McCartney et al., 1996; Pfister et al., 2000). Any change in atmospheric circulation patterns can thus influence the westerly fluxes and rainfall patterns in western Europe. Hess and Brezowski (1977) have defined 29 atmospheric circulation types that correspond to a mean air pressure distribution that generally persists for several days in western Europe (zonal, meridian and mixed circulations). Zonal atmospheric circulations are associated with more than 55% of winter rainfall, followed by almost equal contributions of meridian and mixed circulations (approximately 20%). During summer months, mixed atmospheric circulations cause more or less 45% of total rainfall, while zonal and meridian circulation contributions vary between 25 and 30%. Amongst the zonal atmospheric circulation types that include northwest- to southwest-oriented airflows, the westerly component has had a growing influence on winter rainfall since the 1970s.

During winter, an overall increase of 230 mm of rainfall due to the westerly component (5-year moving average) was observed between 1954 and 1994 (fig. 2A). Thus, the contribution of this circulation type to total winter rainfall increased from 20% during the 1950s to more than 50% during the 1990s (fig. 2B). For the westerly component of zonal atmospheric circulations, the 5-year average of days with rainfall increased from 15 days at the end of the 1950s to more than 35 days at the beginning of the 1990s. Winter rainfall variability in the Alzette basin is consequently mainly due to fluctuations in the atmospheric circulation patterns (Pfister et al., 2000).

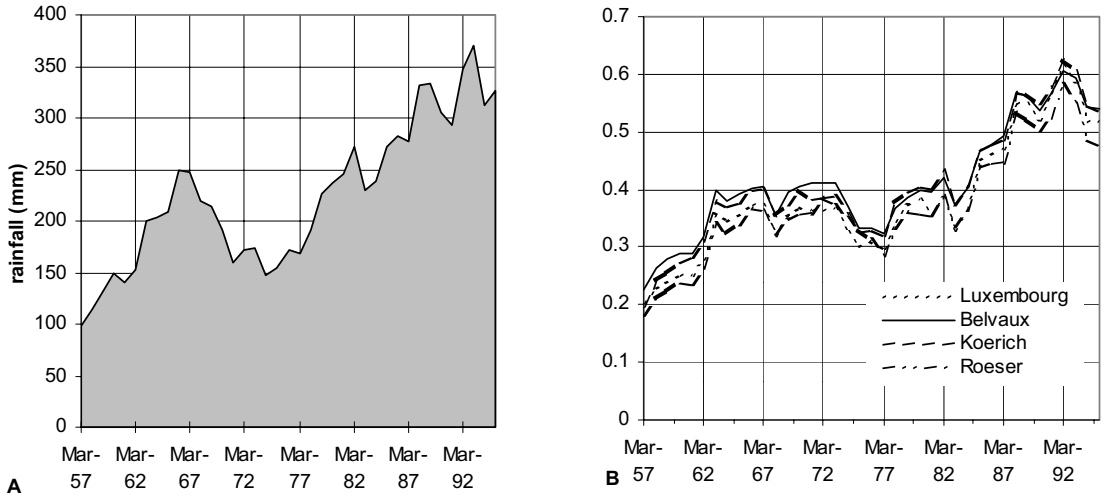

Fig. 2 5-year moving average of rainfall (Belvaux) due to the westerly component (A) and 5-year moving average of the contribution to total rainfall by the westerly component (B)

Westerly atmospheric fluxes are circulating between high pressure cells (centered over the Azores) and low pressure cells (centered above Greenland and Iceland). An oscillation of the strength and the position of these cells occurs on an interannual and interdecennial time-scale (McCartney, 1996). The atmospheric circulation type is part of a very complex energy exchange system between the Atlantic Ocean and the atmosphere. The Gulf Stream brings warm water to high latitudes. This water is consequently cooling down and thus liberating a lot of energy to the atmosphere. This cooling process is subject to an interdecennial variability that has direct consequences on the atmospheric circulation patterns. Between 1930 and 1971 the Labrador Sea water temperature increased, while between 1972 and 1993 the water has been cooling down (McCartney et al., 1996). The positioning of the high pressure and low pressure cells (Azores and Greenland) was enhancing a progressive reduction of the cooling process of the Labrador Sea between 1950 and 1960. Thus, less energy was evacuated towards the atmosphere. Reversely, in the 1970s and the 1980s, a change in the positioning of the high and low pressure cells induced a progressive cooling of the Labrador Sea, enhancing the loss of energy from the ocean towards the atmosphere.

The Labrador Sea water temperature has almost continuously decreased between the 1970s (3.5°C) and the 1990s (2.7°C). This decrease has been linked to the annual and winter rainfall totals due to westerly atmospheric fluxes in the Grand-duchy of Luxembourg (fig. 3). The highest rainfall totals due to the westerly atmospheric fluxes obviously are strongly correlated to low Labrador Sea water temperatures and vice-versa.

Regardless of the origin of the atmospheric circulation types that bring more or less rainfall to western Europe, and also regardless of the maximum daily rainfall intensities, extreme streamflow is always generated by extreme rainfall events. In this respect, the total length of rainfall events that totalised the highest rainfall values, as well as the corresponding daily rainfall intensities have been studied. Since the 1980s there is a simultaneous increase in duration and intensity of extreme rainfall events in the Alzette basin (Pfister, 2000). Rainfall events longer than 21 days and with daily intensities higher than 50 mm/day appeared on several occasions since the 1980s, while such events had not been observed between 1953 and 1980.

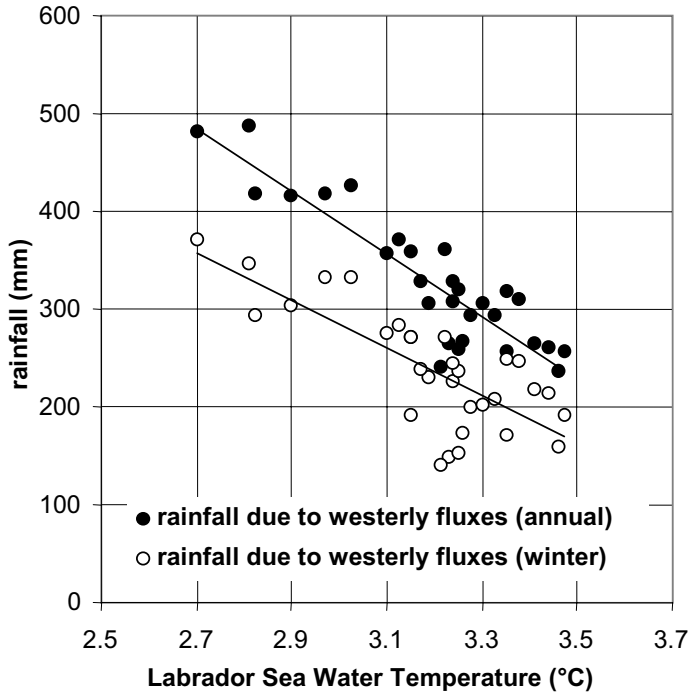

Fig. 3 Rainfall contributions due to westerly fluxes in relation to Labrador Sea water temperature

Since the beginning of the 1990s, the Alzette has been subject to a large number of heavy floods. The Alzette streamflow in the Esch/Alzette streamgauge station has been studied via a 5-year moving average. Various fluctuations of streamflow thus appeared over the last decades, such as high annual streamflow at the end of the 1960s and at the beginning of the 1980s (0.6 m^3/s) and low annual streamflow at the end of the 1970s and at the end of the 1980s (0.3 m^3/s). These fluctuations are equally seen for both summer and winter months (fig. 4A).

Since the 1980s, the evolution of daily maximum streamflow during winter months is totally different from that observed for mean daily streamflow (fig. 4B). Between the end of the 1950s and the beginning of the 1970s, maximum daily streamflow was very contrasted, with values ranging from 1.1 to 2.5 m^3/s. Since the 1970s, daily maximum streamflow has increased significantly. Maximum daily streamflow values are since then varying between 2 and 2.5 m^3/s. At the same time, maximum daily streamflow observed during summer months has had a similar evolution to mean daily streamflow. These observations thus indicate a clear change in maximum daily streamflow since the 1980s.

The analysis of maximum streamflow has been extended to the winter rainfall events of maximum cumulated rainfall heights. For each of these extreme events, all corresponding mean daily streamflow values were determined for the period 1955-1995. It clearly appeared that mean daily streamflow increased (Pfister, 2000). Thus, maximum streamflow for extreme rainfall events was rarely higher than 2 m^3/s and did not last longer than two weeks until the end of the 1970s. Since the 1980s, mean daily streamflow reached values above 3 and even 4 m^3/s.

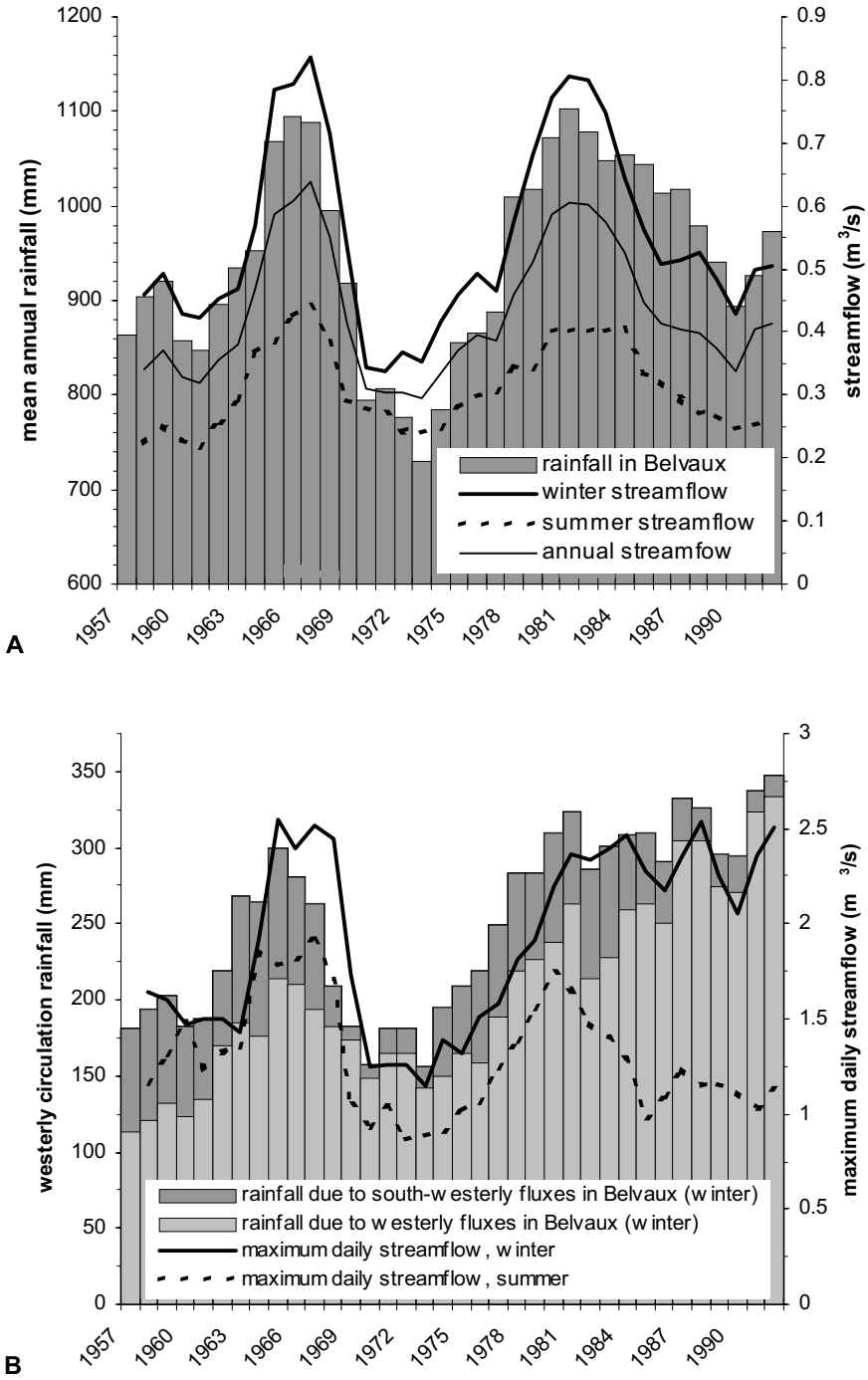

Fig. 4 5-year moving average of mean annual, winter and summer streamflow of the Alzette and mean annual rainfall in Belvaux (1954-1995) (A) ; 5-year moving average of maximum winter and summer streamflow and rainfall due to westerly and south-westerly fluxes in Belvaux (1954-1995) (B).

CONCLUSION

The analysis of long rainfall and streamflow observation series in the Alzette basin has shown the strong influence of the temporal and structural variability of rainfall on the hydrological behaviour of the Alzette. The increase of maximum daily streamflow of the Alzette has been clearly correlated to a redistribution of winter rainfall totals during the last decades.

The growing influence of the westerly atmospheric circulation over the past decades has led to an increase in winter rainfall due to single rainfall periods. The related change in winter rainfall

distribution has an important impact on the Alzette daily maximum streamflow (Pfister et al., 2000). Similar results were reported by Ghio (1995) and Mansell (1997) for other West European countries.

REFERENCES

Ghio M. (1995) 'Les activités humaines augmentent-elles les crues?' Annales de Géographie, 581/582: 118-147.

Hess P. and Brezowski H. (1977) 'Katalog der Grosswetterlagen Europas'. Berichte des Deutschen Wetterdienstes, 15 : 1-14.

Lins H.F. and Michaels P.J. (1996) 'Observed climate variability and change'. In: 'Climate Change 1995: The Science of Climate Change, Contribution of Workgroup I to the Second Assessment Report of the Intergovernmental Panel on Climate Change'. Nicholls N., Gruza G.V., Jouzel J., Karl T.R., Ogallo L.A. and Parker D.E., Eds. Cambridge University Press, Cambridge-New York-Melbourne, 1996. 572 p.

Mansell M.G. (1997) 'The effect of climate change on rainfall trends and flooding risk in the west of Scotland'. Nordic Hydrology, 28: 37-50.

McCartney M.S. (1996) 'North Atlantic Oscillation'. Oceanus, 39: 13.

McCartney M.S., Curry R.G. and Bezdek H.F. (1996) 'North Atlantic's transformation pipeline'. Oceanus, 39: 19-23.

Nicholls N., Gruza G.V., Jouzel J., Karl T.R., Ogallo L.A. and Parker D.E. (Eds.) (1996) 'Climate Change 1995 : The Science of Climate Change'. Contribution of Working Group I to the Second Assessment Report of the Intergovernmental Panel on Climatic Change, Cambridge University Press, Cambridge-New York-Melbourne, 1996. 572p.

Pfister L. (2000) 'Analyse spatio-temporelle du fonctionnement hydro-climatologique du bassin versant de l'Alzette (Grand-duché de Luxembourg) – Détection des facteurs climatiques, anthropiques et physiogéographiques générateurs de crues et d'inondations'. PhD thesis, Université Louis Pasteur, Strasbourg, 240 p.

Pfister L., Humbert J. and Hoffmann L. (2000) 'Recent trends in rainfall-runoff characteristics in the Alzette river basin, Luxembourg'. Climatic Change, 45: 323-337.

Dr. Laurent Pfister and Dr. Lucien Hoffmann
Centre de Recherche Public - Gabriel Lippmann
Cellule de Recherche en Environnement et Biotechnologies (CREBS)
162a, avenue de la Faïencerie
L-1511 Luxembourg

pfister@crpgl.lu, hoffmann@crpgl.lu

Topic 5: Application of procedures for the determination of extreme precipitation events for questions concerning hydrology and water resources management

Generation of hydrometeorological reference conditions for the assessment of flood hazard in large river basins (Proceedings of International Workshop, Koblenz, 6. and 7. March 2001). CHR-Report No. I-20

Application of a Water Balance Model for Calculating the Impact of Extreme Rainfall Events

Karl-Gerd Richter, Martin Ebel and Karl Ludwig
Wasserwirtschaft Wasserbau
Karlsruhe, Germany

Abstract Flood protection is one of the most important objectives of water management in practice. Extreme rainfalls over larger areas cause floods in large basins. The application of the mesoscale rainfall runoff model LARSIM (Large Area Runoff Simulation Model) calculating the impact of extreme rainfall events on flooding in the Rhine catchment is described.

For the Rhine between Switzerland and the German Dutch frontier the mesoscale rainfall runoff model LARSIM is calibrated (1992 – 1997) and verified (1987 – 1992). For three flood events (5/1988, 12/1993 and 1/1995) the results are shown for some gauges.

In addition to this the meterorological situation is calculated for these flood events using the atmospheric Regional Model (REMO) in close co-operation with the Max-Planck-Institute for Meteorology in Hamburg. The output of the atmospheric model REMO is used for the flood simulation. The results of the flood simulation with the model output from REMO will be compared with the results from the flood simulation with measured data.

For the Rhine catchment a daily data base of areal precipitation from 1980 to 1997 is available. Some statistical applications for extreme rainfall events and their impact on floods will be shown for the some subbasins of the Rhine catchment.

INTRODUCTION

Flood protection is one of the most important objectives of a sustainable management of water resources. Since extreme rainfall events represent the major contributor to floods, careful modeling of such events is necessary. Therefore, the water balance model LARSIM (**L**arge **A**rea **R**unoff **S**imulation **M**odel) is used to investigate this type of floods regarding the German part of the Rhine as the study area.

The LARSIM model was calibrated for the time period from 1992 until 1997 and verified from 1987 until 1992. We used three specific flood events (May 1988, December 1993 and January 1995) to portray the results.

With respect to meteorological data, the atmospheric Regional Model (REMO) of the Max-Planck-Institut in Hamburg was employed. The REMO results were utilized as input data for the LARSIM modeling process. Finally, we compared REMO-LARSIM results with a LARSIM simulation on the basis of measured meteorological data.

THE HYDROLOGICAL MODEL LARSIM

The water balance model LARSIM (Bremicker, 2000) simulates the water balance of mesoscale river basins (Becker, 1992). It incorporates the runoff generation in the areas and the translation and retention in river channels. Additionally it is capable of including the processes of interception, evapotranspiration and water storage in soils and aquifers, snow accumulation, snow melt and artificial influences (e.g. storage basins, diversions).
LARSIM combines deterministic hydrological model components, which are generally applicable as far as possible and which are based on easily accessible system data for the land surface. Emphasis is laid on the reliable determination of evapotranspiration by using the MORECS scheme (Thompson,1981). Evapotranspiration and the soil water budget are calculated separately for each different land management type.

Runoff calculation is based on a separation of precipitation into three different runoff components (baseflow, interflow, surface runoff). These runoff components can also be calculated for parts of the basin where runoff was already modified by translation and retention in river channels and by superposition of discharge of several sub-basins. The calculation of the runoff components is based on the Xinanjiang model (Zao, 1977) for soil moisture balance. One of the basic assumptions of the model is that an increase in soil moisture of the model element correlates with an increase of the water saturated areas of the model element. Thus, the percentage of water saturated areas in the model is considered to be variable in time. Precipitation falling on the saturated areas leads to surface runoff. The runoff components of interflow and baseflow are also calculated dependent on the current soil moisture content of the model element as lateral drainage or vertical percolation.

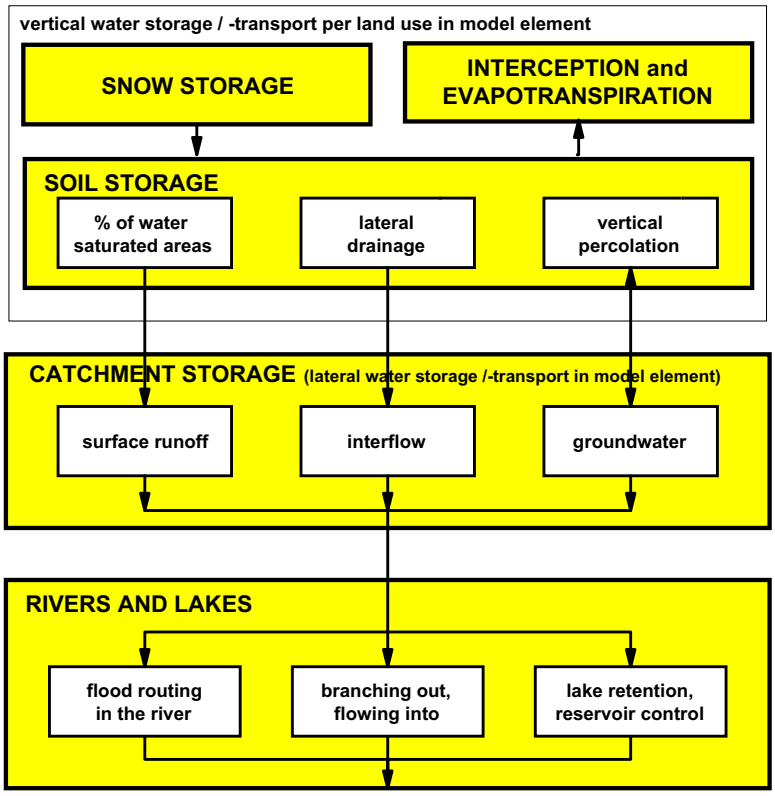

Fig. 1 The LARSIM model scheme

MODEL APPLICATION FOR THE RHINE-BASIN

The hydrological model area covers the Rhine basin from Switzerland to the German-Dutch border (gauge Lobith). The model area is divided into sub-basins using a horizontal grid with size of 1/6 degree, which corresponds to the grid size of the atmospheric model REMO. Therefore, 471 grid elements are used for the roughly 160.000 km² Rhine basin, which is shown in Figure 2.

To adopt the model parameters (Ebel et al., 2000) to the Rhine basin for calibration and verification, daily values of about 1.950 rainfall gauges, 200 climatic stations (temperature, wind velocity, sunshine duration and relative humidity) and 26 runoff-gauges were used.

A special treatment of the Swiss and the French parts of the Rhine basin was necessary, because only limited data were available. For the gauges Perl/Mosel, Andelfingen/Thur, Reckingen/Rhein and Untersiggental/Aare the measured discharge was used as input in the hydrological model.

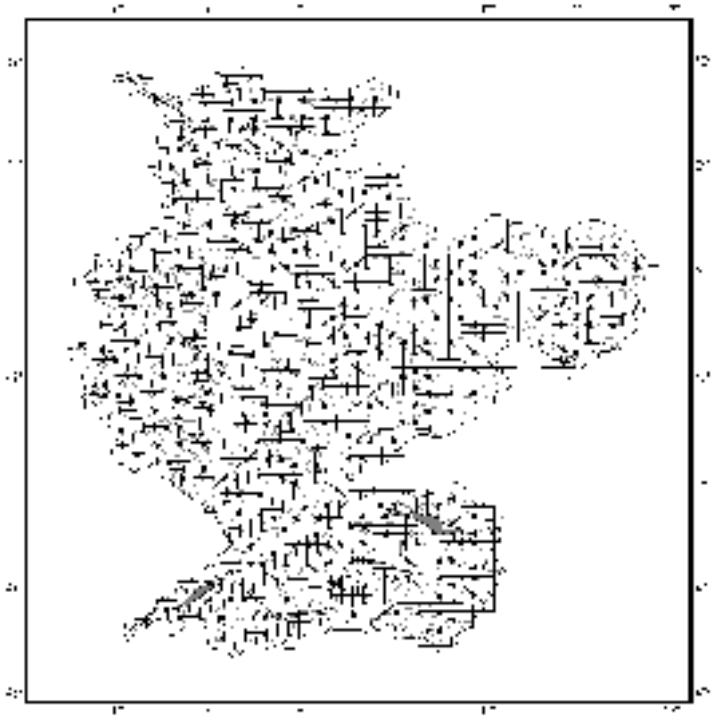

Fig. 2 The Rhine basin with model grid and river network

Six model parameters were calibrated based on daily values of the time series from January 1, 1992 until December 31, 1997 and verified for the time series from January 1, 1987 until December 31, 1992. To test the performance of the model measured and calculated discharges for the 26 runoff-gauges were compared statistically (e.g. using the coefficient of determination and the model efficiency (Nash & Sutcliffe, 1970).

A high correlation between measured and calculated discharges both in the calibration and the verification period results, particularly for gauges with basins areas of more than 2000 km². In Figure 3 the measured and calculated runoff for the gauges Maxau/Rhein, Bollendorf/Sauer, Frankfurt/Main can be seen. The coefficients of determination of the hydrological model LARSIM of these gauges are shown in Figure 4. In most cases they lie between 0.80 and 0.98 for the calibration period and also for the validation period. For or the whole period it was found to be 0.96 for the runoff-gauge Düsseldorf (last plot of Figure 3). This value shows also the capability of LARSIM to simulate adequately extreme events on a long term period.

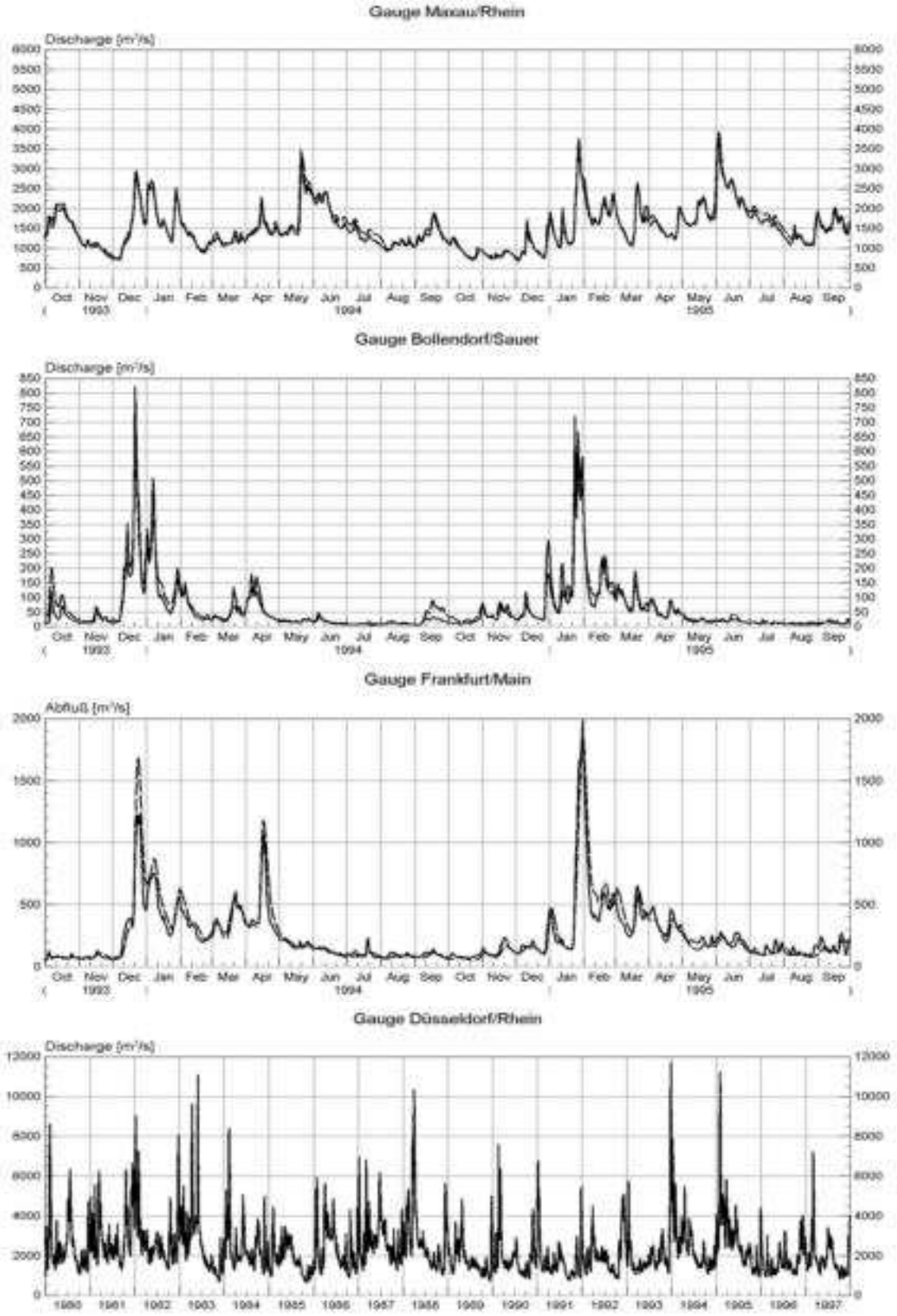

Fig. 3 Model application for the gauges Maxau/Rhein, Frankfurt/Main, Bollendorf/Sauer and Düsseldorf/Rhein (broken line = calculated runoff, continuous line = measured runoff)

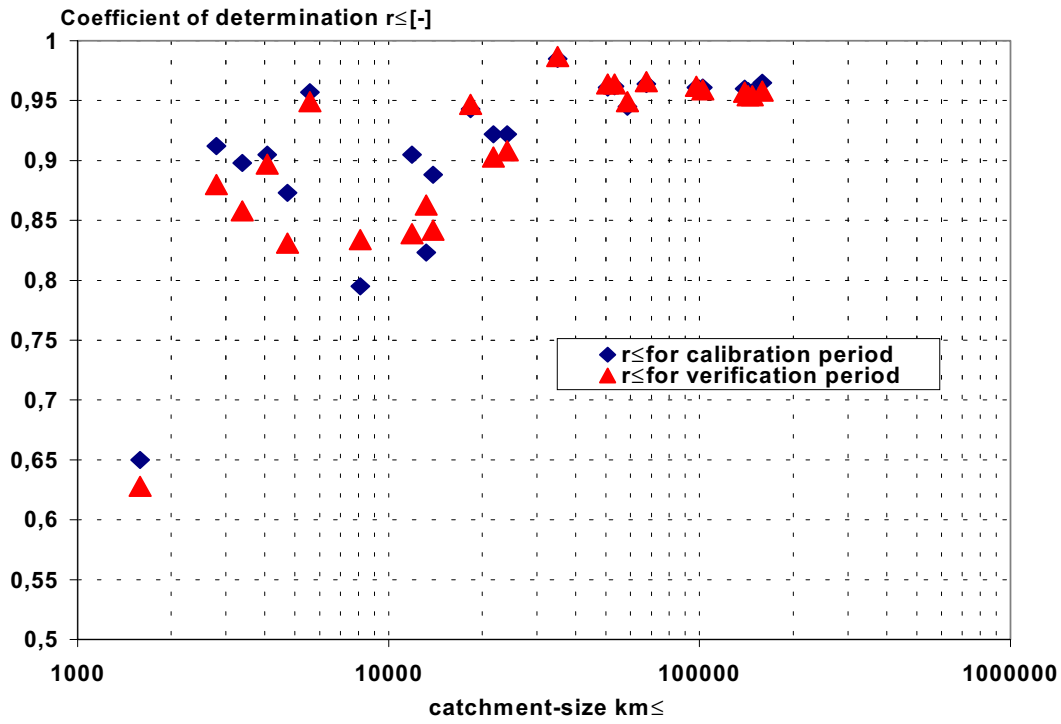

Fig 4 Coefficient of determination for the calibration and verification period

CALCULATION OF EXTREME EVENTS WITH THE COUPLED MODEL REMO-LARSIM

The major objective was to couple the atmospheric model REMO (Jacob,1995) with the hydrological model LARSIM, to simulate extreme rainfall runoff events (Richter et al. 2001). In a first step, the meteorological parameters were calculated with the atmospheric model REMO.

The model areas of the atmospheric model covers a region between 0 and 30 degree East and 45 to 75 degree North with a horizontal grid mesh size of 1/6 degree. REMO is a regional hydrostatic, numerical circulation model to calculate the three-dimensional atmospheric fields of the wind vector, temperature, humidity and precipitation. The grid size is consistent to the grid size of the hydrological model. For the three flood events March 1988, December 1993 and January 1995 the atmospheric conditions were calculated with the atmospheric model REMO. The model results for precipitation, temperature, relative humidity, wind velocity and radiation are used as input for the hydrological model LARSIM to calculate floods.

The model results for these recent flood events in the Rhine basin are shown in Figure 5, 6 and 7. The precipitation averaged across each model element (based on REMO output) has been compared to the one calculated with measured rainfall data. They correspond well in larger subbasins. On some days a time delay in the calculated precipitation can be seen. The quality of the flood simulations (with meteorological input from REMO results) with the hydrological model LARSIM strongly depends on the reliability of the meteorological input. For gauges with larger areas, the calculated and measured floods are corresponding well, provided there is no time delay in the calculated precipitation.

In the next step the atmospheric model REMO and the hydrological model LARSIM are coupled directly by using a common hydrological model for the vertical water transport in the soil. For the flood event 3/1988 the model parameters from LARSIM have been fully coupled to REMO. The model parameters of the vertical transport scheme (Xinanjiang) have been applied to REMO.

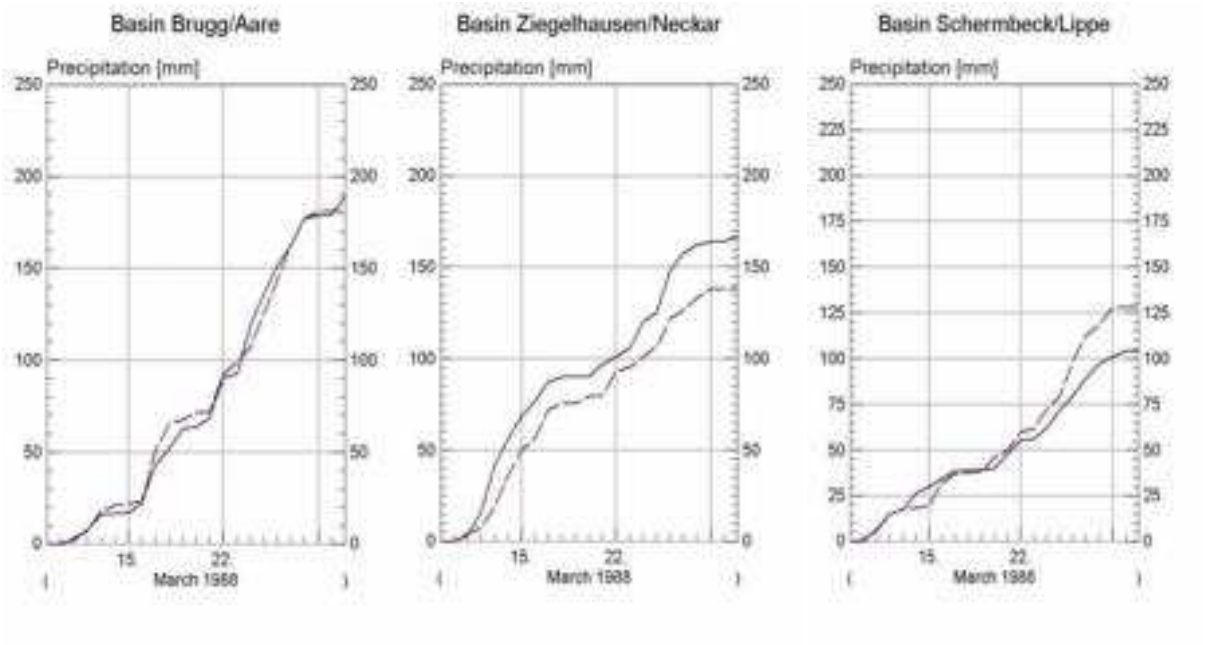

a) measured accumulated rainfall (continuous line) and with REMO calculated rainfall (broken line)

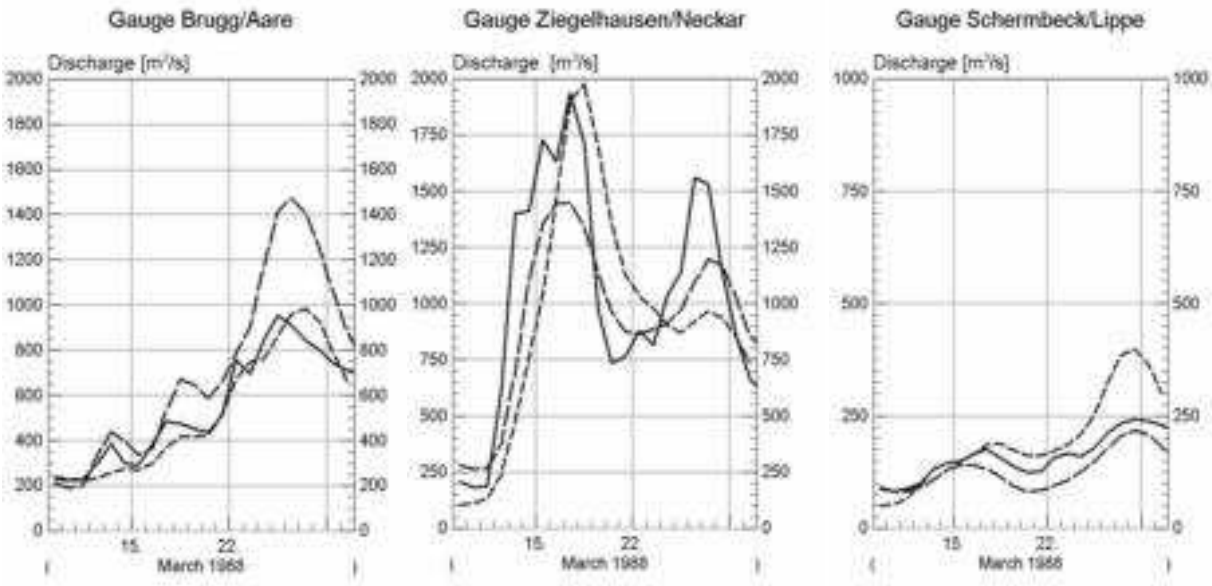

b) measured runoff (continuous line), with measured rainfall calculated runoff (long broken line) and with calculated rainfall (REMO) calculated runoff (short broken line)

Fig. 5 Model results for extreme rainfall-runoff event (flood event March 1988)

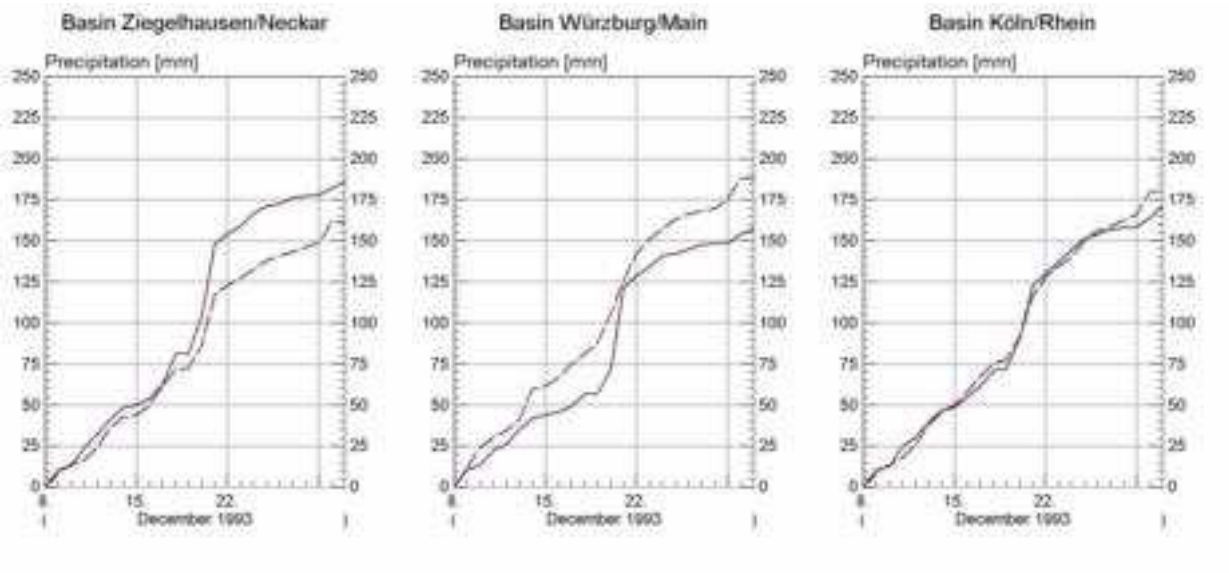

a) measured accumulated rainfall (continuous line) and with REMO calculated rainfall (broken line)

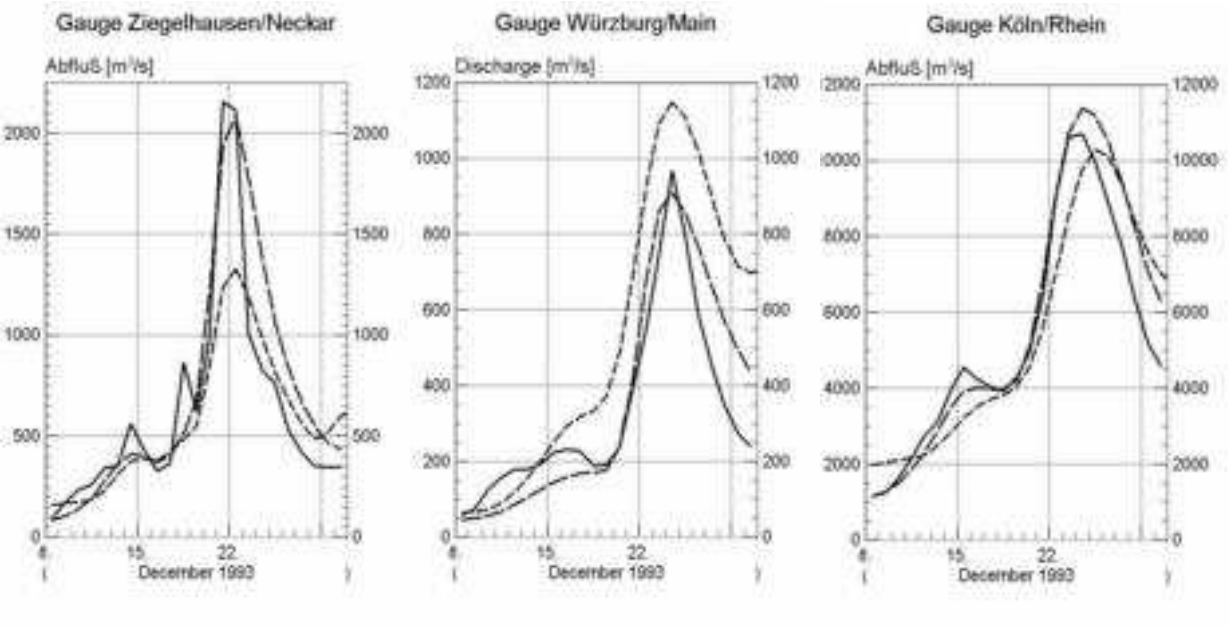

b) measured runoff (continuous line), with measured rainfall calculated runoff (long broken line) and with calculated rainfall (REMO) calculated runoff (short broken line)

Fig. 6 Model results for extreme rainfall-runoff event (flood event December 1993)

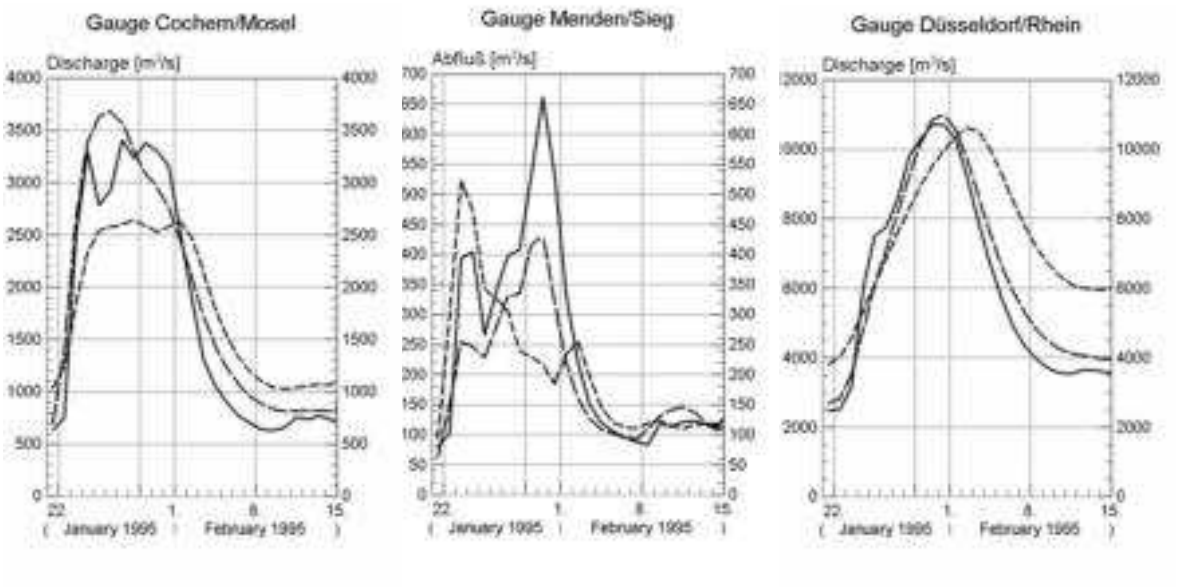

a) measured accumulated rainfall (continuous line) and with REMO calculated rainfall (broken line)

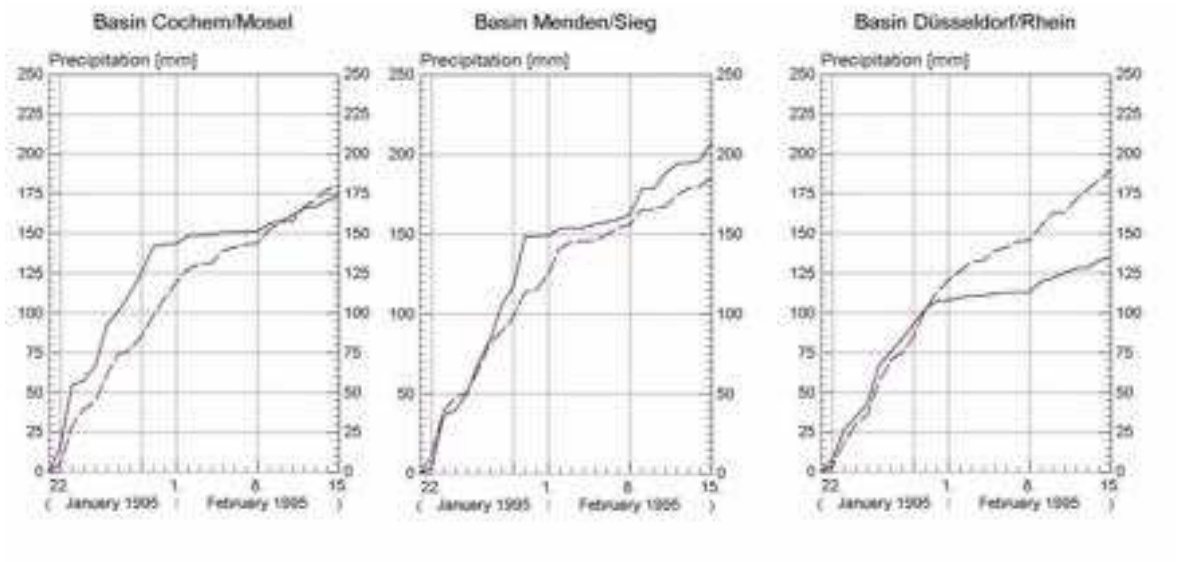

b) measured runoff (continuous line), with measured rainfall calculated runoff (long broken line) and with calculated rainfall (REMO) calculated runoff (short broken line)

Fig. 7 Model results for extreme rainfall-runoff event (flood event January 1995)

For each model element of LARSIM the accumulated runoff (baseflow + interflow + direct runoff) has been calculated using measured rainfall data for the period from March 9 until March 31, 1988 (Figure 8a). The difference of these values and the ones calculated using REMO output without model coupling were calculated (Figure 8b) as well as the difference using the calculated runoff with the coupled REMO-LARSIM model (Figure 8c).

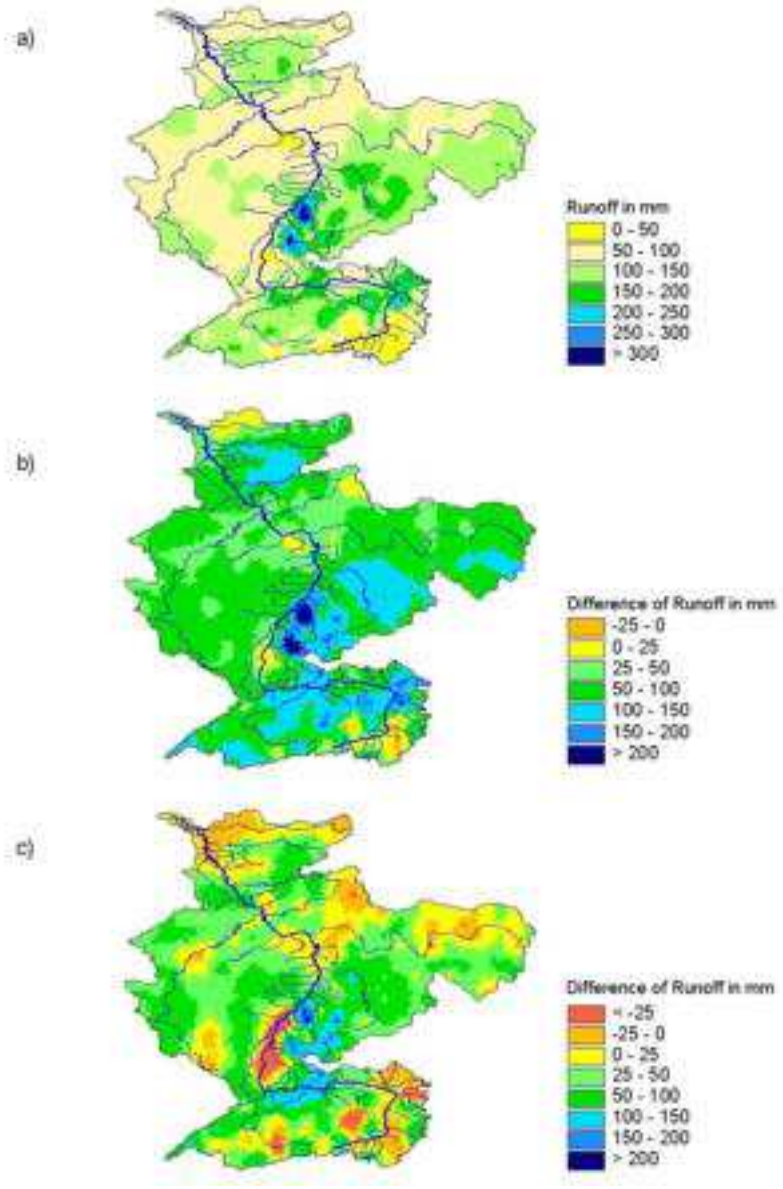

Fig. 8
a) Accumulated runoff between March 9,1988 and March 31,1988 (flood event March 1988) using measured rainfall data
b) difference between calculated runoff with measured data and runoff calculated with REMO output without model coupling
c) difference between calculated runoff with measured data and runoff calculated with output of the coupled REMO-LARSIM model

In most parts of the evaluated area the total accumulated runoff using measured rainfall data (a) varies between 50 and 200 mm with maxima in the Neckar basin.
The computed runoff calculated with uncoupled REMO output is in most regions significantly higher. Especially in the Neckar basin, where most of the runoff was produced in reality, maximum differences of up to 200 mm for this 22 day period appear.
Using the output of the coupled REMO-LARSIM model these differences are reduced substantially in large parts of the Rhine basin, even though significant differences remain in some regions. In general

the coupling of REMO and LARSIM therefore leads to a more realistic calculation of precipitation and runoff.

CONCLUSION AND RESULTS

For a period of nearly twenty years the hydrological model LARSIM has been applied to the Rhine basin using a mesoscale approach. Differences between the measured and the calculated discharge are remarkably low.

In a further step the hydrological model LARSIM was coupled to the atmospheric model REMO to improve the simplified hydrological cycle implemented in the present version of REMO. This approach was evaluated for three flood events leading to the following results:

-The precipitation averaged across each model element (based on REMO output) corresponds well with the one calculated using measured rainfall data.

-On some days a time delay in the calculated precipitation can be seen.

-The quality of the flood simulations (with meteorological input from REMO results) with the hydrological model LARSIM strongly depends on the reliability of the meteorological input.

A direct coupling of the atmospheric model REMO and the hydrological model LARSIM significantly improves the calculation of rainfall for large areas and yields more realistic runoff values.

During the evaluated 22 day period of a flood event, it only results in a small change of values of precipitation and river discharge. For long-term and/or climatological simulations a stronger response of the model results to the direct coupling can be expected.

REFERENCES

Becker A. (1992) Methodische Aspekte der Regionalisierung. In: Regionalisierung in der Hydrologie. Mitteilung XI der Senatskommission für Wasserforschung, Deutsche Forschungsgemeinschaft. S. 16-32.

Bremicker M. (2000) Das Wasserhaushaltsmodell LARSIM –Modellgrundlagen und Anwendungsbeispiele. Freiburger Schriften zur Hydrologie, Band 11, Institut für Hydrologie der Universität Freiburg i Br..

Bremicker M., Ludwig K., Richter K.-G. (1997) Effiziente Erstellung mesoskaliger Wasserhaushaltsmodelle. "Deutsche Gewässerkundliche Mitteilungen, Heft 5, 41. Jahrgang, Koblenz.

Ebel. M, Ludwig K., Richter K.-G. (2000) Mesoskalige Wasserhaushaltsmodellierung im Rheineinzugsgebiet mit LARSIM, Hydrologie und Wasserbewirtschaftung, Heft 6, Koblenz.

Jacob D. (1995) REMO - a model for climate research and weather forecast. In: Conference proceedings of the first study conference on BALTEX, Visby, Sweden. International BALTEX Secretariat, Publication No. 3, p. 99.

Nash J.E., Sutcliffe, J.V. (1970) River flow forecasting through conceptual models. 1. A discussion of principles. J. Hydrology, 10, pp. 282-290.

Richter, K.-G., Jacob D., Ebel M., Lenz, C.-J. (2001) Regionales Klimamodell zur Vorhersage meteorologischer und hydrologischer Extremereignisse am Beispiel des Rheinein-zugsgebietes, In Johannes Sutmoeller und Ehrhard Raschke (Hrsg): Modellierung in meso- bis makroskaligen Flusseinzugsgebieten. - Tagungsband zum gleichnamigen Workshop am 16./17. November 2000 in Lauenburg, GKSS 2001/15.

Thompson N., Barrie I.A., Ayles M. (1981) The Meteorological Office rainfall and evaporation calculation system: MORECS (July 1981). Hydrological Memorandum No. 45, Meteorological Office (GB).

Zhao R.J. (1977) Flood forecasting method for humid regions of China. East China Institute of Hydraulic Engineering, Nanjing, China.

Dr.-Ing. Karl-Gerd Richter
Dipl.-Hydr. Martin Ebel
Dr.-Ing. Karl Ludwig
c/o Dr.-Ing. Karl Ludwig
Beratender Ingenieur Wasserwirtschaft-Wasserbau
Herrenstr. 14
76133 Karlsruhe
karl-gerd.richter@t-online.de

Generation of hydrometeorological reference conditions for the assessment of flood hazard in large river basins (Proceedings of International Workshop, Koblenz, 6. and 7. March 2001). CHR-Report No. I-20

The Development of A Stochastic Rainfall Model for UK Flood Modelling

Harvey J. E Rodda
Peter Brett Associates
Reading, United Kingdom

Abstract A method has been developed to produce stochastic rainfall events which can be used as input into a river flood model for the UK. Firstly the basic event shapes, as a series of concentric ellipses, were produced using the Arc Info GIS from inputting just four parameters – a centre point, the long axis length and orientation, and the short axis length. The ellipses were then moved over the UK to represent the path taken by the rainfall. As the ellipses were moved, the rainfall was modified firstly by a rainfall profiling factor using techniques taken from the Flood Estimation Handbook and secondly the effect of orographic enhancement was incorporated using maps provided by the UK Meteorological Office. Over two hundred stochastic events were generated in this way from varying the parameters describing the size, orientation, movement and intensity of the rainfall using information from historical events. Clusters of events were also generated in order to represent the rainfall footprint associated with the passage of a number of depressions across the UK in close succession. The maximum rainfall and the rainfall for selected points for each event were compared with published rainfall maps and observations at 40 rain gauges (corresponding to the selected points) for calibration. Once calibrated the rainfall for each event was downloaded into a file on an hourly basis, and used as input for the rainfall runoff component of the river flood model.

INTRODUCTION

A flood loss model is currently being tested at Risk Management Solutions. The purpose of this model is to provide the probability of a certain financial loss associated with a given depth of floodwater on a postcode basis for the whole of Great Britain. It will be used by insurance and re-insurance companies for setting premiums, managing the risk of their existing portfolios, and providing risk information to assist in taking on new business. The application of hydrological modelling and mapping for insurance purposes has been increasing over the past decade. A number of peril maps already exist which show the extent of a 100 year flood for each river in Great Britain (e.g. Morris & Flavin, 1996, Environment Agency, 2000). These types of maps are very good for planning purposes, but one major disadvantage is that they do not consider the relationships between the degree of flooding for individual river basins. It is unlikely a 100 year flood will occur for every basin in the country at the same time. Instead when one basin experiences a 100 year flood, it is important to know what the return period of flooding is in neighbouring or distant basins. This is of particular relevance for the insurance industry where a primary insurer will need to know whether losses can be paid without requiring coverage from a re-insurer. The RMS model is able to address this limitation as it is an event-based model, where the inundation associated with a large number of flood events is calculated.

The complete model has four components: a stochastic rainfall model through which a series of flood producing rainfall events are generated; a rainfall-runoff model to derive peak flows, a hydrodynamic model to calculate the depth and extent of floodplain inundation, and the loss model to calculate the damage and subsequent financial losses on a postal code basis. This current paper will discuss the development of the stochastic rainfall model.

HISTORIC FLOOD EVENT DATA

The basis for the model development was the creation of a database of UK flood events from 1870 to 2000. A total of 528 individual events were selected from a variety of sources. Most events prior to 1930 were taken from an existing database of extreme hydrological events (British Hydrological Society, 1999). Events since 1981 were taken from documented annual hydrological reviews in the Hydrological Data UK Yearbooks (Institute of Hydrology, 1981-1999). Events for the period between 1930 and 1981 were taken from a variety of publications (e.g., British Rainfall 1870-1969; Holford, 1976; Perry, 1981; DOE, 1993,). Flood events were selected based on observational rather than hydrological measurements because this was format which the flooding was reported in most of the above sources, and only limited flow records were available for the earlier part of the study period. Records of maximum annual flows (Institute of Hydrology, 2000) were used to ensure major flood events had not been missed. The information on the date and location of flood events, the rivers affected, the meteorological conditions and any damage to buildings, property, and loss of life was listed in the database. This intensive data search provided a wide distribution in the magnitudes of flood events. Man made flood events such as dam-bursts, canal wall collapses, and burst water mains were not included in the database. The causes of the flooding were listed for each event, it was clear that the majority of these were rainfall induced flood events, only 38 were listed as snowmelt events and all of these involved the effect of rain falling on snow.

RAINFALL CLASSIFICATION

An analysis of the rainfall maps and the synoptic meteorology associated with the flood events led to the classification of four types of rainfall events: frontal, mesoscale convective complexes (MCC), thunderstorms, and east coast; examples of each are given in Figure 1.

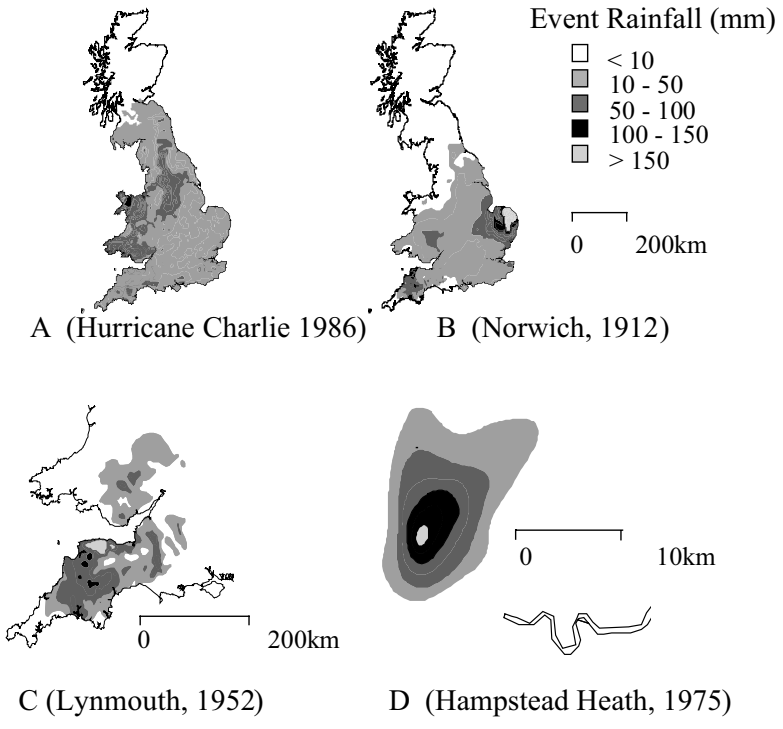

Figure 1. Examples of frontal (A), East Coast (B), MCC (C) and thunderstorm (D) rainfall types with the event dates, and names or areas affected.

Frontal events encompassed all types and combinations of fronts (warm, cold, occluded, stationary) associated with the westerly track of Atlantic depressions. The rainfall footprints were characterised by a wide area of rain heaviest over western parts of Britain. MCCs are rare in the British Isles,

initiated from deep convection and occur frequently over continental interiors (Browning & Hill, 1984). They are characterised by clusters of intense thunderstorm cells within a mesocale region of stratiform rain, which forms a shallow depression. (Collier & Hardaker, 1996). They occur only during summer in the UK, mostly in the South and Southwest, originating from the Bay of Biscay. MCCs have been responsible for the largest 24 hour rainfalls in the UK and also some of the most devastating floods (e.g. Lynmouth, 1952). Thunderstorm events are more scattered and less intense than MCCs, and without the defined depression. These generally only cause localised flooding when they occur over urban areas (e.g. London, 1975). East coast events are depressions travelling in a westerly direction that become quasi-stationary over the North Sea and produce on-shore easterly winds. In the winter these would cause snow, but in the summer they bring heavy and prolonged rainfall and notable flooding (e.g. the Norwich floods of 1912).

STOCHASTIC EVENT GENERATION

The meteorological characteristics of a subset of 72 events were investigated in more detail. These were in most cases the more extreme events but also events where quality rainfall maps (rainfall footprints) and information on rainfall durations and intensity were available. The values of specific parameters were then obtained from the 72 events, these were the long axis and short axis of the rainfall maps (defined by the area of rain > 25mm), the axis orientation, the storm direction and translational speed (taken from synoptic meteorology maps), the rainfall intensity, and the rainfall duration. Frontal events had the additional parameter of being single or multiple events. During the collection of data for the database it was found that flooding from frontal events resulted from a single depression or in many cases from a sequence of depressions moving across the country. A cumulative density function (CDF) of each of these parameters were plotted and then a stratified sampling regime was undertaken in order to derive values for a stochastic event set. The stratified sampling is illustrated in Figure 2, the principle being that the CDF is divided into slices and values are sampled randomly within each slice. The slices are selected so that there are a greater number of slices from the extreme end of the distribution. This will ensure that a higher number of more extreme events are present in the stochastic set. Values were sampled for each CDF although in some cases specific rules were set to ensure that the stochastic events made sense meteorologically. The rules were based on considering the relationships between the parameters. For example the storm duration had an inverse relationship with translational speed – the faster the speed the shorter the rainfall duration.

The set of the stochastic parameter values were then used to generate areas of rainfall, or rainfall footprints over Great Britain. Different sets of parameter values were used for the different rainfall classifications. The basic shape for the rainfall was taken as an ellipse. This is because the investigation of the historical events showed that rainfall footprints generally had a long axis and a short axis, and the boundary between the areas of rain and no rain was curved. Also ellipses could be generated automatically using the Arc/Info GIS with just four parameters – the long and short axis lengths, the long axis bearing and the centre point. Three concentric ellipses were chosen for each individual rainfall event with different maximum rainfall intensities within each one. Again this reflected the evidence from historical events where rainfall values were highest in a central area and lower towards the edges. An additional parameter was required for the ellipse generation, the centre point. This was also derived using a stochastic sampling technique by first selecting an anchor line of either specific longitude or latitude and then randomly sampling points along that line in defined slices. Figure 3 shows the anchor line for frontal events, 7.5 degrees west. The anchor line for East Coast and MCC events were different to reflect the source areas and movement of these events – East Coast along the Greenwich meridian and MCCs as 50 degrees latitude. Thunderstorm events were not considered along an anchor line instead their spatial distribution was defined using a 100 km by 100 km grid over the country.

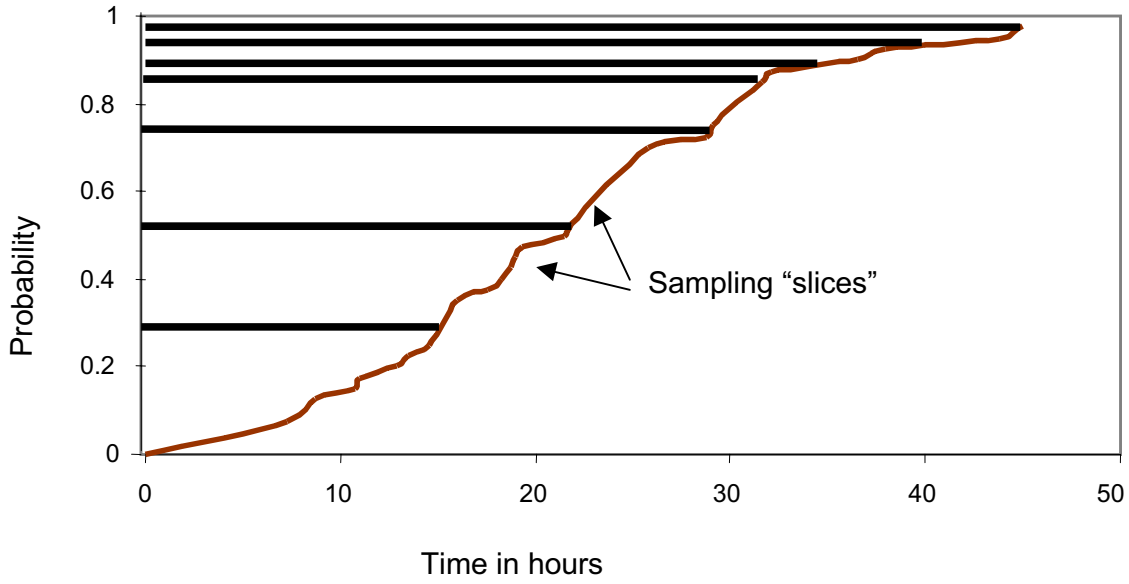

Figure 2. An example of stratified sampling, where the same number of samples are randomly selected for each slice giving a greater number of samples from the extreme end of the distribution.

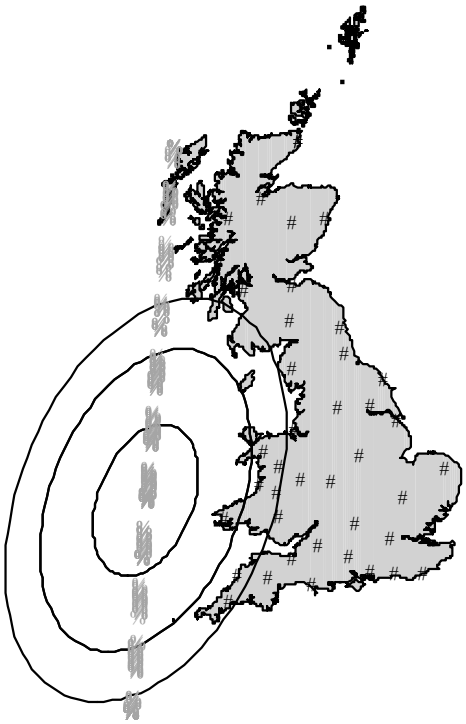

Figure 3. A stochastic frontal rainfall ellipse and its starting location in relation to the UK.

STOCHASTIC RAINFALL TRANSFORMATION

A large number of stochastic rainfall events were generated, approximately 400 frontal events, 50 MCC and East Coast events, and 200 thunderstorm events. The rainfall ellipses were used to provide hourly rainfall totals for the rainfall runoff component of the model. The ellipses were moved across the country using an automated procedure in Arc/Info. During the course of the movement the rainfall intensity was modified using a rainfall profile taken from the Flood Estimation Handbook - FEH (Institute of Hydrology, 2000) and orographic enhancement grids taken from the meteorological office (Hill, 1983). The FEH rainfall profiles were designed to simulate the growth and decay of rainfall over a point. For fast moving events with translational speeds over 50 km/h the use of a profile was not considered necessary as the movement of the rainfall footprint itself would produce a realistic profile over a point. The profiling was only used for slow moving events < 20km/h to simulate the effect of "rainout" which had been observed in many of the historical events, where a slow moving or stationary rainstorm eventually dissipates. An intermediate smoothed profile was used for events with a translational speed between 20 and 50 km/h. The orographic enhancement grids were used to represent the proven increase of rainfall with altitude from a number of factors. They took account of wind speed and direction, and could contribute rainfall of up to an extra 5 mm/hour. The combination of the rainfall profile and orographic enhancement on the rainfall ellipse as it moved across the country produced a realistic total rainfall footprint for the event (Figure 4). Since the stochastic rainfall was purely synthetic no rigorous rainfall calibration could be made. However a sanity check was undertaken by comparing the estimated rainfalls for selected durations and return periods (e.g. 100 year 24 hour rainfall) at 40 gauges around the country with the total stochastic event rainfall at the same location.

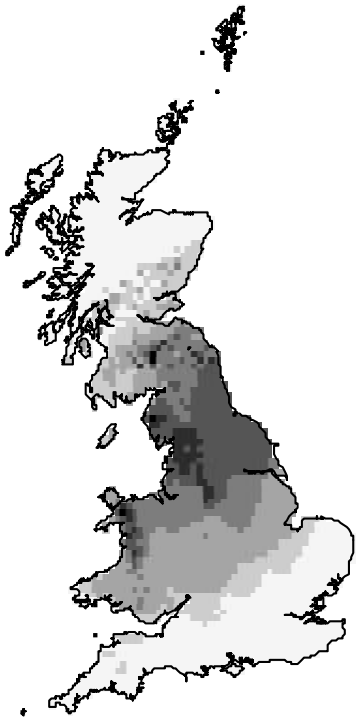

Figure 4. Total 24 hour rainfall from a stochastic frontal rainfall event.

FURTHER MODEL CALCULATIONS

As mentioned in the introduction, the stochastic rainfall model is one of the four components of the UK flood loss model. The stochastic rainfalls were used as an input to the rainfall runoff component of the model in order to calculate the maximum event discharge. Totals were averaged over each

catchment on an hourly basis and then modified using a stochastic antecedent wetness model to calculate a hydrologically effective rainfall. The effective rainfall was fed into a modified unit hydrograph approach, based on the Flood Estimation Handbook (Institute of Hydrology, 2000).

Flood routing was required since the maximum discharge at a point downstream was dependant on the time when flood peaks from upstream basins would arrive. The wave speeds were calculated using the RIBAMAN (Hydraulics research, 1994) model and the routing sequence was defined by using the USGS hydro1k coding system (Verdin 1997). The rainfall runoff model is currently being tested and calibrated using observed discharge data from flood events in April 1998 and October 2000. In this case observed rainfall data and antecedent conditions are being used. When the calibration is completed stage/discharge rating equations will then used to calculate the maximum depth for each outlet. The extent and depth of floodwater along the segment length was derived using a combination of a 50m DEM, interpolation techniques and some basic hydrodynamic principles. This component of the model has been developed concurrently with the rainfall runoff model and is also being independently calibrated using mapped flood extent data from historical events.

REFERENCES

British Hydrological Society (1999) Chronology of Hydrological Events Database, http://www.dundee.ac.co/geog/~che.

Browning, K. A. & Hill, F. F. (1984) Structure and evolution of a mesoscale convective system near the British Isles. *Quart. J. Roy. Met Soc*. 110, 897–913.

Collier, G. C. & Hardaker, P. J. (1996) Estimating probable maximum precipitation using a storm model approach. *J Hydrol*. 183, 277-306.

Department of the Environment (DOE) (1995) *The Occurrence and Significance of Erosion, Deposition and Flooding in Great Britain*. Her Majesty's Stationary Office, London.

Hill F. F. (1983) The use of average annual rainfall to derive estimates of orographic enhancement of frontal rain over England and Wales for different wind directions. *J. Climatology* **3**, 113-129.

Holford, I. (1976*) British Weather Disasters*. David and Charles, Newton Abbot, UK.

Hydraulics Research (1994) *RIBAMAN User Manual Version 1.22A*, HR Wallingford, UK.

Institute of Hydrology (1981-1999) *Hydrological Data UK Yearbook.* Wallingford, UK.

Institute of Hydrology (2000) *Flood Estimation Handbook*. Wallingford, UK.

Morris, D.G. & Flavin, R.W. (1996) Flood Risk Map for England and Wales. *Institute of Hydrology Report No. 30*, Wallingford, UK.

Perry, A. H. (1981) *Environmental Hazards in the British Isles*. George Allen and Unwin, London.

Verdin, K.L. (1997) A System for Topologically Coding Global Drainage Basins and Stream Networks. In: *Proc. 17th Annual ESRI Users Conference*, San Diego, California, July 1997.

Dr. Harvey J. E Rodda
Peter Brett Associates
16 Westcote Road
Reading
RG30 2DE
UK

Hrodda@pba.co.uk

KHR-VERÖFFENTLICHUNGEN **PUBLICATIONS DE LA CHR**

CHR/KHR (1978): Das Rheingebiet, Hydrologische Monographie. Staatsuitgeverij, Den Haag/
Le bassin du Rhin. Monographie Hydrologique. Staatsuitgeverij, La Haye. ISBN 90-12017-75-0
Nicht mehr Lieferbar

Berichte der KHR **Rapports de la CHR**

1-1 GREBNER, D. (1982): Objektive quantitative Niederschlagsvorhersagen im Rheingebiet. Stand 1982 (nicht mehr lieferbar) / Prévisions objectives et quantitatives des précipitations dans le bassin du Rhin. Etat de la question en 1982 (édition épuisée)

1-2 GERHARD, H.; MADE, J.W. VAN DER; REIFF, J.; VREES, L.P.M. DE (1983): Die Trocken- und Niedrigwasserperiode 1976. (2. Auflage 1985) / La sécheresse et les basses eaux de 1976 (2ème édition, 1985). ISBN 90-70980-0 1 -0

1-3 HOFIUS, K. (1985): Hydrologische Untersuchungsgebiete im Rheingebiet / Bassins de recherches hydrologiques dans le bassin du Rhin. ISBN 90-70980-02-9

1-4 BUCK, W.; KIPGEN, R.; MADE, J.W. VAN DER; MONTMOLLIN, F. DE; ZETTL, H.; ZUMSTEIN, J.F. (1986): Berechnung von Hoch- und Niedrigwasserwahrscheinlichkeit im Rheingebiet / Estimation des probabilités de crues et d'étiages dans le bassin du Rhin. ISBN 90-7098003-7

1-5 TEUBER, W.; VERAART, A.J. (1986): Abflußermittlung am Rhein im deutsch-niederländischen Grenzbereich / La détermination des débits du Rhin dans la région frontalière germano-hollandaise. ISBN 90-70980-04-5

1-6 TEUBER, W. (1987): Einfluß der Kalibrierung hydrometrischer Meßflügel auf die Unsicherheit der Abflußermittlung. Ergebnisse eines Ringversuchs / Influence de l'étalonnage des moulinets hydrométriques sur l'incertitude des déterminations de débits. Résultats d'une étude comparative. ISBN 90-70980-05-3

1-7 MENDEL, H.-G. (1988): Beschreibung hydrologischer Vorhersagemodelle im Rheineinzugsgebiet / Description de modèles de prévision hydrologiques dans le bassin du Rhin. ISBN 90-7098006-1

1-8 ENGEL, H., SCHREIBER, H.; SPREAFICO, M., TEUBER, W.; ZUMSTEIN, J.F. (1990): Abflußermittlung im Rheingebiet im Bereich der Landesgrenzen / Détermination des débits dans les régions frontalières du bassin du Rhin. ISBN 90-70980-10-x

1-9 CHR/KHR (1990): Das Hochwasser 1988 im Rheingebiet / La crue de 1988 dans le bassin du Rhin. ISBN 90-70980-11-8

1-10 NIPPES, K.-R. (1991): Bibliographie des Rheingebietes / Bibliographie du bassin du Rhin. ISBN 90-70980-13-4

1-11 BUCK, W.; FELKEL, K.; GERHARD, H., KALWEIT, H.; MALDE, J. VAN; NIPPES, K.-R., PLOEGER, B., SCHMITZ, W. (1993): Der Rhein unter der Einwirkung des Menschen - Ausbau, Schiffahrt, Wasserwirtschaft / Le Rhin sous l'influence de l'homme - Aménagement, navigation, gestion des eaux. ISBN 90-70980-17-7

1-12 SPREAFICO, M.; MAZIJK, A. VAN (Red.) (1993): Alarmmodell Rhein. Ein Modell für die operationelle Vorhersage des Transportes von Schadstoffen im Rhein. ISBN 90-70980-18-5

1-13 SPREAFICO, M., MAZIJK, A. VAN (réd.) (1997): Modèle d'alerte pour le Rhin. Un modèle pour la prévision opérationnelle de le propagation de produits nocifs dans le Rhin. ISBN 9070980-23-1

1-14 EMMENEGGER, CH. et al. (1997): 25 Jahre KHR. Kolloquium aus Anlaß des 25jährigen Bestehens der KHR / 25 ans de la CHR. Colloque à l'occasion du 25e anniversaire de la CHR. 1SBN 90-70980-24-x

1-15 ENGEL, H. (1997): Fortschreibung der Monographie des Rheingebietes für die Zeit 1971-1990 / Actualisation de la Monographie du Bassin du Rhin pour la période 1971-1990. ISBN 90-7098025-8

1-16 GRABS, W. (ed.) (1997): Impact of climate change on hydrological regimes and water resources management in the Rhine basin. ISBN 90-70980-26-6

1-17 ENGEL, H. (1999): Eine Hochwasserperiode im Rheingebiet. Extremereignisse zwischen Dez. 1993 und Febr. 1995. ISBN 90-70980-28-2

1-18 KOS, Th.J.M.; SCHEMMER, H.; JAKOB, A. (2000): Feststoffmessungen zum Vergleich von Messgeräte und Messmethoden im Rhein, 10-12 März 1998. ISBN 90-36953-54-5

1-19 BARBEN, M.; HODEL, H. P.; KLEEBERG, H. B.; SPREAFICO, M.; WEINGARTNER, R. (2001): Übersicht über Verfahren zur Abschätzung von Hochwasserabflüssen – Erfahrungen aus den Rheinanliegerstaaten. ISBN 90-36954-11-8

Katalog/Catalogue 1 SPROKKEREEF, E. (1989): Verzeichnis der für internationale Organisationen wichtigen Meßstellen im Rheingebiet / Tableau de stations de mesure importantes pour les organismes internationaux dans le bassin du Rhin. ISBN 90-70980-08-8

Berichte unter der Schirmherrschaft der KHR **Rapports sous l'égide de la CHR**

II-1 MADE, J.W. VAN DER (1982): Quantitative Analyse der Abflüsse (nicht mehr lieferbar) / Analyse quantitative des débits (édition épuisée)
II-2 GRIFFIOEN, P.S. (l 989): Alarmmodell für den Rhein / Modèle d'alerte pour le Rhin. ISBN 9070980-07-x
II-3 SCHRÖDER, U. (1990): Die Hochwasser an Rhein und Mosel im April und Mai 1983 / Les crues sur les bassins du Rhin et de la Moselle en avril et mai 1983. ISBN 90-70980-09-6
II-4 MAZIJK, A. VAN; VERWOERDT, P., MIERLO, J. VAN, BREMICKER, M.; WIESNER, H. (199 1): Rheinalarmmodell Version 2.0 - Kalibrierung und Verifikation / Modèle d'alerte pour le Rhin version 2.0 - Calibration et vérification. ISBN 90-70980-12-6
II-5 MADE, J.W. VAN DER (1991): Kosten-Nutzen-Analyse für den Entwurf hydrometrischer Meßnetze / Analyse des coûts et des bénéfices pour le projet d'un réseau hydrométrique. ISBN 9070980-14-2
II-6 CHR/KHR (1992): Contributions to the European workshop Ecological Rehabilitation of Floodplains, Arnhem, The Netherlands, 22-24 September 1992. ISBN 90-70980-15-0
II-7 NEMEC, J. (1993): Comparison and selection of existing hydrological models for the simulation of the dynamic water balance processes in basins of different sizes and on different scales. ISBN 90-70980-16-9
II-8 MENDEL, H.-G. (1993): Verteilungsfunktionen in der Hydrologie. ISBN 90-70980-19-3
II-9 WITTE, W., KRAHE, P.; LIEBSCHER, H.-J. (1995): Rekonstruktion der Witterungsverhältnisse im Mittelrheingebiet von 1000 n. Chr. bis heute anhand historischer hydrologischer Ereignisse. ISBN 90-70980-20-7
II-10 WILDENHAHN, E.; KLAHOLZ, U. (1996): Grobe Speicherseen im Einzugsgebiet des Rheins. ISBN 90-70980-21-5
II-11 SPREAFICO, M., LEHMANN, C., SCHEMMER, H.; BURGDORFFER, M.; KOS, T.L. (1996): Feststoffbeobachtung im Rhein, Beschreibung der Meßgeräte und Meßmethoden. ISBN 90-70980-22-3
II-12 SCHÂDLER, B. (Red.) (1997): Bestandsaufnahme der Meldesysteme und Vorschläge zur Verbesserung der Hochwasservorhersage im Rheingebiet. Schlußbericht der IKSR-Arbeitseinheit 'Meldesysteme / Hochwasservorhersage' - Projektgruppe 'Aktionsplan Hochwasser' / Annonce et prévision des crues dans le bassin du Rhin. Etat actuel et propositions d'amélioration. Rapport final de l'unité de travail 'Systèmes d'annonce / prévision des crues' - Groupe de projet 'Plan d'action contre les inondations'. ISBN 90-70980-27-4
II-13 DRÖGE, B., HENOCH, H.; KELBER, W.; MAHR, U.; SWANENBERG, T.; THIELEMANN, T., THURM, U. (1999): Entwicklung eines Längsprofils des Rheins. Bericht für die Musterstrecke von Rhein-km 800 - 845. Arbeitsgruppe 'Sedimenttransport im Rhein' Projekt 3. ISBN 90-70980-29-0
II-14 MAZIJK, A. VAN; LEIBUNDGUT, CH.; NEFF, H.-P. (1999): Rhein-Alarm-Modell Version 2. 1. Erweiterung um die Kalibrierung von Aare und Mosel. Kalibrierungsergebnisse von Aare und Mosel aufgrund der Markierversuche 05/92, 11/92 und 03/94. ISBN 90-70980-30-4
II-15 KWADIJK, J.; DEURSEN, W. VAN (1999): Development and testing of a GIS based water balance model for the Rhine drainage basin. ISBN 90-70980-31-2
II-16 MAZIJK, A. VAN; GILS, J.A.G. VAN; WEITBRECHT, V.; VOLLSTEDT, S. (2000): ANALYSE und EVALUIERUNG der 2D-MODULE zur Berechnung des Stofftransportes in der Windows-Version des RHEINALARMMODELLS in Theorie und Praxis. ISBN 90-36953-55-3

Einige Informationen über die:

DIE INTERNATIONALE KOMMISSION FÜR DIE HYDROLOGIE DES RHEINGEBIETES (KHR):

Die KHR ist eine Organisation, in der wissenschaftliche Institutionen der Rheinanliegerstaaten gemeinsam hydrologische Grundlagen für die nachhaltige Entwicklung im Rheingebiet erarbeiten.

Mission und Aufgaben der KHR sind:
- Erweiterung der Kenntnisse über die Hydrologie des Rheingebietes durch:
- gemeinsame Untersuchungen
  - Austausch von Daten, Methoden und Informationen
  - Entwicklung standardisierter Verfahren
  - Veröffentlichungen in einer eigenen Schriftenreihe
- Beiträge zur Lösung von grenzüberschreitenden Problemen durch die Entwicklung, Verwaltung und Bereitstellung von:
  - Informationssystemen (KHR-Rhein-GIS)
  - Modellen, wie z. B. Wasserhaushaltsmodelle und das Rhein-Alarmmodel

Die Länder, die sich daran beteiligen, sind:
die Schweiz, Österreich, Deutschland, Frankreich, Luxemburg und die Niederlande.

Beziehung zur UNESCO und WMO.
Die KHR wurde 1970 anlässlich der UNESCO-Empfehlung zur Förderung einer engeren Zusammenarbeit in internationalen Flussgebieten gegründet. Seit 1975 erfolgt die Fortsetzung der Arbeiten im Rahmen des Internationalen Hydrologischen Programms (IHP) der UNESCO und des Operationellen Hydrologischen Programms (OHP) der WMO.

Auszug aus den KHR-Aktivitäten für das Jahr 2001:

Hochwasser
Das Projekt "Übersicht von angewandten Verfahren zur Abschätzung von Hochwasserabflüssen für mittelgroße Einzugsgebiete" soll dazu beitragen, ein Werkzeug bereit-zustellen, das es erlaubt, das im Hinblick auf verfügbare Messungen optimale Modell bzw. die geeignetste Modellkombination zu identifizieren.
Mit dem Projekt "DEFLOOD" wird ein Beitrag zur Unter-stützung des nachhaltigen Hochwassermanagements geleistet. Es zielt darauf ab, anhand von Referenzhochwassern Methoden für die Analyse der Wirksamkeit von Maßnahmen zur Hochwasserrückhaltung im Rheineinzugsgebiet zu entwickeln.

Quelques informations sur la:

LA COMMISSION INTERNATIONALE POUR L'HYDROLOGIE DU BASSIN DE RHIN (CHR)

La CHR est une organisation regroupant les instituts scientifiques des Etats riverains du Rhin dans le but d'établir des bases hydrologiques pour un développement durable dans le bassin du Rhin.

Mission et tâches de la CHR :
- Elargir les connaissances sur l'hydrologie du bassin versant du Rhin par le biais :
  - de la recherche commune
  - de l'échange de données, méthodes et information
  - du développement de procédures normalisées
  - de publications dans les séries CHR
- Contribuer à la résolution de problèmes transfrontaliers par la réalisation, la gestion et la mise à disposition de :
- systèmes d'information (SIG Rhin CHR)
- modèles, par exemple des modèles de gestion des eaux et le Modèle d'Alarme pour le Rhin

Les pays suivants apportent leur collaboration :
la Suisse, l'Autriche, l'Allemagne, la France, le Luxembourg et les Pays-Bas.

Relation avec l'UNESCO et l'OMM.
La CHR a été fondée en 1970 sur la recommandation de l'UNESCO en vue de favoriser une collaboration plus étroite entre les bassins versants internationaux. Depuis 1975, les activités se poursuivent dans le cadre du Programme Hydrologique International (PHI) de l'UNESCO et du Programme Hydrologique Opérationnel (PHO) de l'OMM.

Sélection des activités de la CHR en 2001 :

Crues
Le projet "Inventaire des méthodes utilisées pour la détermination des débits de crues dans les bassins versants de taille moyenne" vise à contribuer au développement d'un instrument permettant de déterminer le modèle optimal ou la combinaison la plus appropriée de modèles à utiliser en fonction des mesures disponibles.
Le projet "DEFLOOD" contribue à une gestion durable des crues. L'objectif est de développer des méthodes pour analyser l'efficacité des mesures de réduction des niveaux de crues dans le bassin versant du Rhin en se basant sur des crues de référence.

Sediment
Sedimentation und Erosion können zu Problemen hinsichtlich der Fahrwassertiefe für die Schifffahrt, zu Austrocknung sowie zu einer Unterhöhlung von Fundamenten, Schädigung der Natur und Beeinträchtigung der Landschaftswerte führen. Die KHR-Untersuchungen richten sich im Jahr 2001 auf die Untersuchung von morphologischen Modellen, die im Rheineinzugsgebiet eingesetzt werden.

Rhein-GIS
Das geographische Informationssystem ist eine Datenbank des Rheineinzugsgebietes mit digitalisierten geographischen und hydrologischen Kenngrößen. Diese Datenbank umfasst auch meteorologische Zeitreihen.
Das Rhein-GIS der KHR wird bei stets mehr Untersuchungen, bei denen die KHR als Partner fungiert, eingesetzt.
Das System wird 2001 um neue Klimadaten erweitert und mit einer anwenderfreundlichen Benutzeroberfläche versehen.

Das Rhein-Alarmmodell sagt bei Schadstoffeinleitungen den Verlauf der Verunreinigung vorher. Die Anwenderfreundlichkeit und Zuverlässigkeit des Modells wurde neulich in Zusammenarbeit mit den niederländischen Anwendern des Modells erheblich verbessert.

Nähere Informationen über die KHR können Sie auf der Website www.chr-khr.org finden.

Sédiments
La sédimentation et l'érosion peuvent provoquer des problèmes de profondeur du chenal pour la navigation, de tarissement, d'affaiblissement de fondations, de dommages à la nature et de nuisance aux intérêts paysagers. En 2001, l'étude de la CHR a concentré ses efforts sur les modèles morphologiques qui sont utilisés dans le bassin versant du Rhin.

SIG Rhin
Le Système d'Information Géographique est une base de données pour le bassin versant du Rhin et contient des données de base géographiques et hydrologiques numérisées. Cette base de données comprend aussi des séries temporelles météorologiques.
Le SIG Rhin de la CHR est de plus en plus utilisé lors d'études auxquelles participe la CHR. Le système a été enrichi par de nouvelles données climatologiques et a été doté d'une interface utilisateur conviviale.

Le Modèle d'Alarme pour le Rhin prévoit la propagation de la contamination lors de rejets de substances toxiques. Une bonne collaboration avec les utilisateurs du modèle a permis d'améliorer considérablement sa convivialité ainsi que sa fiabilité en 2001.

Pour de plus amples informations sur la CHR, consultez le site Internet : www.chr-khr.org

Enige gegevens betreffende de :

DE INTERNATIONALE COMMISSIE VOOR DE HYDROLOGIE VAN HET RIJNGEBIED (CHR)

De CHR is een organisatie, waarin de wetenschappelijke instituten van de Rijnoeverstaten gezamenlijk hydrologische grondslagen voor een duurzame ontwikkeling in het Rijngebied uitwerken.

Missie en taken van de CHR:
- Uitbreiden van de kennis over de hydrologie van het Rijnstroomgebied door:
  - gemeenschappelijk onderzoek
  - uitwisseling van gegevens, methoden en informatie
  - ontwikkeling van gestandaardiseerde procedures
  - publicaties in de CHR-reeksen
- Bijdragen aan het oplossen van grensoverschrijdende problemen door het maken, beheren en beschikbaar stellen van:
  - informatiesystemen(CHR Rijn GIS)
  - modellen, b.v. waterhuishoudingsmodellen en het Rijn Alarmmodel

Samenwerkende landen zijn:
Zwitserland, Oostenrijk, Duitsland, Frankrijk, Luxemburg en Nederland.

Relatie met UNESCO en WMO.
De CHR werd in 1970 opgericht naar aanleiding van een advies van de UNESCO om een nauwere samenwerking tussen internationale stroomgebieden te bevorderen. Sinds 1975 worden de werkzaamheden voortgezet in het kader van het Internationale Hydrologische Programma (IHP) van de UNESCO en van het Operationele Hydrologische Programma (OHP) van de WMO.

Selectie uit CHR-werkzaamheden in 2001:

Hoogwater
Het project "Overzicht van toegepaste methoden voor het schatten van hoogwaterafvoeren voor middelgrote stroomgebieden" moet ertoe bijdragen om een instrument te ontwikkelen, waarmee in relatie tot de beschikbaarheid van metingen het optimale model of de meest geschikte combinatie van modellen kan worden bepaald.
Met het project "DEFLOOD" wordt een bijdrage geleverd aan de ondersteuning van duurzaam hoogwatermanagement. Het doel is methoden te ontwikkelen ter analysering van de effectiviteit van maatregelen ter verlaging van hoogwaterstanden in het Rijnstroomgebied op basis van referentie hoogwaters.

Some information on the:

INTERNATIONAL COMMISSION FOR THE HYDROLOGY OF THE RHINE BASIN (CHR)

The CHR is an organisation in which the scientific institutes of the Rhine riparian states develop joint hydrological measures for sustainable development of the Rhine basin.

CHR's mission and tasks:
- Acquiring knowledge of the hydrology of the Rhine basin through:
  - joint research
  - exchange of data, methods and information
  - development of standardised procedures
  - publications in the CHR series
- Making a contribution to the solution of cross-border problems through the formulation, management and provision of:
  - information systems (CHR Rhine GIS)
  - models, e.g. models for water management and the Rhine Alarm model

Co-operating countries:
Switzerland, Austria, Germany, France, Luxembourg and the Netherlands.

Relationship with UNESCO and WMO.
The CHR was founded in 1970 following advice by UNESCO to promote closer co-operation between international river basins. Since 1975, the work has been continued within the framework of the International Hydrological Programme (IHP) of the UNESCO and the Operational Hydrological Programme (OHP) of the WMO.

Selection of CHR activities in 2001:

High water
The "Summary of allied processes for estimating high water discharges for meso-scale catchment areas" project is to contribute to the development of a tool, to identify the best model or combination of models in the context of available measurements.
The "DEFLOOD" project will contribute to sustainable high water management. The objective is to develop methods for analysing the effectiveness of measures to reduce high waters in the Rhine basin on the basis of high water references.

Sediment
Sedimentatie en erosie kunnen leiden tot problemen bij de vaargeuldiepte voor de scheepvaart, tot verdroging, ondermijning van fundamenten, schade aan de natuur en aantasting van de landschappelijke waarden. Het CHR onderzoek concentreert zich in 2001 op bestudering van de morfologische modellen die in het Rijnstroomgebied worden gebruikt.

Rijn GIS
Het Geografische Informatiesysteem is een databank voor het Rijnstroomgebied met gedigitaliseerde geografische en hydrologische basisgegevens. Deze databank omvat ook meteorologische tijdreeksen.
Het CHR Rijn-Gis wordt bij steeds meer onderzoeken ingezet, waarbij de CHR partner is.
Het systeem werd in 2001 uitgebreid met nieuwe klimaatgegevens en voorzien van een gebruiksvriendelijke user interface.

Het Rijn Alarmmodel voorspelt bij lozingen van schadelijke stoffen het verloop van de verontreiniging. In goede samenwerking met de gebruikers van het model is de gebruiksvriendelijkheid en robuustheid van het model in 2001 aanzienlijk verbeterd.

Meer informatie over de CHR kunt u vinden op de website: www.chr-khr.org

Sediment
Sedimentation and erosion can lead to problems in the navigable depth for shipping, to dehydration, to undermining of foundations, as well as to damage to nature and the landscape. CHR research in 2001 concentrated on the study of morphological models used in the Rhine catchment area.

Rhine GIS
The Geographical Information System is a database for the Rhine catchment area, holding digitised geographical and hydrological parameters. The database also covers meteorological time series.
The CHR Rhine GIS is used in increasingly more studies, to which the CHR is a partner.
In 2001, the system was expanded with new climatic data and equipped with a user-friendly GUI.

The Rhine Alarm model forecasts the progress of pollution following the discharge of harmful substances. In co-operation with its users, the model's user friendliness and sturdiness was considerably improved in 2001.

For more information on the CHR, refer to the web site: www.chr-khr.org

KOLOPHON

Publikation der CHR/KHR
Sekretariat , Postfach17
8200 AA Lelystad
Niederlande
Email: info@chr-khr.org
Website: www.chr-khr.org

Übersetzungen: Password Translations, Heino

Drucker: Veenman drukkers, Ede

ISBN: 90-36954-18-5

Secretariaat CHR/KHR
Zuiderwagenplein 2

Postbus 17
8200 AA Lelystad
Niederlande/Pays-Bas